THE HONG KONG POLYTECHNIC UNIVERSITY
香港理工大學
Pao Yue-kong Library
包玉剛圖書館

Copyright Undertaking

This thesis is protected by copyright, with all rights reserved.

By reading and using the thesis, the reader understands and agrees to the following terms:

1. The reader will abide by the rules and legal ordinances governing copyright regarding the use of the thesis.
2. The reader will use the thesis for the purpose of research or private study only and not for distribution or further reproduction or any other purpose.
3. The reader agrees to indemnify and hold the University harmless from and against any loss, damage, cost, liability or expenses arising from copyright infringement or unauthorized usage.

IMPORTANT

If you have reasons to believe that any materials in this thesis are deemed not suitable to be distributed in this form, or a copyright owner having difficulty with the material being included in our database, please contact lbsys@polyu.edu.hk providing details. The Library will look into your claim and consider taking remedial action upon receipt of the written requests.

Pao Yue-kong Library, The Hong Kong Polytechnic University, Hung Hom, Kowloon, Hong Kong

http://www.lib.polyu.edu.hk

ACTIVE MANAGEMENT OF DISTRIBUTION SYSTEMS WITH DISTRIBUTED ENERGY RESOURCES

JIAYONG LI

PhD

The Hong Kong Polytechnic University

2018

The Hong Kong Polytechnic University

Department of Electrical Engineering

Active Management of Distribution Systems with Distributed Energy Resources

Jiayong Li

A thesis submitted in partial fulfillment of the requirements for the degree of Doctor of Philosophy

April 2018

CERTIFICATE OF ORIGINALITY

I hereby declare that this thesis is my own work and that, to the best of my knowledge and belief, it reproduces no material previously published or written, nor material that has been accepted for the award of any other degree or diploma, except where due acknowledgement has been made in the text.

____________________(Signed)

Jiayong LI (Name of student)

I would like to dedicate this thesis to my loving parents ...

Abstract

Over the last decade, the world has witnessed a widespread adoption of distributed energy resources (DERs) in the distribution networks (DNs) due to the rapid advances in renewable DER technologies. This trend may bring about lot of economic and environmental benefits. However, it also introduces adverse impacts on the DN operations because of the uncertainty and intermittency of renewable DERs. These impacts include but are not limited to the severe voltage variations and significant load ramps. In order to mitigate these effects, the potential of DERs has been explored to provide ancillary services, e.g. voltage regulation and frequency control. On the other hand, since DERs are geographically dispersed over the entire DN, it is considerably challenging in coordinating them. Therefore, this thesis focuses on addressing these concerns by developing advanced management approaches.

To overcome the complexity in coordinating various devices and promote a competitive energy trading environment, a novel transactive energy trading framework is proposed with detailed designs for the end-use customers. Particularly, the author innovatively integrates a novel Nash bargaining based bilateral energy trading mechanism with an efficient distributed optimal power flow (OPF) technique to maximize the benefit of customers and to enhance the system reliability and security. With some rigorous analysis, the proposed model is converted into a two-stage problem, where the first stage determines the optimal energy trading and dispatch decisions, and the second stage settles the optimal payments. To implement this framework in a decentralized manner, an advanced distributed algorithm is developed. Numerical results demonstrate the economic and technical advantages of this framework.

To address the severe voltage variations caused by the intermittent photovoltaic (PV) output, a distributed online voltage control algorithm is developed based on

dual ascent method. Conventional distributed algorithms implement voltage control only when the algorithms converge, while the proposed algorithm is able to carry out voltage control immediately. In particular, a closed-form solution is derived for the PV controllers to locally update the active and reactive power set-points based on local voltage measurements and information exchange with their neighboring PV systems. The objective is to minimize the total loss, while maintaining the bus voltages within the acceptable ranges. The effectiveness and robustness of the proposed algorithm are verified in case studies.

To mitigate the significant load ramps caused by the diurnal pattern of PV power, the author proposes a novel look-ahead dispatch model for the DNs with multiple distributed ESSs. The dispatch problem is formulated as a finite horizon optimization problem and is carried out utilizing model predictive control method (MPC) that takes both current and future information into account. Thus, the short-sightedness can be avoided. The numerical results show that the proposed model can bring about a significant reduction of maximum ramp and power losses.

To alleviate the PV ramp event (PRE) induced voltage violations, a robust dispatch model is proposed that enables systematic coordination between on-load tap changer (OLTC) and PV inverters. Particularly, this model is formulated as a two-stage robust optimization problem, where the first stage determines the OLTC step and maximum admissible PV output (MAPO), and the second stage evaluates the feasibility of the first stage result under all possible realizations of PRE. MAPO is proposed to quantify the operational PV hosting capacity. Column-and-constraint generation algorithm is employed to solve the problem. Case study on IEEE 33-bus distribution system validates the effectiveness of the proposed model in eliminating PRE induced voltage violations.

Publications Arising from the Thesis

Journal Papers

1. **Jiayong Li**, Zhao Xu, Jian Zhao and Can Wan, "A Coordinated Dispatch Model for Distribution Network Considering PV Ramp", *IEEE Transactions on Power Systems*, 2018, Published.

2. **Jiayong Li**, Chaorui Zhang, Zhao Xu, Jianhui Wang, Jian Zhao and Ying-Jun (Angela) Zhang, "Distributed Transactive Energy Trading Framework in Distribution Networks", *IEEE Transactions on Power Systems*, 2018, in Press.

3. **Jiayong Li**, Zhao Xu, Jian Zhao and Chaorui Zhang, "Distributed Online Voltage Control in Active Distribution Networks Considering PV Curtailment", submitted to *IEEE Transactions on Industrial Informatics*.

4. **Jiayong Li**, Zhao Xu, Jian Zhao, Songjian Chai, Yi Yu and Xu Xu, "Model Predictive Control Based Ramp Minimization in Active Distribution Network Using Energy Storage Systems", submitted to *Electric Power Components and Systems*.

5. Chaorui Zhang, **Jiayong Li**, Ying-Jun (Angela) Zhang and Zhao Xu, "Optimal Location Planning of Renewable Distributed Generation Units in Distribution Networks: An Analytical Approach", *IEEE Transactions on Power Systems*, 2018, Published.

6. Jian Zhao, Zhao Xu, Jianhui Wang, Cheng Wang and **Jiayong Li**, "Robust Distributed Generation Investment Accommodating Electric Vehicle Charging

in a Distribution Network", *IEEE Transactions on Power Systems*, 2018, in Press.

7. Xu Xu, Jian Zhao, Zhao XU, Songjian Chai, **Jiayong Li** and Yi Yu, "Stochastic Optimal TCSC Placement in Power System Considering High Wind Power Penetration", *IET Generation, Transmission & Distribution*, 2018, Published.

Conference Papers

1. **Jiayong Li**, Can Wan and Zhao Xu, "Robust offering strategy for a wind power producer under uncertainties", *2016 IEEE International Conference on Smart Grid Communications.*

2. **Jiayong Li**, Jian Zhao and Zhao Xu, "Optimal real-time scheduling of energy storage systems to accommodate PV generation in distribution networks", *2018 IEEE PES Innovative Smart Grid Technologies Asia.*

Acknowledgements

I am very grateful to all those people who helped, supported and accompanied me during my four-year Ph.D. study in HK PolyU.

First and foremost, I want to express my deepest appreciation to my chief supervisor, Professor Zhao Xu, for his continuous guidance, encouragement and support throughout my Ph.D. study. He is always very kind and patient in offering me insightful suggestions and detailed comments to improve my research works. It is my great honor to have him as my research advisor and closely learn from him. Moreover, I have been deeply inspired by his optimistic attitude to life and enthusiasm on research. I will always remember his endless kindness, strong support and continuous patience.

I would like to express my deep gratitude to Professor Jianhui Wang, for hosting and advising me so kindly during my 5-month visit at Argonne National Laboratory. It was my privilege to discuss with and learn from him.

Furthermore, I would also like to express special thanks to my beloved parents, Fulun Li and Xijun Li, for their unconditional love, support and encouragement throughout my life. I also owe many thanks to my dear fiancée, Mungkai Yik, for giving me so many enjoyable moments and providing me continuous support and encouragement whenever I encountered difficulties in these four years.

I would also like to express many thanks to the research members of our group for their precious friendship and help. Especially, I would like to thank Dr. Can Wan and Dr. Jian Zhao for providing me valuable help on my research path.

Last but not least, I would like to acknowledge the support from Ph.D. studentship awarded by The Hong Kong Polytechnic University.

Table of contents

List of figures

List of tables

Abbreviations

ADMM Alternating Direction Method of Multipliers

ADN Active Distribution Network

AMI Advanced Metering Infrastructure

CCG Column-and-Constraint Generation

DER Distributed Energy Resource

DESS Distributed Energy Storage System

DG Distributed Generator

DN Distribution Network

DR Demand Response

DSO Distribution System Operator

ESS Energy Storage System

FRP Flexible Ramping Product

HVAC Heating Ventilation Air Conditioning System

ICT Information and Communication Technology

ISO Independent System Operator

MAPO Maximum Admissible PV Output

MPC Model Predictive Control

OLTC On-Load Tap Changer

OPF Optimal Power Flow

PV Photovoltaic

PEV Plug-in Electric Vehicle

PRE PV Ramp Event

RES Renewable Energy Source

SDP Semi-definite Programming

SOC Second-order Cone

SOCP Second-order Cone Programming

TE Transactive Energy

TET Transactive Energy Trading

Chapter 1

Introduction

1.1 Background

Over the last decade, the world has witnessed an increasing adoption of Distributed Energy Resources (DERs) boosted mainly by the rapid advances in renewable DER technologies, e.g. distributed solar photovoltaic (PV) panels and wind turbines. According to a recent report [1], the global total installed capacity of DERs has reached 132.4 GW by the end of 2017 and is estimated to increase by approximately 400 GW in the following decade. Although DERs have various definitions, a commonly used one is summarized as: DERs are electricity-generating resources located within the electric distribution network (DN) [2]. The typical scale of DERs ranges from 1 kW to 10 MW, which is much smaller than the conventional power plants. Thus, it makes DERs ready to be adopted by the end-use customers. Thanks to the declining installation cost and favorable government policies, the end-use customers have become the main force in adopting DERs during recent years. For example, over 230,000 houses in California have installed rooftop PV systems by 2014 because of the generous Million Solar Roofs Initiative Scheme supported by the California Public Utilities Commission [3, 4]. The distributed PV capacity in China has also experienced a fast growth in the past few years, reaching 3.73 GW by the end of 2016, and the growth rate has already exceeded the growth rate of the utility-scale

PV [5]. Other countries like Australia, Canada and Germany have also carried out attractive subsidy schemes to encourage the customers to install renewable DERs [6].

The widespread adoption of DERs may bring about lots of economic, environmental and technical benefits. Firstly, it will reduce greenhouse gas emission and energy dependence on fossil fuels as most DERs are renewable energy based. Secondly, DERs are capable of relieving transmission line overload and reducing transmission losses since they are located close to the end-users. In addition, adopting DERs is more economical and faster than upgrading transmission network and central power plants to address the problem of ever-growing load demand. Thirdly, DERs have the potential to provide ancillary service to the system, e.g. voltage control, frequency regulation, contingency reserves and black start services, and thus playing an import role in enhancing the system reliability, security and resilience [7]. Fourthly, DERs is able to reduce the customers' electricity usage cost by enabling local power supply. The advantages of DER are not limited to the mentioned above. On the other hand, the proliferation of DERs is dramatically changing the paradigm of the power systems. Traditionally, the end-use customers are pure electricity consumers and the energy is delivered from the large-scale central power plants to the customers via the transmission networks and distribution networks. But now an increasing proportion of load demand can be supplied by the local DER generations. Besides, since the output of renewable DERs is inherently intermittent and uncertain, the high penetration of DERs also introduces significant challenges to the power system operation. For example, the fluctuation of renewable DERs' output will cause unexpected operation constraint violations, such as voltage violations and distribution line overload [8].

Thanks to the widespread adoption of the smart electric appliances, such as plug-in electric vehicles (PEVs), heating ventilation air conditioning system (HVAC), and intelligent kitchen appliances, there is an increasing level of flexibility on the demand side. By 2016, over 750 thousand electric vehicles have been registered worldwide [9]. In order to better utilize the demand side flexibility to mitigate the adverse impact of DER generations, demand response (DR) has been proposed.

According to the Federal Energy Regulatory Commission, DR is defined as the changes in load consumption by the end-users from their normal electric usage pattern in response to changes in electricity prices, or to incentive payment designed to induce lower electricity use at times of high wholesale market prices or when system reliability is jeopardized [10]. The recent emergence of advanced metering infrastructures (AMIs) and information and communication technologies (ICTs) facilitates the implementation of DR. DR may reduce the customers' cost and improve the system reliability under proper schemes. However, the inappropriate implementation of DR will threaten the normal operation of the distribution system. For instance, a large number of customers may shift their load demand to the period of low electricity price, which may create new peaks and leads to the overload in the DN [11]. Therefore, it is crucially important to properly coordinate DERs and DR.

The distribution network is an electric network that carries the power from the transmission network to the individual customers. It typically starts with the substation that connects with the transmission system or subtransmission system via the step-down transformers. With rare exception, the distribution networks are radial, which means there is only one path for the power to be transmitted from the substation to the end-users [12]. Hence, the power flow is unidirectional in the traditional distribution network that has no local generation facilities. Such a distribution network is called passive network since no active measures can be taken except load shedding when a contingency takes place. However, with the adoption of DERs, the application of advanced ICTs and installation of smart meters, the distribution networks are evolving to active networks that enable effective real-time monitoring, communication and control [13]. In active distribution networks, the objectives of the system operation not only include supplying customers with power of high quality, but also include enhancing the system reliability, security, flexibility and efficiency through the coordination of all kinds of devices [14]. The transition of distribution networks may benefit the customers and society by lowering the electricity price and improving the energy utilization efficiency. Nevertheless, it also introduces considerable complexity to the distribution network operation. For example, the power flow pattern in the active distribution networks become much more complex compared to the unidirectional pattern [15]. In this respect, advanced control strategies are required to handle all potential complexities.

Since the ratio between the resistance and reactance of the distribution line is considerably larger than that of the transmission line [12], the active and reactive power flow will cause comparable voltage drops on the distribution lines. It is likely that the voltage magnitudes on the customers' side deviate too much from the normal values, which inevitably causes detrimental effect on the electric devices. Hence, one major task in the distribution system is to ensure the nodal voltages within the pre-specified limits by utilizing voltage regulation devices, e.g. on-load tap changer (OLTC), voltage regulator, capacity bank, etc [16]. However, with increasing penetration of DERs, the system is more likely to encounter unexpected voltage violations because of uncertain and intermittent output of renewable DERs. The voltage will fluctuate in such a fast rate that the aforementioned conventional regulation devices may not react timely in response to the voltage violations. In addition, these devices cannot be adjusted too frequently; otherwise, their life spans will be shortened significantly. Fortunately, it has been widely recognized that DERs have the potential to address the voltage problem because they are mostly electronic interface based and thus their active and reactive power output can be adjusted quickly and flexibly to some extent [17].

Generally, a large proportion of DERs are owned by the different customers and are geographically dispersed over the entire distribution network [18]. On one hand, the customers' behaviors will inevitably exert a great influence on the distribution network operation. On the other hand, they may be indifferent to the system operation since they are usually self-interested with the primary goal of reducing their payments or improving their profits. In this regard, new business model is required to encourage customers to actively provide support to the system operation. Traditionally, the electricity market, either wholesale market or retail market, inhibits the direct participation of the end-use customers because of the high entry threshold. Hence, customers are passive participants as they have no choice but to accept the prices offered by the utility company for the energy consumption and production. These markets have been used in many countries for years. However, they cannot adapt to the evolution of distribution networks as they fail to fully unlock the technical and economic values of DERs and controllable loads. Moreover, due to the economies of scale in electric industry, it is likely that customers are unable to recover their capital costs of DER installation within the traditional electricity markets. Therefore, it is necessary to create a competitive distribution market that enables active participation of customers. In such a market, the customers with controllable loads are willing to provide support to the system operation in exchange of economic reward and the customers with DER installations, defined as prosumers, are allowed to sell the excess energy at a competitive price. Besides, the distribution system operator can procure the required service locally from the customers instead of the upstream transmission network.

1.2 Research Motivations

As mentioned in the previous section, one biggest challenge introduced by the proliferation of DERs and controllable loads is the considerable complexity in coordinating and controlling a large number of dispersed devices. It is crucially important to overcome this complexity, otherwise it would lead to the reduction of system reliability, security and efficiency. Transactive energy (TE) is a newly emerged concept that sheds new light on addressing this complexity. According to Gridwise Architecture Council (GWAC), TE is defined as a set of mechanisms that combine economic and control techniques to achieve an optimal, reliable and secure operation outcome of an electric system considering the system operating constraints [19]. Specifically, it uses economic techniques to stimulate the self-interested customers to align their activities with the requirement of the entire system. So far, several related studies have been carried out, including the cost-benefit analysis [20], case studies in small systems [21] and preliminary transactive market designs [22]. However, most related research works only focus on the conceptual discussion without detailed designs. Therefore, the transactive energy system (TES) is still at its infancy stage and more efforts should be paid to build up a practical design. In addition, TE based framework is inherently a decentralized scheme, but most existing applications are carried out in a centralized manner. In this regard, decentralized or distributed approaches should be applied to implement TE based framework in practice.

On the other hand, there is a great need to create a competitive distribution market that enables active participation of the end-use customers to fully unlock the economic and technical values of DERs and controllable loads. In this market, customers have multiple choices other than buying/selling energy from/to the utility company. For instance, they are allowed to conduct bilateral energy trading with other customers. Nonetheless, it is likely that this market is not compatible with the distribution system operation since customers are self-interested and their selfish behaviors may give rise to the violation of system operation constraints, such as voltage violation. Previous works like [23–25] do not address this problem properly as they often overlook the impact on the system operation. Hence, it is necessary to deal with the market issues and the operation issues in a holistic manner. Since TE has the potential to resolve the conflict of interest, it is reasonable to apply the TE concept to the decentralized energy trading. However, to the best of the author's knowledge, few works have studied the decentralized energy trading under the TE framework. Therefore, further investigation is needed to create a competitive distribution market that integrates the TE concept.

Despite the economic and environmental benefits of the renewable DERs like rooftop PV systems, the proliferation of them also poses significant challenges to the distribution system operation due to their uncertain and intermittent nature. Specifically, the voltage variation will become more remarkable and frequent, which cannot be properly addressed by the approaches using the traditional voltage regulation devices, e.g. OLTC, voltage regulator and capacity bank. In the regard, the potential of PV inverters has been explored to provide voltage control by adjusting the active and reactive power output to some extent. Many studies [26–29] have been conducted focusing on the voltage control within the distribution networks (DNs) using the PV inverters. These studies can be categorized into three classes, namely the centralized control, decentralized control and distributed control. Under the centralized control, various PV systems are remotely controlled by a central controller who determines the dispatch result based on the collected operation information and issues the command to the individual PV systems. Such a scheme works effectively in dealing with the long-term operation, e.g. hourly dispatch. But it encounters significant challenges when addressing the real-time operation problem since it cannot respond to the fast variation of system condition timely. More importantly, the centralized scheme is not robust as it subjects to a single point failure. The decentralized scheme does not require mutual communication between any pair of entities. Each entity determines its power set-points merely based on the local measurements. A typical decentralized control scheme is the voltage-reactive power droop control. The decentralized control is robust against the component failure, but it often results in sub-optimality and sometimes instability due to lack of coordination [30]. The distributed scheme combines the merits of the centralized scheme and decentralized scheme and thus more appropriate for the real-time voltage regulation. Several distributed algorithms have been developed recently [31–33]. However, the voltage control algorithms in most works cannot be implemented online since the command can be applied only when the algorithms converge. Therefore, it is necessary to develop an online distributed voltage control algorithm in order to enhance the PV hosting capacity of a distribution system.

The widespread adoption PV systems will also cause significant load ramps during the sunrise and the sunset because of the diurnal pattern of solar PV energy [34]. Specifically, the PV generation is only available during daytime. When adding this effect to the net load, it would lead to a sharp decrease and steep increase of net load during the sunrise and the sunset, respectively. Typically, the magnitudes of these ramps are large but the durations are short. Thus, fast-start generators must be called on to follow the net load but it would inevitably cause considerable economic loss due to the high operation cost of these generators. Actually, the present ramping capability offered by the fast start resources is insufficient to resolve the ramping problem of the near future [35]. It is foreseen that the ramping effect will be increasingly severe in the next few years because of the rapid grow of renewable DERs. Moreover, the ramping effect in DNs will be translated into the transmission network and exacerbate the scarcity of ramping capability. But few works have yet studied the ramping problem in DNs. Therefore, it is necessary to develop effective approaches to mitigate the ramping effect in distribution networks using local resources like the distributed energy storage systems (ESSs). DESS is capable of storing the excess solar PV energy during the peak PV generation periods and releasing it during the peak-load periods. The recent advance in DESS, especially in the lithium-ion battery, paves a way for the implementation of the proposed approach [36].

Last but not least, the cloud movement will result in sudden change of PV power output, which is defined as PV ramp event (PRE). This ramp event will give rise to severe voltage violation without proper coordination between the conventional voltage regulation devices and smart PV inverters. Furthermore, the PV ramp events are hard to predict as they are chaotic. Therefore, effective measures should be taken to prevent the PV ramp event induced voltage violation.

1.3 Objectives and Primary Contributions

As discussed previously, the research on transactive energy based market design is till at its early stage. Moreover, the conventional approaches are unsuitable to address the emerging challenges introduced by the proliferation of DERs. In particular, the severe voltage violations and the shortage of ramping capability is threatening the reliability and security of the distribution system operation.

To fill these research gaps, the author developed advanced approaches for the active management of modernized distribution networks in the following four aspects. The main contributions are summarized as below.

1) A novel distributed transactive energy trading framework is developed with detailed designs to accommodate the high penetration of PV generations in

distribution networks. In particular, the bilateral energy trading among customers is seamlessly integrated with the optimal power flow (OPF) technique to ensure the trading outcome do not violate the system operation constraints. Besides, the Nash bargaining theory is employed to design a fair and competitive energy trading mechanism. Furthermore, an advanced distributed algorithm is developed based on the alternating direction method of multipliers (ADMM) to implement the proposed transactive energy trading framework. The optimality and the convergence of the proposed algorithm is guaranteed. Different from most ADMM based distributed algorithms that requires to solve the optimization subproblems iteratively, the author derives closed-form formulas for the update of variables to greatly enhance the computational efficiency.

2) The author develops a distributed online voltage control algorithm based on the dual ascent method considering PV curtailment. In the proposed algorithm, the active and reactive power (P-Q) set-points of different PV systems can be updated in a distributed manner based on local voltage measurements and communications between neighboring PV systems. Different from most existing works (e.g.[ref list]), the proposed distributed voltage control algorithm can be implemented online. That is, the results at each iteration can be applied directly to the PV systems for the voltage control. Therefore, the response rate is faster than that using conventional algorithms, where the voltage control cannot be implemented before the algorithms converge. Besides, the author derives a closed-form solution for the PV controllers to locally update P-Q set-points rather than iteratively solving subproblems. The convergence is established analytically and the optimality is guaranteed.

3) The author proposes a novel look-ahead dispatch model for the ramp minimization in an active distribution network. The fast-responding distributed energy storage systems (DESSs) are utilized to offset the ramp-up and ramp-down effects caused by diurnal generation pattern of PV systems. Model predictive control (MPC) method is used to carry out the proposed dispatch model, which

incorporates both current information and newly updated forecast information. Consequently, DESSs can be appropriately scheduled to avoid latent over-charging or over-discharging during some periods. The second-order cone (SOC) relaxed branch flow model is used to model the power flow in the distribution networks. Numerical results demonstrate that the proposed MPC based ramp minimization model can bring about significant reduction of ramping effect and line losses, i.e. more than 80% reduction of maximum ramp and roughly 50% reduction of line losses.

4) A coordinated dispatch model is proposed to eliminate the voltage violations induced by the PV ramp event (PRE). Specifically, the author models the PREs as an uncertainty set and formulates the intra-hour dispatch model as a two-stage robust optimization problem considering the coordination of OLTC and smart PV systems. In the first stage, maximum admissible PV outputs (MAPO) and the OLTC step position are co-optimized to reinforce the coordination, where MAPO is proposed to quantify the PV hosting capacity for the following one hour. In the second stage, the feasibility of the first stage decision variables is evaluated for any realization of PREs. The column-and-constraint generation (CCG) algorithm is utilized to solve the problem.

1.4 Outlines of the Thesis

The thesis is organized as follows. In Chapter 2, a novel distributed transactive energy framework is presented with detailed designs for the customers in distribution networks. In Chapter 3, a distributed online voltage control algorithm is developed for distribution networks with multiple PV systems based on dual ascent method. In Chapter 4, a model predictive control based look-ahead dispatch model is proposed for ramp minimization in distribution networks using DESSs. In Chapter 5, a two-stage robust optimization based intra-hour dispatch model is presented to alleviate the PRE induced voltage violations using OLTC and PV systems. In Chapter 6, the authors concludes this thesis and casts some ideas on the future works.

Chapter 2

Distributed Transactive Energy Trading Framework in Distribution Networks

2.1 Introduction

Transactive energy (TE) is a newly emerged concept aiming to address the economic and technical issues in power systems in a holistic manner. According to the Gridwise Architecture Council (GWAC), transactive energy system is defined as a set of mechanisms that use economic based instruments to achieve the dynamic balance between the generation and consumption while considering operation constraints of a power system [37]. It is a multi-agent system that enables active participation of customers to contribute to the enhancement of the system reliability, security and efficiency. There are several works related with transactive energy system. In [38], a transactive control strategy with a double-auction market is proposed for commercial buildings to coordinate the internal electric appliances. In [39], a transactive energy framework is presented for the decision making of virtual power plants. However, these works overlook the impact of TE on the power system operation. In [22], a day-ahead transactive market model is proposed for the distribution system operator (DSO) to manage the distribution level operation and to participate in the wholesale market. Nonetheless, it does not consider the P2P energy trading between customers. Ref.[20] conducts a cost-benefit analysis for the transactive energy sharing within a microgrid. Ref.[40] carries out a case study of the transactive energy trading in a distribution system. However, these works only focus on conceptual discussion and preliminary study without details. Up to now, the research on applying TE to distribution system operation is still at its very early stage.

Economic and system operating issues are two major concerns of a TE based framework. Current policies of most countries encourage self-consumption of solar PV energy so as to mitigate its adverse influence. But it is not preferable to PV prosumers who may have excess PV generation after meeting their own load especially during the peak irradiance period. In order to improve the economic benefit to PV prosumers and other consumers, some energy sharing and trading mechanisms have been developed in recent research works. Ref. [41] presents an energy sharing mechanism with an internal pricing model for prosumers within a microgrid. Ref. [42] investigates the interconnected microgrids and proposes a holistic model for energy scheduling and trading. Ref. [43] develops a distributed model for energy trading among multiple microgrids. In [44], a study on energy exchange is carried out using DC based interconnected nanogrids. There are also some works [45, 46] focusing on game-theoretic approach based energy trading in smart grid, which are summarized in [46]. Nevertheless, few existing works have dealt with the economic issues of energy trading and the technical issues of distribution system operation in a holistic way.

Traditionally, distribution systems are managed by distribution system operators in a centralized manner. However, with the proliferation of DERs and household automation products, it becomes challenging to centrally control customer-owned assets due to privacy concerns and complex communication and control requirements. In this regard, distributed operation and control has been extensively studied in recent research works [33, 47–50]. In [47], a distributed dispatch method is proposed based on primal-dual subgradient algorithm. In [48], an ADMM based distributed algorithm is developed for the optimal power flow (OPF) problem in distribution systems. In [33], a distributed method is used to optimize the active and reactive power set-points of DER inverters. In [49, 50], distributed approaches are applied to voltage regulation.

In this chapter, the author develops a transactive energy trading (TET) framework for customers considering the operating constraints of the distribution network. In particular, it seamlessly integrates the bilateral energy trading mechanism with the optimal power flow (OPF) technique. In order to preserve the autonomy and privacy of customers, the author develops a distributed algorithm with closed-form solutions to solve the transactive energy trading problem. The optimality of the energy trading is guaranteed using the proposed distributed algorithm.

The nomenclature of symbols used in this chapter is given as follows,

Indices and Set

$\mathcal{E}$	Distribution Line set
$\mathcal{N}$	Distribution node set
$t/\mathcal{T}$	Index and set of time slots
k	Iteration index

Parameters

$\underline{d}_{i,t}/\overline{d}_{i,t}$	Lower/Upper bound of agent i's load demand at time t
$D_{i,t}$	Preferred load demand of agent i at time t
E_i	Total required energy of agent i over the entire optimization horizon
$p^g_{i,t}$	Aggregated PV generation of agent i at time t
$q^d_{i,t}$	Reactive power demand of agent i at time t
$\underline{Q}_{i,t}/\overline{Q}_{i,t}$	Lower/Upper bound of reactive power output of agent i's PV system at time t
r_i/x_i	Resistance/Reactance of the ith line
$\underline{v}_i/\overline{v}_i$	Lower/Upper bound of the squared voltage magnitude at node i
α_i	Sensitivity of the agent i's discomfort cost to the demand deviation
γ	Iteration step size
λ^b_t/λ^s_t	Electricity price for buying/selling energy from/to the utility company at time t

Variables

$e_{ij,t}$	Energy amount agent i purchases from agent j at time t
$l_{i,t}$	Squared line current magnitude of line i at time t
$p^d_{i,t}$	Aggregated load demand of agent i at time t
$q^g_{i,t}$	Reactive power output of agent i's PV system at time t
$p_{i,t}/q_{i,t}$	Active/Reactive power injection at the ith node at time t
$P_{i,t}/Q_{i,t}$	Active/Reactive power flow on the ith line at time t
$v_{i,t}$	Squared voltage magnitude of node i at time t
ϕ_{ij}	Payment from agent i to agent j

2.2 System Model and Problem Formulation

In this section, the author designs a novel TET framework by integrating a Nash bargaining based bilateral energy trading mechanism with the OPF technique. Then, the author transforms the original problem into an equivalent two-stage problem.

2.2.1 System Model

Consider a distribution network $\mathcal{G} := (\mathcal{N}, \mathcal{E})$, where $\mathcal{N} := \{0, 1, \ldots, N\}$ represents the node set and $\mathcal{E}$ represents the line set. Each node except the substation node (indexed as 0) has a unique parent node A_i and a set of child nodes, denoted by C_i. It is assumed that each directed line points from a node i to its unique parent node A_i. Thus, the line from i to A_i can be uniquely labeled as i and the line set can be expressed as $\mathcal{E} := \{1, \ldots, N\}$. Given a radial distribution network, the branch flow model [51] can be used to represent the power flow equations as

$$v_{i,t} - v_{A_i,t} = 2(r_i P_{i,t} + x_i Q_{i,t}) - l_{i,t}(r_i^2 + x_i^2) \quad i \in \mathcal{E} \tag{2.1a}$$

$$\sum_{j \in C_i} (P_{j,t} - l_{j,t} r_j) + p_{i,t} = P_{i,t} \quad i \in \mathcal{N} \tag{2.1b}$$

$$\sum_{j \in C_i} (Q_{j,t} - l_{j,t} x_j) + q_{i,t} = Q_{i,t} \quad i \in \mathcal{N} \tag{2.1c}$$

$$l_{i,t} = \frac{P_{i,t}^2 + Q_{i,t}^2}{v_{i,t}} \quad i \in \mathcal{N} \tag{2.1d}$$

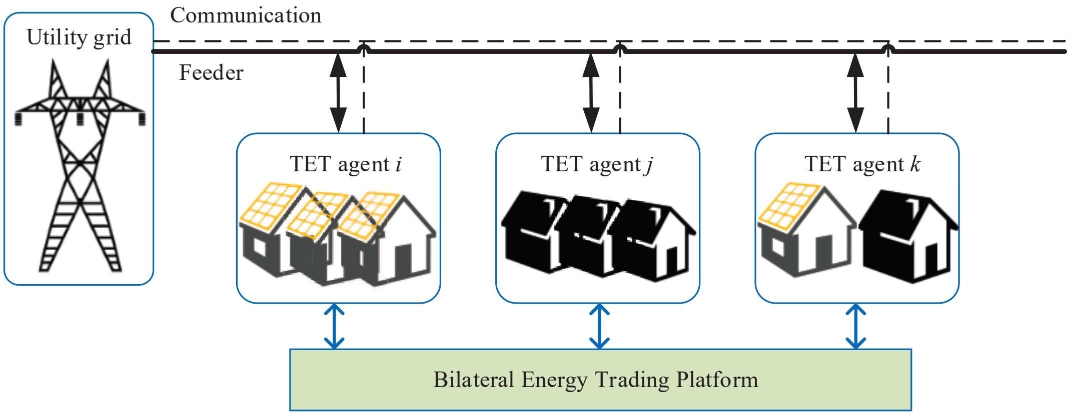

Fig. 2.1 Transactive energy trading framework in a distribution system

Note (2.1d) is nonconvex. Hence, the second order cone relaxtion from [51] will be applied to convexify it. Specifically, the equality constraint (2.1d) is first relaxed into an inequality constraint as (2.2) which is then reformulated into a second order cone (SOC) constraint as (2.3).

$$P_{i,t}^2 + Q_{i,t}^2 \leq v_{i,t} l_{i,t} \quad i \in \mathcal{N} \tag{2.2}$$

$$\|(2P_{i,t}, 2Q_{i,t}, l_{i,t} - v_{i,t})\| \leq l_{i,t} + v_{i,t} \tag{2.3}$$

Note that the SOC relaxation is generally exact for the radial distribution networks according to [51]. The numerical results also validate the exactness of the relaxation in this application.

2.2.2 TET Agent Model

For a better energy trading coordination, TET agent is introduced to represent the aggregation of customers on the same node as illustrated in Fig. 2.1, where the solid black line represents the distribution feeder line and the dashed black line represents communication line. It is entrusted to fulfil the energy management and trading on behalf of the local customers. Besides, the TET agent is also responsible for maintaining the reliable and secure operation of the entire distribution system together with other TET agents.

It is assumed that each agent has some flexible demand. For simplicity, only the aggregated demand of each agent i is modelled, denoted as $p^d_{i,t}$, without considering the detailed composition of the demand. The aggregated demand is simply termed as the demand in the rest of this chapter. Thus, each demand subjects to

$$\underline{d}_{i,t} \leq p^d_{i,t} \leq \overline{d}_{i,t} \quad t \in \mathcal{T} \tag{2.4}$$

$$\sum_{t \in \mathcal{T}} p^d_{i,t} \geq E_i \tag{2.5}$$

Each agent can schedule its demand across time as long as it satisfies (2.4) and (2.5). Nevertheless, the deviation from the preferred value will incur discomfort cost that is defined as

$$C^{dis}_{i,t}(p^d_{i,t}) = \alpha_i \left(p^d_{i,t} - D_{i,t}\right)^2 \quad t \in \mathcal{T} \tag{2.6}$$

It is assumed that each PV system operates at the maximum power point so as to harvest as much solar energy as possible. Thus, the aggregated PV generation of agent i, denoted as $p^g_{i,t}$, is a predicted parameter. Note if agent i does not have PV installations, then $p^g_{i,t}$ is simply set as 0. In addition, the PV reactive power of agent i, denoted as $q^g_{i,t}$, is adjustable and subjects to

$$\underline{Q}_{i,t} \leq q^g_{i,t} \leq \overline{Q}_{i,t} \tag{2.7}$$

where $\underline{Q}_{i,t} = -\overline{Q}_{i,t}$ and $\overline{Q}_{i,t} = \min\left(\sqrt{S_i^2 - (p^g_{i,t})^2},\ p^g_{i,t} \times tan\theta\right)$; S_i is the rated apparent power of the PV system and θ denotes the power factor angle associated with the minimum allowed power factor.

2.2.3 Bilateral Energy Trading and Payoff Function

Bilateral energy trading

Let $e_{ij,t}$ denote the energy amount that agent i purchases from agent j in time slot t. Then, the consensus on the amount of bilateral energy trading can be expressed as

$$e_{ij,t} = -e_{ji,t} \quad i \in \mathcal{N},\ j \in \mathcal{N} \backslash i,\ t \in \mathcal{T} \tag{2.8}$$

It is assumed that the payment between each pair of agents is settled at the end of the entire optimization horizon. Let ϕ_{ij} denote the payment from agent i to agent j. Then, the consensus on payment is expressed as

$$\phi_{ij} = -\phi_{ji} \quad i \in \mathcal{N},\ j \in \mathcal{N} \backslash i \tag{2.9}$$

Hence, the total payment of agent i to other agents can be written as

$$\Phi_i(\boldsymbol{\phi}_i) = \sum_{j \in \mathcal{N} \backslash i} \phi_{ij} \tag{2.10}$$

where $\boldsymbol{\phi}_i$ is the vector of $\{\phi_{ij} | j \in \mathcal{N} \backslash i\}$.

Payoff function

The payoff function of each agent i is defined as the cost reduction arising from TET. Hence, the cost functions without and with TET should be introduced first. The cost without TET is composed of the utility bill and the discomfort cost, that is

$$\widetilde{C}_i(\mathbf{p}_i^d) = \sum_{t \in \mathcal{T}} \left(\widetilde{B}_{i,t}(p_{i,t}^d) + C_{i,t}^{dis}(p_{i,t}^d) \right) \tag{2.11}$$

where $\mathbf{p}_i^d$ is the vector of $\{p_{i,t}^d | t \in \mathcal{T}\}$ and $\widetilde{B}_{i,t}(p_{i,t}^d)$ is the utility bill without TET defined as

$$\widetilde{B}_{i,t}(p_{i,t}^d) = \lambda_t^b \left[p_{i,t}^d - p_{i,t}^g \right]^+ - \lambda_t^s \left[p_{i,t}^g - p_{i,t}^d \right]^+ \tag{2.12}$$

where $[\cdot]^+$ denotes the projection operator onto the non-negative orthant, i.e. $[x]^+ = \max(x, 0)$; λ_t^b denotes the electricity price in the retail market which is typically set at a fixed level by the utility company; and λ_t^s denotes the feed-in tariff. Generally, λ_t^b is considerably higher than λ_t^s [41].

The cost with TET consists of the utility bill, the discomfort cost and the payment to other agents, that is

$$C_i(\mathbf{p}_i^d, \mathbf{e}_i, \boldsymbol{\phi}_i) = \sum_{t \in \mathcal{T}} \left(B_{i,t}(p_{i,t}^d, e_{ij,t}) + C_{i,t}^{dis}(p_{i,t}^d) \right) + \Phi_i(\boldsymbol{\phi}_i) \tag{2.13}$$

where $\mathbf{e}_i$ is the vector of $\{e_{ij,t}|\forall j \in \mathcal{N}\backslash i,\ \forall t \in \mathcal{T}\}$ and $B_{i,t}(p_{i,t}^d, e_{ij,t})$ is the utility bill with TET, which is written as

$$B_{i,t}(p_{i,t}^d, e_{ij,t}) = \lambda_t^b \Delta_{i,t}^+ - \lambda_t^s \Delta_{i,t}^- \tag{2.14}$$

where $\Delta_{i,t}^+ = \left[p_{i,t}^d - p_{i,t}^g - \sum_{j\in\mathcal{N}\backslash i} e_{ij,t}\right]^+$ and $\Delta_{i,t}^- = \left[p_{i,t}^g - p_{i,t}^d + \sum_{j\in\mathcal{N}\backslash i} e_{ij,t}\right]^+$, represent the energy extraction/injection from/to the utility company, respectively,

Therefore, the payoff function for each agent i is defined as

$$\begin{aligned} U_i(\mathbf{p}_i^d, \mathbf{e}_i, \boldsymbol{\phi}_i) &= \widetilde{C}_i(\tilde{\mathbf{p}}_i^d) - C_i(\mathbf{p}_i^d, \mathbf{e}_i, \boldsymbol{\phi}_i) \\ &= \widetilde{C}_i(\tilde{\mathbf{p}}_i^d) - W_i(\mathbf{p}_i^d, \mathbf{e}_i) - \Phi_i(\boldsymbol{\phi}_i) \end{aligned} \tag{2.15}$$

where $W_i(\mathbf{p}_i^d, \mathbf{e}_i) := \sum_{t\in\mathcal{T}} \left(B_{i,t}(p_{i,t}^d, e_{ij,t}) + C_{i,t}^{dis}(p_{i,t}^d)\right)$, and $\tilde{\mathbf{p}}_i^d$ is the optimal solution to the following problem.

$$\min_{\mathbf{p}_i^d} \quad \widetilde{C}_i(\mathbf{p}_i^d) \tag{2.16a}$$

$$\text{s.t.} \quad \underline{d}_{i,t} \leq p_{i,t}^d \leq \overline{d}_{i,t} \qquad t \in \mathcal{T} \tag{2.16b}$$

$$\sum_{t\in\mathcal{T}} p_{i,t}^d \geq E_i \tag{2.16c}$$

Due to (2.10), it can be derived that the sum of individual payoff equals to the overall social cost reduction, i.e.

$$\sum_{i\in\mathcal{N}} U_i(\mathbf{p}_i^d, \mathbf{e}_i, \boldsymbol{\phi}_i) = \sum_{i\in\mathcal{N}} \widetilde{C}_i(\tilde{\mathbf{p}}_i^d) - \sum_{i\in\mathcal{N}} W_i(\mathbf{p}_i^d, \mathbf{e}_i) \tag{2.17}$$

2.2.4 Nash Bargaining based Transactive Energy Trading

The transactive energy trading problem is modelled as a Nash bargaining problem as it is often used to determine a fair allocation of a total surplus among multiple players. Moreover, the Nash bargaining solution satisfies the following four axioms: invariant to affine transformation, Pareto optimality, independent of irrelevant alternatives, and symmetric [52]. Thus, the TET problem is formulated as (2.18) by taking system operating constraints into account.

$$\max \ \prod_{i=1}^{N} U_i(\mathbf{p}_i^d, \mathbf{e}_i, \boldsymbol{\phi}_i) \tag{2.18a}$$

$$\text{over } p_{i,t}^d, q_{i,t}^g, e_{ij,t}, \phi_{ij}, p_{i,t}, q_{i,t}, P_{i,t}, Q_{i,t}, l_{i,t}, v_{i,t}$$

$$\text{s.t. } (2.4), (2.5) \text{ and } (2.7) \tag{2.18b}$$

$$(2.8) \text{ and } (2.9) \tag{2.18c}$$

$$(2.1a)\text{-}(2.1c) \text{ and } (2.2) \tag{2.18d}$$

$$p_{i,t} = p_{i,t}^g - p_{i,t}^d \quad i \in \mathcal{N} \backslash 0, \ t \in \mathcal{T} \tag{2.18e}$$

$$q_{i,t} = q_{i,t}^g - q_{i,t}^d \quad i \in \mathcal{N} \backslash 0, \ t \in \mathcal{T} \tag{2.18f}$$

$$\underline{v}_i \le v_{i,t} \le \overline{v}_i \quad i \in \mathcal{N}, \ t \in \mathcal{T} \tag{2.18g}$$

where (2.18b) summarizes local scheduling constraints for each agent; (2.18c) is associated with bilateral energy trading; (2.18d)-(2.18f) are power flow equations and (2.18g) is voltage constraints. It can be observed from (2.17) that the optimal solution to (2.18) also minimizes the total operating cost with TET, i.e. $\sum_{i \in \mathcal{N}} W_i(\mathbf{p}_i^d, \mathbf{e}_i)$; otherwise, some agents can be better off due to the improvement of the total cost reduction while keeping the other agents' payoffs unchanged. Therefore, the following theorem can be obtained.

Theorem 1 *The proposed TET problem (2.18) is equivalent to the following two-stage problem, where the first stage problem **S1** solves the optimal energy trading along with system dispatch and the second stage problem **S2** solves the corresponding optimal bilateral payment.*

S1: multi-period OPF problem

$$\min \ \sum_{i \in \mathcal{N}} W_i(\mathbf{p}_i^d, \mathbf{e}_i)$$

$$\text{over } p_{i,t}^d, q_{i,t}^g, e_{ij,t}, p_{i,t}, q_{i,t}, P_{i,t}, Q_{i,t}, l_{i,t}, v_{i,t}$$

$$\text{s.t. } (2.1a)\text{-}(2.1c), (2.2)\text{-}(2.5), (2.7), (2.8), (2.18e)\text{-}(2.18g)$$

S2: payment bargaining problem

$$\max_{\phi_{ij}} \prod_{i=1}^{N} \left(\widetilde{C}_i(\widetilde{\mathbf{p}}_i^d) - W_i(\mathbf{p}_i^{d*}, \mathbf{e}_i^*) - \Phi_i(\boldsymbol{\phi}_i)\right)$$
$$\text{s.t. } (2.9)$$

where $(\mathbf{p}_i^{d*}, \mathbf{e}_i^*)$ is the optimal solution to **S1**.

Due to the convexity, both **S1** and **S2** can be solved in a centralized fashion by cutting-edge solvers. However, the centralized optimization requires the complete information of the entire system, which violates the privacy of individual TET agent. In this regard, a distributed algorithm for TET problem is needed, which is introduced in the next section.

2.3 Distributed Algorithm for TET Problem

In this section, an ADMM based distributed algorithm is developed for solving the two-stage TET problem. Firstly, the multi-period OPF problem **S1** is decoupled into multiple single-period OPF subproblems using Lagrangian relaxation. Then, a distributed algorithm is developed for the single-period subproblem by employing a recent proposed distributed OPF technique [48]. Subsequently, the distributed algorithm is also used to solve the second stage problem **S2**. Furthermore, closed form solutions are derived to the optimization subproblems of **S1** and **S2**, which greatly speeds up each iteration.

2.3.1 Decoupling of Temporally Coupled Constraint

In **S1**, the constraint (2.5) couples the decision variables of all time slots, which inhibits **S1** to be solved separately at each time slot. Hence, **S1** is reformulated by relaxing (2.5). Let π_i, $\mathbf{y}_t := \{p_{i,t}^d, q_{i,t}^g, e_{ij,t}, p_{i,t}, q_{i,t}, P_{i,t}, Q_{i,t}, l_{i,t}, v_{i,t} | i \in \mathcal{N}\}$ and $\mathcal{Y}_t$ denote the Lagrangian multiplier for (2.5), the vector composed of the variables of **S1** at time slot t and the feasible region of $\mathbf{y}_t$, respectively. Then, the Lagrangian of

S1 is given as

$$\begin{aligned} L &= \sum_{i\in\mathcal{N}} W_i(\mathbf{p}_i^d, \mathbf{e}_i) + \sum_{i\in\mathcal{N}} \pi_i(E_i - \sum_{t\in\mathcal{T}} p_{i,t}^d) \\ &= \sum_{t\in\mathcal{T}} L_t(\mathbf{y}_t, \boldsymbol{\pi}) + \sum_{i\in\mathcal{N}} E_i\pi_i \end{aligned} \tag{2.21}$$

where $L_t(\mathbf{y}_t, \boldsymbol{\pi}) := \sum_{i\in\mathcal{N}} \Big(B_{i,t}(p_{i,t}^d, e_{ij,t}) + C_{i,t}^{dis}(p_{i,t}^d) - \pi_i p_{i,t}^d\Big)$, and $\boldsymbol{\pi}$ is a vector consisting of all π_i.

The strong duality holds for problem **S1** according to Slater's condition [71]. Hence, there is zero duality gap between problem **S1** and its dual problem **S1′** as shown below, which means the transformation of the problem is accurate.

$$\textbf{S1}'\textbf{:} \qquad \max_{\boldsymbol{\pi}\geq\mathbf{0}} \sum_{t\in\mathcal{T}} \Big(\min_{\mathbf{y}_t\in\mathcal{Y}_t} L_t(\mathbf{y}_t, \boldsymbol{\pi})\Big) + \sum_{i\in\mathcal{N}} E_i\pi_i$$

Note that the inner level problem is decoupled into multiple single-period optimization subproblems that can be solved in parallel. Next, the subscript t is dropped for conciseness and the single-period subproblem is formulated as

$$\min \sum_{i\in\mathcal{N}} \Big(B_{i,t}(p_i^d, e_{ij}) + C_{i,t}^{dis}(p_i^d) - \pi_i p_i^d\Big) \tag{2.22a}$$

$$\text{over } \{p_i^d, q_i^g, e_{ij}, p_i, q_i, P_i, Q_i, l_i, v_i | i \in \mathcal{N}\}$$

$$\text{s.t. (2.1a)-(2.1c), (2.2), (2.4), (2.7), (2.8), (2.18e)-(2.18g)} \tag{2.22b}$$

Suppose for a given $\boldsymbol{\pi}^k$, the optimal solution of (2.22) can be obtained for each time slot t, denoted as $p_{i,t}^{d,k}$. Then dual ascent method [53] can be used to solve **S1′** with the Lagrangian multiplier π_i being iteratively updated as

$$\pi_i^{k+1} = \Big[\pi_i^k + \gamma\Big(E_i - \sum_{t\in\mathcal{T}} p_{i,t}^{d,k}\Big)\Big]^+ \tag{2.23}$$

However, the major challenge lies in the calculation of $\mathbf{y}_t$ since the centralized method is impractical for (2.22) due to privacy concern. Therefore, a distributed algorithm will be developed in the following subsection.

2.3.2 Distributed Algorithm for Single-period OPF Problem

Due to the strong coupling between each agent's decision variables $\mathbf{x}_i := \Big\{p_i, q_i, P_i, Q_i, l_i, v_i, \{e_{ij} | j \in \mathcal{N} \backslash i\}\Big\}$ with those of others, ADMM cannot be directly applied to (2.22). Thus, problem (2.22) should be reformulated into a problem with a decomposable structure. Toward this end, a set of auxiliary variables $\mathbf{z}_{j(i)}$ is introduced that is constituted by the duplicate of relevant elements of $\mathbf{x}_j$. $\mathbf{z}_{j(i)}$ can be visualized as agent i's observation of agent j's partial information contained in $\mathbf{x}_j$. In this application, $\mathbf{z}_{j(i)}$ is explicitly defined as

$$\mathbf{z}_{j(i)} := \begin{cases} \Big(p^z_{i(i)}, q^z_{i(i)}, P^z_{i(i)}, Q^z_{i(i)}, l^z_{i(i)}, v^z_{i(i)}, \{e^z_{ik(i)} | k \in \mathcal{N} \backslash i\}\Big) & j = i \\ \Big(P^z_{j(i)}, Q^z_{j(i)}, l^z_{j(i)}, e^z_{ji(i)}\Big) & j \in C_i \\ \Big(v^z_{j(i)}, e^z_{ji(i)}\Big) & j = A_i \\ \Big(e^z_{ji(i)}\Big) & \text{otherwise} \end{cases} \tag{2.24}$$

where the superscript z is used to indicate the auxiliary variables. Then, (2.22) is reformulated as the problem below.

$$\min_{\mathbf{x},\mathbf{z}} \sum_{i \in \mathcal{N}} f_i(\mathbf{x}_i) \tag{2.25a}$$

$$\text{s.t. } v^z_{i(i)} - v^z_{A_i(i)} = 2(r_i P^z_{i(i)} + x_i Q^z_{i(i)}) - l^z_{i(i)}(r_i^2 + x_i^2) \qquad i \in \mathcal{N} \backslash 0 \tag{2.25b}$$

$$\sum_{j \in C_i} (P^z_{j(i)} - l^z_{j(i)} r_j) + p^z_{i(i)} = P^z_{i(i)} \qquad i \in \mathcal{N} \tag{2.25c}$$

$$\sum_{j \in C_i} (Q^z_{j(i)} - l^z_{j(i)} x_j) + q^z_{i(i)} = Q^z_{i(i)} \qquad i \in \mathcal{N} \tag{2.25d}$$

$$e^z_{ij(i)} = -e^z_{ji(i)} \qquad j \in \mathcal{N} \backslash i,\ i \in \mathcal{N} \tag{2.25e}$$

$$(P^x_i)^2 + (Q^x_i)^2 \le l^x_i v^x_i \qquad i \in \mathcal{N} \tag{2.25f}$$

$$\underline{v}_i \le v^x_i \le \overline{v}_i \qquad i \in \mathcal{N} \tag{2.25g}$$

$$\underline{p}_i \le p^x_i \le \overline{p}_i \qquad i \in \mathcal{N} \tag{2.25h}$$

$$\underline{q}_i \le q^x_i \le \overline{q}_i \qquad i \in \mathcal{N} \tag{2.25i}$$

$$\mathbf{x}_j - \mathbf{z}_{j(i)} = 0 \qquad j \in \mathcal{N},\ i \in \mathcal{N} \tag{2.25j}$$

where the variables with superscript x correspond to the original decision variables; $\mathbf{x} := \{\mathbf{x}_i | i \in \mathcal{N}\}$ and $\mathbf{z} := \{\mathbf{z}_{j(i)} | j \in \mathcal{N}, i \in \mathcal{N}\}$; $f_i(\mathbf{x}_i) = \lambda^b[-p_i^x - \sum_{j\in\mathcal{N}\setminus i} e_{ij}^x]^+ - \lambda^s[p_i^x + \sum_{j\in\mathcal{N}\setminus i} e_{ij}^x]^+ + \alpha_i(p_i^x - p_i^g + D_i)^2 + \pi_i p_i^x$; (2.25h) and (2.25i) are reduced from (2.4), (2.7), (2.18e) and (2.18f); $\underline{p}_i$, $\overline{p}_i$, $\underline{q}_i$ and $\overline{q}_i$ are parameters derived from (2.4), (2.7), (2.18e) and (2.18f). The consensus constraint (2.25j) is enforced to ensure the equivalence between (2.22) and (2.25). It is written explicitly as below with a slight abuse of notations.

$$0 = \mathbf{x}_j - \mathbf{z}_{j(i)} := \begin{cases} \Big(p_i^x - p_{i(i)}^z, q_i^x - q_{i(i)}^z, P_i^x - P_{i(i)}^z, Q_i^x - Q_{i(i)}^z, \\ \quad l_i^x - l_{i(i)}^z, v_i^x - v_{i(i)}^z, \{e_{ik}^x - e_{ik(i)}^z | k \in \mathcal{N}\setminus i\}\Big) & j = i \\ \Big(P_j^x - P_{j(i)}^z, Q_j^x - Q_{j(i)}^z, l_j^x - l_{j(i)}^z, e_{ji}^x - e_{ji(i)}^z\Big) & j \in C_i \\ \Big(v_j^x - v_{j(i)}^z, e_{ji}^x - e_{ji(i)}^z\Big) & j = A_i \\ \Big(e_{ji}^x - e_{ji(i)}^z\Big) & \text{otherwise} \end{cases}$$

For mathematical conciseness, (2.25) can be written compactly as the problem below.

$$\min_{\mathbf{x},\mathbf{z}} \quad \sum_{i\in\mathcal{N}} f_i(\mathbf{x}_i) \tag{2.26a}$$

$$\text{s.t.} \quad \sum_{j\in\mathcal{N}} \mathbf{A}_{ij}\mathbf{z}_{j(i)} = 0 \qquad i \in \mathcal{N} \tag{2.26b}$$

$$\mathbf{x}_i \in \mathcal{X}_i \qquad i \in \mathcal{N} \tag{2.26c}$$

$$\mathbf{x}_j - \mathbf{z}_{j(i)} = 0 \qquad j \in \mathcal{N},\ i \in \mathcal{N} \tag{2.26d}$$

where $\mathbf{A}_{ij}$ is a constant matrix and $\mathcal{X}_i$ is a convex set. (2.26b) summarizes (2.25b)-(2.25e), and (2.26c) summarizes (2.25f)-(2.25i).

Then, the author applies the consensus version of ADMM [53] to (2.26) by relaxing (2.26d). Denote the Lagrangian multipliers for (2.26d) as $\boldsymbol{\mu}_{j(i)}$. For a given penalty parameter $\rho > 0$, the augmented Lagrangian is defined as

$$\begin{aligned} \mathcal{L}_\rho(\mathbf{x}, \mathbf{z}, \boldsymbol{\mu}) &= \sum_{i\in\mathcal{N}} \mathcal{L}_{\rho,i}^x\Big(\mathbf{x}_i, \{\mathbf{z}_{i(j)}, \boldsymbol{\mu}_{i(j)} | j \in \mathcal{N}\}\Big) \\ &= \sum_{i\in\mathcal{N}} \mathcal{L}_{\rho,i}^z\Big(\{\mathbf{x}_j, \mathbf{z}_{j(i)}, \boldsymbol{\mu}_{j(i)} | j \in \mathcal{N}\}\Big) \end{aligned} \tag{2.27}$$

where

$$\mathcal{L}^{x}_{\rho,i}\Big(\mathbf{x}_i,\{\mathbf{z}_{i(j)},\boldsymbol{\mu}_{i(j)}|j\in\mathcal{N}\}\Big) :=f_i(\mathbf{x}_i)+\sum_{j\in\mathcal{N}}\Big(\langle\boldsymbol{\mu}_{i(j)},\mathbf{x}_i-\mathbf{z}_{i(j)}\rangle+\frac{\rho}{2}\|\mathbf{x}_i-\mathbf{z}_{i(j)}\|^2\Big)$$
$$\mathcal{L}^{z}_{\rho,i}\Big(\{\mathbf{x}_j,\mathbf{z}_{j(i)},\boldsymbol{\mu}_{j(i)}|j\in\mathcal{N}\}\Big) :=f_i(\mathbf{x}_i)+\sum_{j\in\mathcal{N}}\Big(\langle\boldsymbol{\mu}_{j(i)},\mathbf{x}_j-\mathbf{z}_{j(i)}\rangle+\frac{\rho}{2}\|\mathbf{x}_j-\mathbf{z}_{j(i)}\|^2\Big)$$

where $\langle\cdot,\cdot\rangle$ denotes the operation of inner product.

The basic idea of ADMM for solving (2.26) is to cyclically minimize its augmented Lagrangian $\mathcal{L}_\rho(\mathbf{x},\mathbf{z},\boldsymbol{\mu})$ over one of the three categories of variables, $\mathbf{x},\mathbf{z}$ and $\boldsymbol{\mu}$, while fixing the other two. Owing to decomposability of the Lagrangian $\mathcal{L}_\rho(\mathbf{x},\mathbf{y},\boldsymbol{\mu})$ as well as the constraints (2.26b) and (2.26c), the update of each category of variables can be executed in a distributed manner by solving the local subproblems of each agent. At each iteration k, the ADMM based distributed algorithm consists of the following three steps.

(**A1**) Upon receiving the latest updated $\mathbf{z}^k_{i(j)}$ and $\boldsymbol{\mu}^k_{i(j)}$ from others, each agent i updates $\mathbf{x}_i$ as (2.28) and sends relevant elements of $\mathbf{x}_i$ to others.

$$\mathbf{x}^{k+1}_i := \operatorname*{arg\,min}_{\mathbf{x}_i\in\mathcal{X}_i}\ \mathcal{L}^{x}_{\rho,i}\Big(\mathbf{x}_i,\{\mathbf{z}^k_{i(j)},\boldsymbol{\mu}^k_{i(j)}|j\in\mathcal{N}\}\Big) \tag{2.28}$$

(**A2**) Upon receiving the relevant elements of the latest updated $\mathbf{x}^{k+1}_j$ from others, each agent i updates $\mathbf{z}_{j(i)}$ as (2.29) and sends $\mathbf{z}_{j(i)}$ to agent j.

$$\mathbf{z}^{k+1}_{(i)} := \operatorname*{arg\,min}_{\mathbf{z}_{(i)}\in\mathcal{Z}_i}\ \mathcal{L}^{z}_{\rho,i}\Big(\{\mathbf{x}^{k+1}_j,\mathbf{z}_{j(i)},\boldsymbol{\mu}^k_{j(i)}|j\in\mathcal{N}\}\Big) \tag{2.29}$$

where $\mathbf{z}_{(i)} := \{\mathbf{z}_{j(i)}|j\in\mathcal{N}\}$ and $\mathcal{Z}_i := \{\mathbf{z}_{(i)}|\sum_{j\in\mathcal{N}}\mathbf{A}_{ij}\mathbf{z}_{j(i)}=0\}$.

(**A3**) Each agent i updates $\boldsymbol{\mu}_{j(i)}$ as (2.30) and sends it to agent j.

$$\boldsymbol{\mu}^{k+1}_{j(i)} := \boldsymbol{\mu}^k_{j(i)}+\rho(\mathbf{x}^{k+1}_j-\mathbf{z}^{k+1}_{j(i)})\quad j\in\mathcal{N} \tag{2.30}$$

The convergence of the above iterations to the optimal solution of (2.26) is guaranteed according to [48]. The termination condition is given as

$$r^k \leq \varepsilon, \quad s^k \leq \varepsilon \tag{2.31}$$

where $r^k := \|\mathbf{x}^k - \mathbf{z}^k\|$ denotes the primal residue, $s^k := \rho\|\mathbf{z}^k - \mathbf{z}^{k-1}\|$ denotes the dual residue, and ε is the tolerance.

Proposition 1 *At each iteration k*

(a) The subproblem (2.28) for updating $\mathbf{x}_i$ can be solved by each agent i with closed form solution.

(b) The subproblem (2.29) for updating $\mathbf{z}_{(i)} := \{\mathbf{z}_{j(i)} | j \in \mathcal{N}\}$ can be solved by each agent i with closed form solution.

Proof 1 *The proof of (a) is deferred to Appendix A.*

The proof of (b) is given as follows. (2.29) can be reformulated as

$$\min_{\mathbf{z}_{(i)}} \; G_i(\mathbf{z}_{(i)}) \tag{2.32a}$$

$$s.t. \; \sum_{j \in \mathcal{N}} \mathbf{A}_{ij} \mathbf{z}_{j(i)} = 0 \tag{2.32b}$$

where $G_i(\mathbf{z}_{(i)}) = \sum_{j \in \mathcal{N}} \Big(- \langle \boldsymbol{\mu}_{j(i)}, \mathbf{z}_{j(i)} \rangle + \frac{\rho}{2}\|\mathbf{x}_j - \mathbf{z}_{j(i)}\|^2 \Big)$. Since (2.32) is a convex quadratic optimization problem with linear equality constraints, it can be generalized as

$$\min_{\mathbf{z}_{(i)}} \; \frac{1}{2}\mathbf{z}_{(i)}^T \mathbf{Q} \mathbf{z}_{(i)} + \mathbf{c}^T \mathbf{z}_{(i)} \tag{2.33a}$$

$$s.t. \; \mathbf{B}\mathbf{z}_{(i)} = 0 \tag{2.33b}$$

where $\mathbf{Q}$ and $\mathbf{B}$ are constant matrices, and $\mathbf{c}$ is a constant vector. (2.33) has a unique solution that can be expressed as

$$\mathbf{z}_{(i)} = \Big(\mathbf{Q}^{-1}\mathbf{B}^T(\mathbf{B}\mathbf{Q}^{-1}\mathbf{B}^T)^{-1}\mathbf{B}\boldsymbol{Q}^{-1} - \mathbf{Q}^{-1} \Big)\mathbf{c} \tag{2.34}$$

Q.E.D.

2.3.3 Distributed Algorithm for Problem S2

In order to apply the aforementioned consensus version of ADMM, **S2** is also reformulated with the same technique. Here, the original decision variables $\mathbf{x}'_i$ and auxiliary variables $\mathbf{z}'_{j(i)}$ for each agent i are defined as

$$\mathbf{x}'_i := \{\phi^x_{ij} | j \in \mathcal{N}\backslash i\} \tag{2.35}$$

$$\mathbf{z}'_{j(i)} := \begin{cases} \{\phi^z_{ik(i)} | k \in \mathcal{N}\backslash i\} & j = i \\ \phi^z_{ji(i)} & \text{otherwise} \end{cases} \tag{2.36}$$

Then, **S2** is reformulated as the problem below by taking log of the objective function.

$$\min_{\mathbf{x}', \mathbf{z}'} \sum_{i \in \mathcal{N}} -\ln\Big(\theta_i - \sum_{j \in \mathcal{N}\backslash i} \phi^x_{ij}\Big) \tag{2.37a}$$

$$\text{s.t. } \phi^z_{ij(i)} = -\phi^z_{ji(i)} \quad j \in \mathcal{N}\backslash i, \ i \in \mathcal{N} \tag{2.37b}$$

$$\phi^z_{ij(i)} - \phi^x_{ij} = 0 \quad j \in \mathcal{N}\backslash i, \ i \in \mathcal{N} \tag{2.37c}$$

$$\phi^z_{ji(i)} - \phi^x_{ji} = 0 \quad j \in \mathcal{N}\backslash i, \ i \in \mathcal{N} \tag{2.37d}$$

where $\mathbf{x}' := \{\mathbf{x}'_i | i \in \mathcal{N}\}$ and $\mathbf{z}' := \{\mathbf{z}'_{j(i)} | j \in \mathcal{N}, i \in \mathcal{N}\}$; $\theta_i = \widetilde{C}_i(\tilde{\mathbf{p}}^d_i) - W_i(\mathbf{p}^{d*}_i, \mathbf{e}^*_i)$ is a parameter; (2.37c) and (2.37d) are the consensus constraints.

Note that problem (2.37) can also be written into the compact form as (2.26) by replacing $\mathbf{x}_i$ and $\mathbf{z}_{j(i)}$ with $\mathbf{x}'_i$ and $\mathbf{z}'_{j(i)}$, respectively. $f_i(\mathbf{x}'_i)$ is changed to $f_i(\mathbf{x}'_i) := -\ln\Big(\theta_i - \sum_{j \in \mathcal{N}\backslash i} \phi^x_{ij}\Big)$ and (2.26c) is removed. Therefore, the following proposition can be derived.

Proposition 2

*(a) Problem (2.37) can be solved in a distributed manner through the iterative process given by (**A1**)-(**A3**).*

*(b) The problem for updating $\mathbf{x}'_i := \{\phi^x_{ij} | j \in \mathcal{N}\backslash i\}$ shown in (**A1**) can be solved by each agent i in closed form.*

Algorithm 1: Distributed Algorithm for TET Problem

Stage 1: Solve $\mathbf{S1}'$.
Initialize all $\mathbf{z}_{j(i),t}$, $\boldsymbol{\mu}_{j(i),t}$ and π_i. Set the inner and outer loop tolerance levels, ε_1 and ε_2. Initialize the iteration indices, $k = 0$ and $m = 0$;
repeat
  for $t = 1$ **to** T **do**
    while $\|\mathbf{x}_t^k - \mathbf{z}_t^k\| > \varepsilon_1$ **or** $\rho\|\mathbf{z}_t^k - \mathbf{z}_t^{k-1}\| > \varepsilon_1$ **do**
      Each agent i updates $\mathbf{x}_{i,t}$ according to (2.28);
      Each agent i updates $\mathbf{z}_{j(i),t}$ according to (2.29);
      Each agent i updates $\boldsymbol{\mu}_{j(i),t}$ according to (2.30);
      Update inner loop iteration index $k = k + 1$;
    end
  end
  Each agent i updates π_i according to (2.23);
  Update outer loop iteration index $m = m + 1$;
until $\|\boldsymbol{\pi}^m - \boldsymbol{\pi}^{m-1}\| \leq \varepsilon_2$;
Stage 2: Solve $\mathbf{S2}$.
Initialize all $\mathbf{z}'_{j(i)}$ and $\boldsymbol{\mu}'_{j(i)}$. Set the tolerance level ε. Initialize the iteration index $k = 0$;
while $\|\mathbf{x}'^{,k} - \mathbf{z}'^{,k}\| > \varepsilon$ **or** $\rho\|\mathbf{z}'^{,k} - \mathbf{z}'^{,k-1}\| > \varepsilon$ **do**
  Each agent i update $\mathbf{x}'_i$ similarly as (2.28);
  Each agent i update $\mathbf{z}'_{j(i)}$ similarly as (2.29);
  Each agent i update $\boldsymbol{\mu}_{j(i)}$ as $\boldsymbol{\mu}'^{,k}_{j(i)} = \boldsymbol{\mu}'^{,k-1}_{j(i)} + \rho(\mathbf{x}'^{,k}_j - \mathbf{z}'^{,k}_{j(i)})$;
  Update iteration index $k = k + 1$;
end

(c) The problem for updating of $\mathbf{z}'_{j(i)}$ *shown in (**A2**) can be solved by each agent i in closed form.*

Proof 2 *The proof of (a) and (c) is evident just by going through the steps described by (**A1**)-(**A3**). The proof of (b) is given in Appendix A.* ***Q.E.D.***

2.3.4 Implementation

Algorithm 1 summarizes the overall distributed algorithm for solving the transactive energy trading problem, where the outer and inner loops in **Stage 1** represent dual ascent method and ADMM based iterations, respectively. Thanks to the distributed algorithm, each agent only need to disclose partial information to other agents as illustrated by $\mathbf{z}_{j(i)}$ and $\mathbf{z}'_{j(i)}$. The information exchange among TET agents can be facilitated by the advanced information and communication technologies (ICT), e.g. LTE technology, which is designed for high-speed wireless communication.

2.4 Numerical results

In this section, the proposed TET framework is tested on the modified IEEE 37-bus and 123-bus distribution systems for the energy trading of a day. Detailed information of the systems can be found in [54]. Three-phase balanced scenario is considered in the case studies for simplicity. In addition, the distribution nodes are classified into residential nodes and commercial nodes based on their load patterns. It is assumed that each residential node is installed with a PV system with the rated capacity being 200 kVA. The data of the load is simulated using the same technique as our recent work [55] and the PV generation data is calculated using the actual solar irradiance data provided by [56]. Without loss of generality, the purchasing price λ_t^b is set as \$0.8/kWh during the off-peak periods (12:00 a.m.-6:00 a.m.) and \$1/kWh during other periods, and the selling price λ_t^s is set as \$0.4/kWh. All the costs and prices are presented in HK dollars. In order to accelerate the convergence speed of **S1′**, the tolerance level ε_1 for the inner loop is set to be gradually diminished until 10^{-4}. Other parameters are summarized as follows: $\alpha_i = 500$, $\rho = 1$, $\underline{v}_i = 0.95^2$, $\overline{v}_i = 1.05^2$ and $\varepsilon_2 = \varepsilon = 10^{-4}$. Numerical tests are implemented using MATLAB on a computer with an Intel Core i5 of 2.4GHz and 12GB memory.

2.4.1 IEEE 37-bus Distribution System

The nominal voltage value of the 37-bus distribution system is $4.8kV$ and the network topology is shown in Fig. 2.2. Per unit value is used in the case studies.

From the Perspective of the Entire System

Table 2.1 lists the total operating cost of the system with and without TET. It can be seen that TET can bring about roughly 25% relative cost saving resulting from the emergence of bilateral energy trading among TET agents and the reduction of

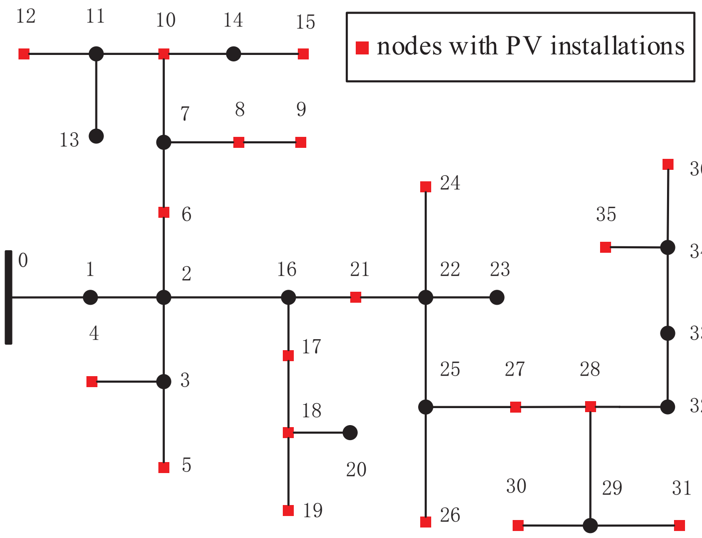

Fig. 2.2 IEEE 37-bus distribution system with PV installations

Table 2.1 Total operating cost of the system with and without TET

Cost without TET $	Cost with TET $	Cost reduction $
18812	14138	4674

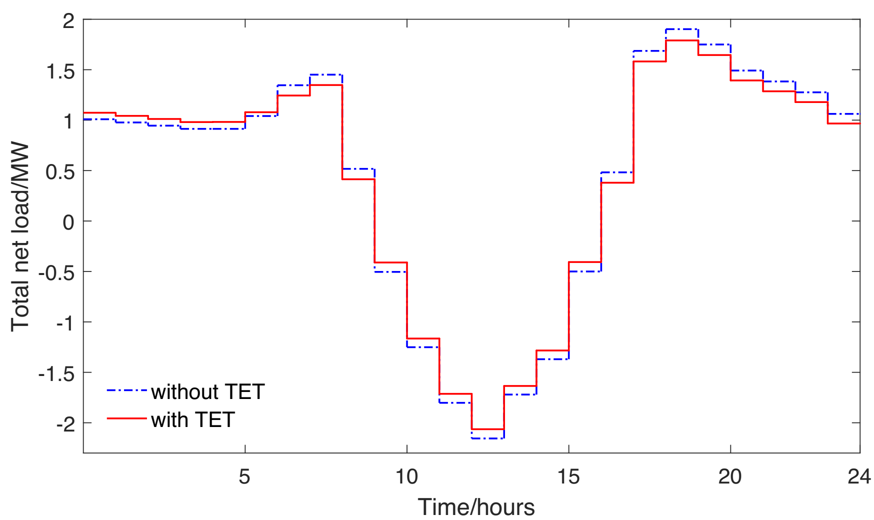

Fig. 2.3 Total net load with and without TET

energy trading between TET agents and the utility company. Fig. 2.3 depicts the hourly net load of the entire system with and without TET. It can be observed that TET fulfil the valley-filling and peak-shaving of the total net load to some extent. The reason is that the introduction of bilateral energy trading encourages

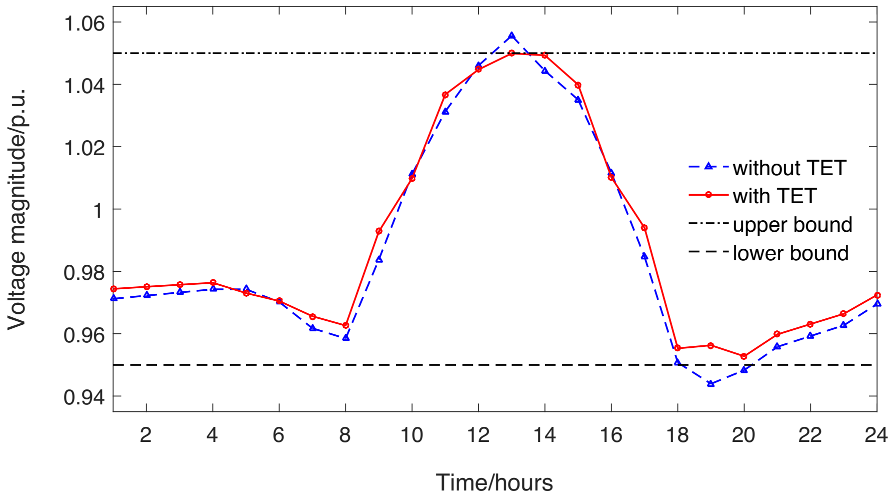

Fig. 2.4 Voltage magnitudes of node 30 with and without TET

load shifting from the periods of peak load to the periods of peak PV generation. Fig. 2.4 shows the voltage profile of node 30 with and without TET. The author only demonstrates the voltage profile of node 30 because it is a terminal node and is more likely to experience voltage violations. Without TET, overvoltage violation is observed at noon when peak PV generation occurs and undervoltage violation is observed at early night when peak load occurs. However, all voltage violations are removed when TET is introduced. The reason is that without TET each agent merely schedules its local power consumptions without systematic coordination with other agents. By contrast, TET takes the system operating constraints into account and thus enables coordinated management of the entire system.

From the Perspective of TET Agents

Table 2.2 Cost comparison with and without TET for agent 1 and 4 ($)

Items	Agent 1	Agent 4
Cost without TET	3163.7	222.9
Utility bill plus discomfort cost	1781.6	373.0
Payment to other agents	1209.0	−323.2
Cost with TET	2990.6	49.7
Payoff	173.1	173.1

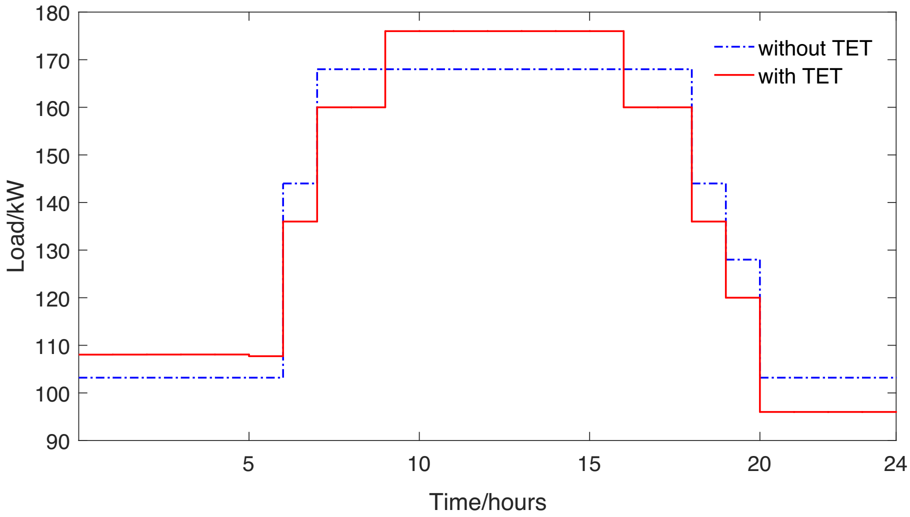

Fig. 2.5 Load schedule of agent 1 with and without TET

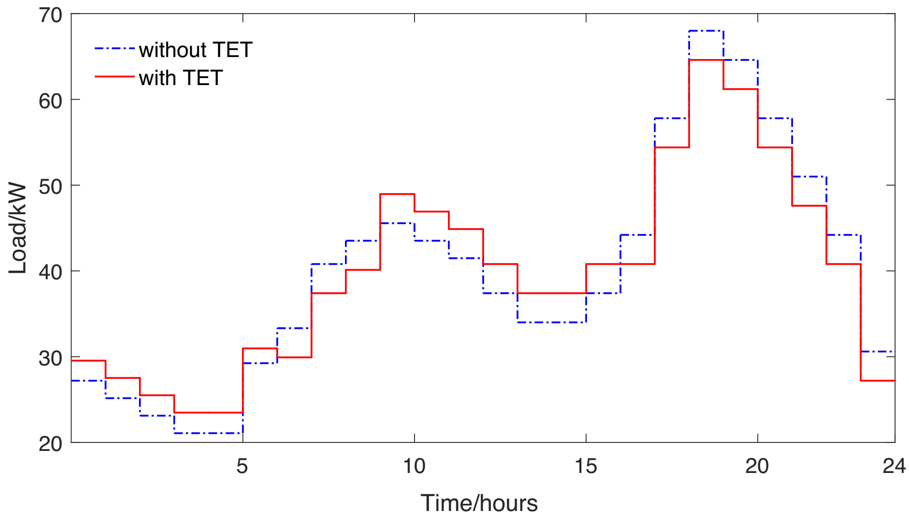

Fig. 2.6 Load schedule of agent 4 with and without TET

To avoid tedious illustration, the author takes agent 1 as a representative for a commercial node and agent 4 as a representative for a residential node. Fig. 2.5 and 2.6 show the load schedule of agent 1 and 4 with and without TET, respectively. It can seen that both agents shift part of their power consumption from the peak load periods (18:00-20:00) to the periods of peak PV generation (10:00-16:00). As a result, more PV power is consumed locally instead of feeding back to the grid during daytime, and less power is consumed during early night. Fig. 2.7 and 2.8 demonstrate the energy procurement of agent 1 and 4 when TET is involved, respectively. The

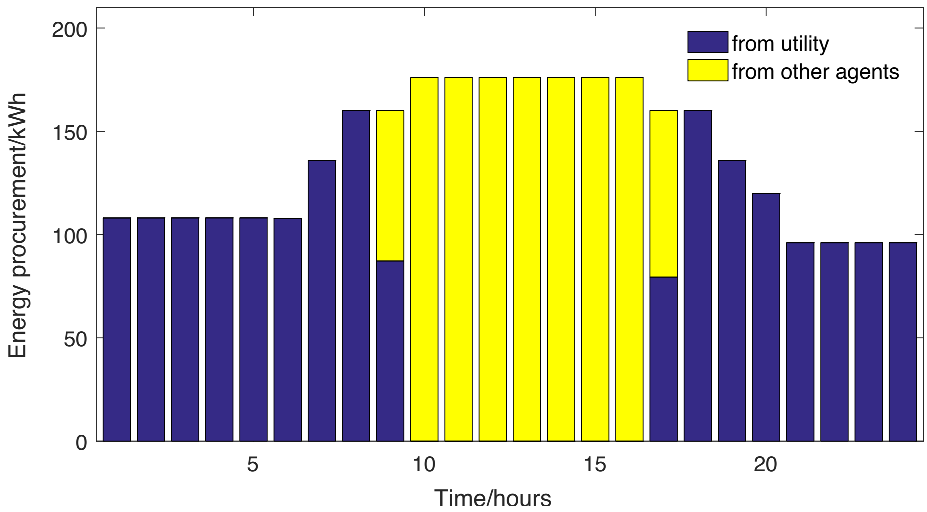

Fig. 2.7 Hourly net load and procurement of agent 1

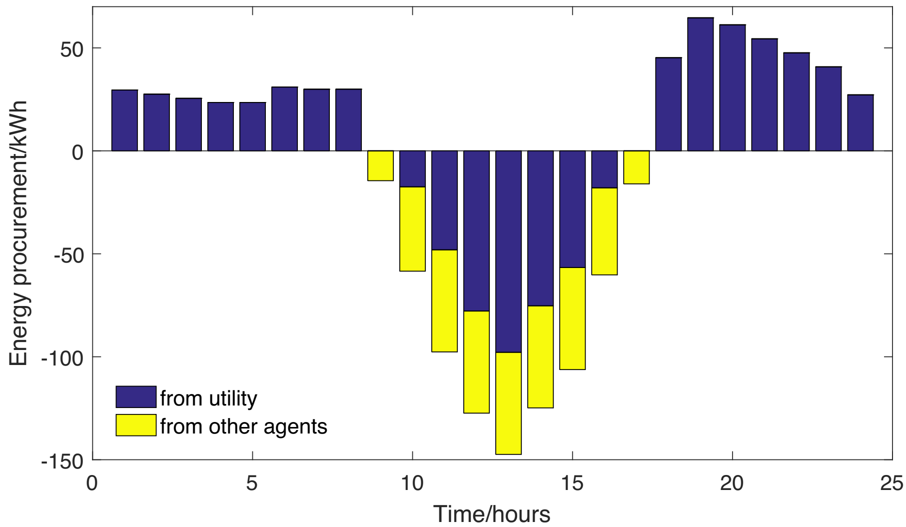

Fig. 2.8 Hourly net load and procurement of agent 4

negative values in Fig. 2.8 mean agent 4 sells energy to the utility company and other agents. It can be observed that TET agents are more willing to trade energy with other agents instead of the utility company because they can procure energy from other agents with a lower price than from the utility company and sell energy to other agents with a higher price than to the utility company. Table 2.2 shows the cost comparison with and without TET for agent 1 and 4. Both agents are awarded with an equal payoff for participating in TET. Therefore, TET is economically and technically feasible for both the entire system and individual agents.

Computational efficiency

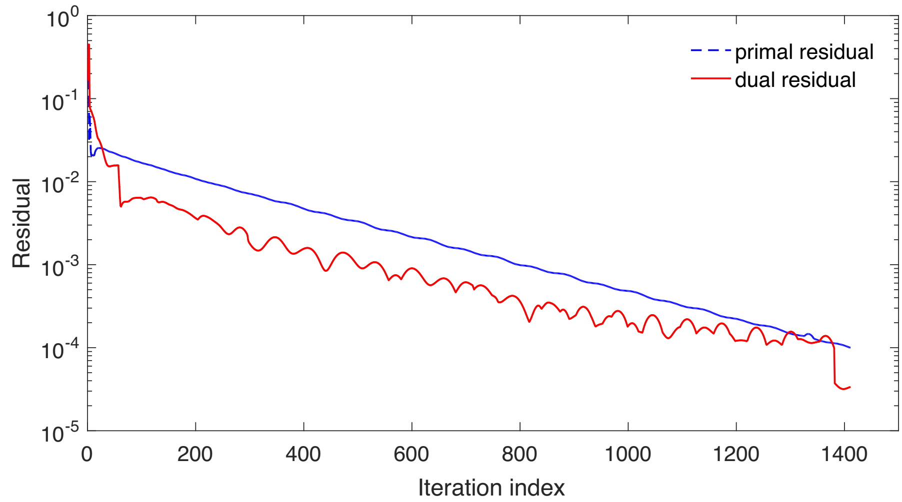

Fig. 2.9 Convergence result of the 1st stage problem for IEEE 37-bus distribution system

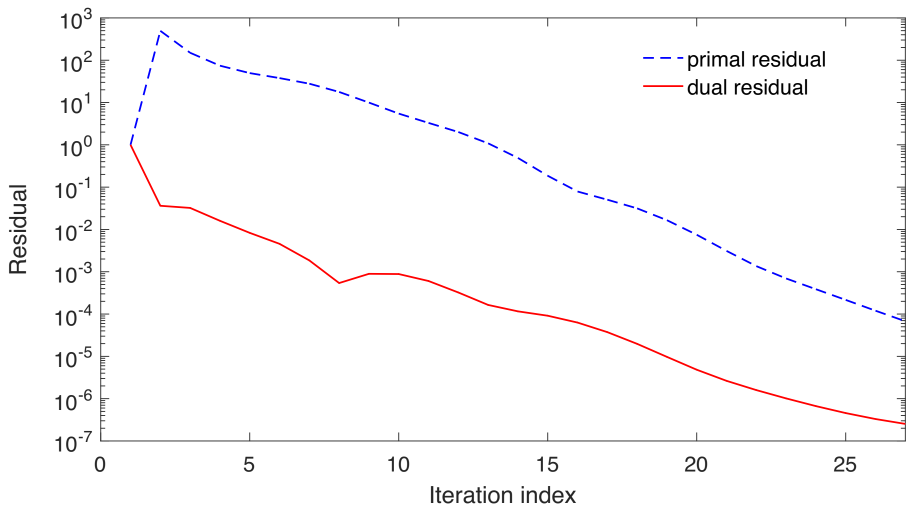

Fig. 2.10 Convergence result of the 2nd stage problem for IEEE 37-bus distribution system

Fig. 2.9 and 2.10 show the convergence result of **S1′** and **S2** using Algorithm 1, respectively. It is observed that the first stage problem takes more iterations to converge due to its great complexity. However, the total computation time for both stages is relatively short, as shown in Table 2.3 where the comparison of computational efficiency using Algorithm 1 and an off-the-shelf solver (SDPT3) [57]

Table 2.3 Computation time for IEEE 37-bus distribution system

Stage	Iteration	Total Time (s)	Time/iteration (s) (Algorithm 1)	Time/iteration (s) (SDPT3)
1st	1411	4.32	3.1×10^{-3}	12.19
2nd	27	0.01	3.8×10^{-4}	2.82

are also demonstrated. Significant time reduction (more than 3000 times faster) is achieved by using Algorithm 1 because of the employment of closed form solutions.

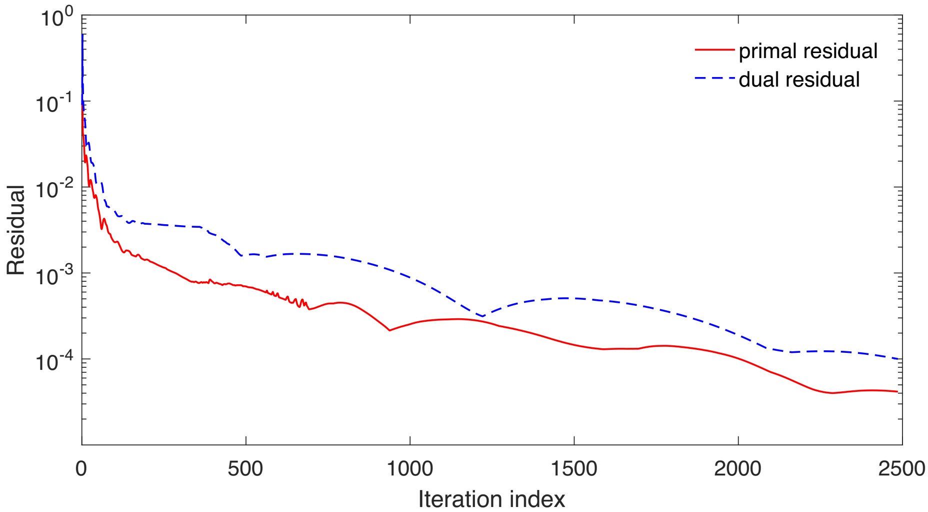

Fig. 2.11 Convergence result of the 1st stage problem for IEEE 123-bus distribution system

2.4.2 IEEE 123-bus Distribution System

In order to verify the implementability of the proposed TET framework and distributed algorithm on large systems, they are tested on the modified IEEE 123-bus distribution system. The computational result is demonstrated as below. Fig. 2.11 and 2.12 depict the convergence result of **S1′** and **S2**, respectively. The total computation time is 20.9s and 0.05s for **S1′** and **S2**, respectively.

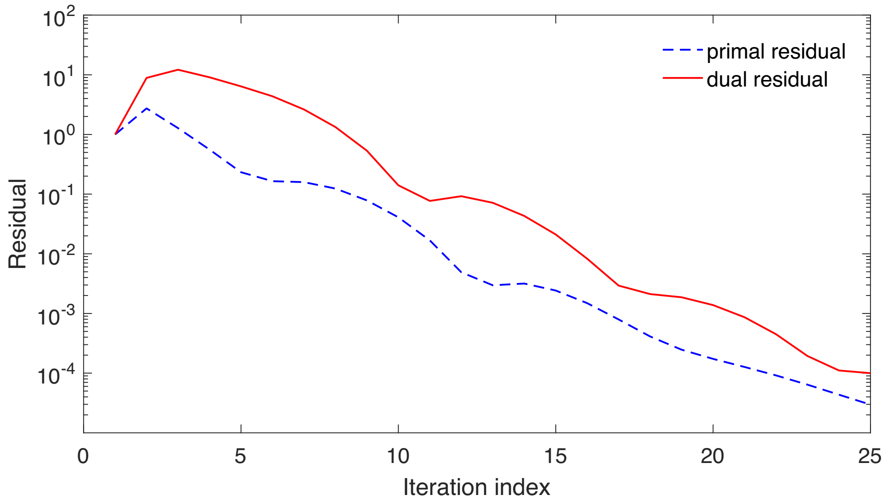

Fig. 2.12 Convergence result of the 2nd stage problem for IEEE 123-bus distribution system

2.5 Summary

In this chapter, a novel TE based energy trading framework is proposed that integrates Nash bargaining based bilateral energy trading and optimal power flow technique. By leveraging the Pareto efficiency of the Nash bargaining solution, the original transactive energy trading problem is transformed into an equivalent two-stage problem. To preserve the privacy and autonomy of individual agents, an advanced ADMM based distributed algorithm is developed for solving the problem. Moreover, the closed form formulas are derived for the update of the variables in order to substantially improve the computational efficiency. Case studies on IEEE 37-bus and 123-bus distribution feeders demonstrate the effectiveness of the proposed framework and the efficiency of the proposed algorithm.

Chapter 3

Distributed Online Voltage Control in Active Distribution Networks

3.1 Introduction

In 2016, the total installed solar photovoltaic (PV) capacity has increased by 97%, driven by the increasing environment concerns, falling manufacturing costs and attractive government incentives [58]. However, the proliferation of PV generations poses significant challenges to the operations of power systems, especially for the low-voltage distribution networks (DNs). In particular, the fast varying solar energy could result in unexpected voltage violations, at a time scale that is not consistent with conventional voltage control using on-load tap changers, step voltage regulators and shunt capacitors [59]. In this regard, PV systems can play an important role to provide voltage support in DNs [17]. Therefore, it is necessary to develop an online control scheme for dispersed PV systems to address the rapid voltage fluctuations.

Different voltgage control strategies using distributed generators (DGs) have been proposed, which can be classified into three categories, i.e. centralized strategy (e.g., [17, 60]), decentralized strategy (e.g. [61, 62]), and distributed strategy (e.g. [32, 63, 31]). Under centralized voltage control, multiple DGs are dispatched centralizedly by DN operator. Centralized control is effective for relatively long term operations (e.g. hourly), but it is hard to deal with real-time operation due to its complex communication and control schemes [64]. Furthermore, it is not robust since it fails to work when a single point failure takes place [63].

Under decentralized voltage control, DGs are locally managed by their own controllers instead of a central one. Generally, decentralized control includes local control and distributed control. Here it particularly refers to the former. Decentralized control, e.g., droop control, only relies on local measurements without any communication. Thus, it has much lower computational complexity compared with centralized voltage control. However, it often results in suboptimality due to the lack of coordination [64].

Under distributed control, DGs cooperate with each other to achieve a global goal predetermined by system operator or DG owners, and only communication between neighboring DGs is required [64]. A research summary on distributed voltage control for DNs can be found in [64]. Therein, dual-decomposition techniques, e.g., dual-ascent method and alternating direction method of multipliers (ADMM), are mostly used to develop distributed algorithms. For example, dual ascent method is employed in [49] to decompose a semi-definite programming (SDP) relaxed optimal power flow (OPF) problem into subproblems such that it can be solved in a distributed manner. In [31], an OPF problem that optimizes the active and reactive power set-points of PV inverters is decomposed based on ADMM and SDP relaxation. ADMM is also combined with second-order cone programming (SOCP) relaxation, to develop distributed algorithms for voltage control problem in [32, 63]. In [65], an ADMM consensus based distributed algorithm for reactive power optimization problem is compared with a dual-ascent based distributed algorithm, but it ignores voltage constraints. The general framework of such kind of distributed voltage control for DGs is illustrated in Fig. 3.1. It shows that multiple SDP/SOCP subproblems have to be solved iteratively before applying the final converged solution to DGs in voltage control. Consequently, the response speed of DGs cannot catch up with the fast variations of system condition, which thwarts an online application.

Apart from duality-based methods, approaches like gradient/subgradient method [66] and heuristic algorithms [67] have been applied to derive distributed control schemes as well. For example, a gradient based distributed algorithm is proposed in [66] to minimize the voltage deviations in a microgrid with a consensus on reactive power utilization. In [59], a local reactive power control framework is developed to minimize the weighted voltage mismatch based on gradient-projection method. However, these strategies will inevitably encounter some problems when the reactive power capacities of inverters are insufficient, especially during peak irradiance period. In such case, PV active power has to be curtailed to ensure the nodal voltages within the acceptable ranges.

In this chapter, an efficient distributed online voltage control algorithm is proposed using dual ascent method. PV curtailment is taken into account to overcome the aforementioned inadequacy of reactive power capacity. The objective is to maintain the voltages within the acceptable ranges and meanwhile to minimize the total loss consisting of network loss and PV curtailment. In the proposed algorithm, the active and reactive power (P-Q) set-points of multiple PV systems can be updated in a distributed manner based on local voltage measurements and communications between neighboring PV systems. Moreover, the proposed distributed voltage control algorithm can be implemented online. That is, each update obtained by the proposed algorithm can be applied directly into voltage control, as shown in Fig. 3.2. Therefore, the response speed is faster than conventional distributed algorithms, where the voltage control cannot be implemented before algorithms converge.

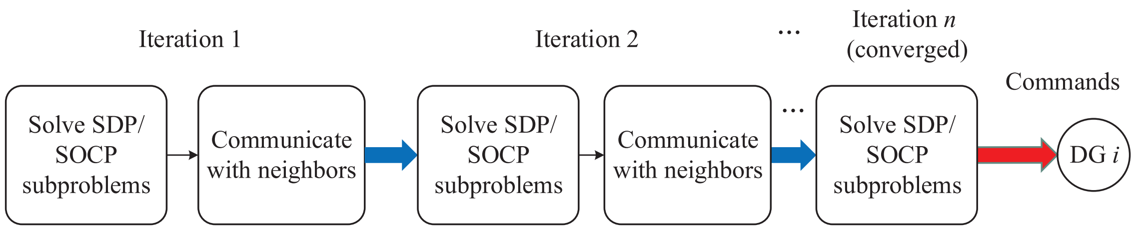

Fig. 3.1 General distributed voltage control framework

The nomenclature of symbols used in this chapter is given as follows,

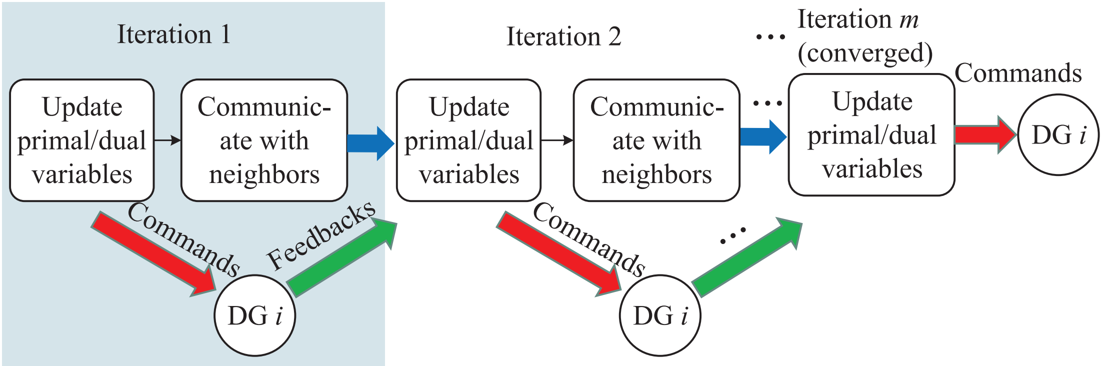

Fig. 3.2 Our proposed distributed online voltage control framework

Indices and Set

$\mathcal{E}$	Line set
$\mathcal{N}$	Bus set
k	Iteration index

Parameters

p_i^l	Active power demand at bus i
p_i^m	Maximum available active power for PV system i
q_i^l	Reactive power demand at bus i
$\underline{q}_i/\overline{q}_i$	Lower/Upper bound of reactive power output of PV system i
r_{ij}	Resistance of the line connecting bus i and bus j
x_{ij}	Reactance of the line connecting bus i and bus j
S_i	Rated apparent power of PV system i
V_0	Nominal voltage magnitude
$\underline{V}_i/\overline{V}_i$	Lower/Upper bound of voltage magnitude at node i
$\underline{\alpha_i}/\overline{\alpha_i}$	Step size for updating $\underline{\mu_i}/\overline{\mu_i}$
$\underline{\beta_i}/\overline{\beta_i}$	Step size for updating $\underline{\nu_i}/\overline{\nu_i}$
$\underline{\gamma_i}/\overline{\gamma_i}$	Step size for updating $\underline{\omega_i}/\overline{\omega_i}$

Variables

p_j	Active power injection at bus j
p_i^s	Active power output of PV system i
q_j	Reactive power injection at bus j
q_i^s	Reactive power output of PV system i

P_{ij}	Active flow on the line from bus i to bus j
Q_{ij}	Reactive flow on the line from bus i to bus j
V_i	Voltage magnitude at bus i
$\underline{\mu_i}/\overline{\mu_i}$	Dual variables associated with voltage constraints
$\underline{\nu_i}/\overline{\nu_i}$	Dual variables associated with PV active power output
$\underline{\omega_i}/\overline{\omega_i}$	Dual variables associated with PV reactive power output

3.2 System Model and Preliminaries

3.2.1 System Model

Consider a radial DN with N+1 buses and N lines represented by a directed graph $\mathcal{G} = (\mathcal{N},\ \mathcal{E})$, where $\mathcal{N} := \{0, 1, \ldots, N\}$ represents the bus set and $\mathcal{E} := (i,\ j) \subset \mathcal{N} \times \mathcal{N}$ represents the line set. Let $\mathbf{A}^0$ of size $N \times (N + 1)$ denote the incidence matrix of $\mathcal{G}$, whose entries are defined as

$$A^0_{ij} = \begin{cases} 1 & \text{line } i \text{ leaves bus } j \\ -1 & \text{line } i \text{ enters bus } j \\ 0 & \text{otherwise} \end{cases}$$

Since $\mathcal{G}$ is a connected tree, the rank of $\mathbf{A}^0$ equals to N [68]. Let $\mathbf{a}_0$ denote the first column of $\mathbf{A}^0$ that corresponds to the substation bus 0 and $\mathbf{A}$ be the rest of $\mathbf{A}^0$, i.e. $\mathbf{A}^0 = [\mathbf{a}_0\ \mathbf{A}]$. Note that $\mathbf{A}$ is a full-rank square matrix and thus invertible.

3.2.2 Branch Flow Model

For radial DNs, branch flow model is well established to represent the power flow equations [51] as (3.1a)-(3.1c)

$$P_{ij} - \sum_{k:j\to k} P_{jk} = -p_j + r_{ij}\frac{P_{ij}^2 + Q_{ij}^2}{V_i^2} \qquad \forall j \in \mathcal{N}/0 \tag{3.1a}$$

$$Q_{ij} - \sum_{k:j\to k} Q_{jk} = -q_j + x_{ij}\frac{P_{ij}^2 + Q_{ij}^2}{V_i^2} \qquad \forall j \in \mathcal{N}/0 \tag{3.1b}$$

$$V_i^2 - V_j^2 = 2\left(r_{ij}P_{ij} + x_{ij}Q_{ij}\right) - \left(r_{ij}^2 + x_{ij}^2\right)\frac{P_{ij}^2 + Q_{ij}^2}{V_i^2} \qquad \forall (i,\ j) \in \mathcal{E} \tag{3.1c}$$

Unfortunately, (3.1a)-(3.1c) are non-convex. Thus, linearized branch flow model (LinDistFlow) will be adopted by neglecting the high order terms and assuming a relatively flat voltage profile, i.e. $V_i \approx 1,\ \forall i$. It has been widely applied in DN optimization problems (e.g.,[69, 60, 65]) and is given by

$$P_{ij} - \sum_{k:j\to k} P_{jk} = -p_j \qquad \forall j \in \mathcal{N}/0 \tag{3.2a}$$

$$Q_{ij} - \sum_{k:j\to k} Q_{jk} = -q_j \qquad \forall j \in \mathcal{N}/0 \tag{3.2b}$$

$$V_i - V_j = r_{ij}P_{ij} + x_{ij}Q_{ij} \qquad \forall (i,\ j) \in \mathcal{E} \tag{3.2c}$$

3.2.3 PV Inverter Dispatch Strategy

Advance control strategies, e.g., optimal inverter dispatch [17], enable PV inverters to adjust both active and reactive power in order to provide voltage support. Let p_i^m denote the maximum available active power for PV system i. The operating region of P-Q set-points can be represented by

$$0 \le p_i^s \le p_i^m \tag{3.3a}$$

$$|q_i^s| \le \sqrt{S_i^2 - (p_i^s)^2} \tag{3.3b}$$

In order to decouple the correlation between active and reactive power, (3.3b) is linearized by imposing restricted limits on q_i^s as (3.4).

$$\underline{q}_i \le q_i^s \le \overline{q}_i \tag{3.4}$$

where $\overline{q}_i = \sqrt{S_i^2 - (p_i^m)^2}$ and $\underline{q}_i = -\overline{q}_i$.

3.3 Problem Formulation

3.3.1 Objective Function

The primary objective of voltage control is to maintain the DN bus voltage magnitudes within the acceptable ranges, while inappropriate control would lead to excessive network loss and PV curtailment. PV curtailment is taken into account for two reasons. First, the adjustment of active power itself can facilitate voltage control directly. Second, it will enlarge the reactive power capacity. However, excessive curtailment results in a waste of energy resources. Thus, PV curtailment cost should be taken into account. In this chapter, the objective is to minimize the weighted total loss consisting of network loss and PV curtailment cost and meanwhile to ensure the nodal voltage magnitudes within the acceptable ranges.

The network loss is given by

$$\text{Loss} = \sum_{\forall(i,j)\in\mathcal{E}} r_{ij} \frac{P_{ij}^2 + Q_{ij}^2}{V_i^2} \approx \sum_{\forall(i,j)\in\mathcal{E}} r_{ij} \frac{P_{ij}^2 + Q_{ij}^2}{V_0^2} \tag{3.5}$$

where V_0 is the voltage magnitude at the substation bus and is assumed to be 1 p.u. without loss of generality; V_i^2 is approximated by V_0^2 since $V_i \approx 1, \ \forall i$.

PV curtailment is evaluated by an exclusive quadratic function in order to reduce communication complexity, which is given as

$$h\left(\mathbf{p}^c\right) = K \cdot \left(\mathbf{p}^c\right)^T \mathbf{R} \mathbf{p}^c \tag{3.6}$$

where $\mathbf{p}^c$ is the vector collecting all p_i^c and p_i^c is curtailment amount of PV system i; $\mathbf{R}$ is a positive definite matrix with positive entries. K is an adjustable parameter. A larger K results in less PV curtailment amount but lower efficiency in eliminating overvoltage violations, vice versa. $h\left(\mathbf{p}^c\right)$ could effectively quantify PV curtailment amount since it is strictly convex and monotonically increasing with respect to $\mathbf{p}^c$.

Thus, the total loss is given as

$$F = \text{Loss} + h\left(\mathbf{p}^c\right) \tag{3.7}$$

3.3.2 Constraints

The constraints include power flow equations, voltage constraints and PV operation constraints. The power flow equations are represented by LinDistFlow model as (3.8)-(3.10).

$$
\begin{aligned}
&(3.2a) - (3.2c) && (3.8)\\
&p_i = p_i^m - p_i^c - p_i^l \quad \forall i \in \mathcal{N}/0 && (3.9)\\
&q_i = q_i^s - q_i^l \quad \forall i \in \mathcal{N}/0 && (3.10)
\end{aligned}
$$

Note that the PV system located at bus i is denoted as PV system i so that the indices of PV systems are identical with the indices of buses.

The bus voltage magnitudes should be maintained within the acceptable ranges as

$$\underline{V}_i \leq V_i \leq \overline{V}_i \quad \forall i \in \mathcal{N}/0 \tag{3.11}$$

PV active power curtailment and reactive power set-point are constrained by

$$
\begin{aligned}
&0 \leq p_i^c \leq p_i^m \quad \forall i \in \mathcal{N}/0 && (3.12)\\
&\underline{q}_i \leq p_i^s \leq \overline{q}_i \quad \forall i \in \mathcal{N}/0 && (3.13)
\end{aligned}
$$

3.3.3 Centralized Optimization Model

The centralized optimization model is given as

$$
\begin{aligned}
\text{CEN1} \quad & \min_{p_i^c, q_i^s} \; F = \text{Loss} + h\left(\mathbf{p}^c\right) && && (3.14\text{a})\\
& \text{s.t. } P_{ij} - \sum_{k:j\to k} P_{jk} = -p_j && \forall j \in \mathcal{N}/0 && (3.14\text{b})\\
& Q_{ij} - \sum_{k:j\to k} Q_{jk} = -q_j && \forall j \in \mathcal{N}/0 && (3.14\text{c})\\
& V_i - V_j = r_{ij}P_{ij} + x_{ij}Q_{ij} && \forall (i,\ j) \in \mathcal{E} && (3.14\text{d})\\
& p_i = p_i^m - p_i^c - p_i^l && \forall i \in \mathcal{N}/0 && (3.14\text{e})\\
& q_i = q_i^s - q_i^l && \forall i \in \mathcal{N}/0 && (3.14\text{f})
\end{aligned}
$$

$$\underline{V}_i \leq V_i \leq \overline{V}_i \qquad \forall i \in \mathcal{N}/0 \tag{3.14g}$$

$$0 \leq p_i^c \leq p_i^m \qquad \forall i \in \mathcal{N}/0 \tag{3.14h}$$

$$\underline{q}_i \leq p_i^s \leq \overline{q}_i \qquad \forall i \in \mathcal{N}/0 \tag{3.14i}$$

CEN1 is a convex quadratic optimization problem with linear constraints. A distributed online algorithm will be developed in the next section to solve it. Towards this end, it will be written in a compact matrix format for clarity. The corresponding compact form for LinDistFlow model is given as

$$-\mathbf{A}^T\mathbf{P} = -\mathbf{p} \tag{3.15a}$$

$$-\mathbf{A}^T\mathbf{Q} = -\mathbf{q} \tag{3.15b}$$

$$\mathbf{a}_0 + \mathbf{A}\mathbf{V} = \mathbf{D}_r\mathbf{P} + \mathbf{D}_x\mathbf{Q} \tag{3.15c}$$

$$\mathbf{p} = \mathbf{p}^m - \mathbf{p}^c - \mathbf{p}^l \tag{3.15d}$$

$$\mathbf{q} = \mathbf{q}^s - \mathbf{q}^l \tag{3.15e}$$

where $\mathbf{D}_r$ and $\mathbf{D}_x$ are $N \times N$ diagonal matrices whose diagonal entries are constituted by r_{ij} and x_{ij}, respectively. Solving $\mathbf{P}$ and $\mathbf{Q}$ and plugging them into (3.15c), LinDistFlow model boils down to

$$\mathbf{V} = \mathbf{R}\mathbf{p} + \mathbf{X}\mathbf{q} - \mathbf{V}^c \tag{3.16}$$

where $\mathbf{V}^c := \mathbf{A}^{-1}\mathbf{a}_0$, $\mathbf{R} := \mathbf{A}^{-1}\mathbf{D}_r\mathbf{A}^{-T}$ and $\mathbf{R} := \mathbf{A}^{-1}\mathbf{D}_x\mathbf{A}^{-T}$. (3.16) reveals linear relationship between nodal power injections and nodal voltage magnitudes. According to Proposition 1 in [69], $\mathbf{R}$ and $\mathbf{X}$ are positive definite (PD) and their entries are positive.

The network loss can be reformulated as

$$\begin{aligned}\text{Loss} &= \sum_{\forall (i,j)\in\mathcal{E}} \left[\left(\sqrt{r_{ij}}P_{ij}\right)^2 + \left(\sqrt{r_{ij}}Q_{ij}\right)^2 \right] \\ &= \|\mathbf{D}_r^{1/2}\mathbf{P}\|_2^2 + \|\mathbf{D}_r^{1/2}\mathbf{Q}\|_2^2 = \mathbf{p}^T\mathbf{R}\mathbf{p} + \mathbf{q}^T\mathbf{R}\mathbf{q}\end{aligned} \tag{3.17}$$

The last equality follows from the substitution of $\mathbf{P}$ and $\mathbf{Q}$. Note that the PV curtailment evaluation in (3.6) shares a similar structure with the network loss in (3.17). It will be demonstrated in the next section that such a modelling of PV curtailment will facilitate the reduction of communication complexity.

By plugging (3.15d) and (3.15e) into (3.16) and (3.17), and dividing the objective function by 2, the compact format of CEN1 is obtained as follows.

$$\min_{\mathbf{p}^c,\mathbf{q}^s} \frac{1}{2}\Big[\left(\mathbf{p}^m-\mathbf{p}^c-\mathbf{p}^l\right)^T\mathbf{R}\left(\mathbf{p}^m-\mathbf{p}^c-\mathbf{p}^l\right) + \left(\mathbf{q}^s-\mathbf{q}^l\right)^T\mathbf{R}\left(\mathbf{q}^s-\mathbf{q}^l\right)\Big] + \frac{K}{2}\left(\mathbf{p}^c\right)^T\mathbf{R}\mathbf{p}^c \tag{3.18a}$$

$$\text{s.t. } \mathbf{V} = \mathbf{R}\left(\mathbf{p}^m-\mathbf{p}^c-\mathbf{p}^l\right) + \mathbf{X}\left(\mathbf{q}^s-\mathbf{q}^l\right) - \mathbf{V}^c \tag{3.18b}$$

$$\underline{\mathbf{V}} \leq \mathbf{V} \leq \overline{\mathbf{V}} \tag{3.18c}$$

$$\mathbf{0} \leq \mathbf{p}^c \leq \mathbf{p}^m \tag{3.18d}$$

$$\underline{\mathbf{q}} \leq \mathbf{q}^s \leq \overline{\mathbf{q}} \tag{3.18e}$$

3.4 Distributed Online Voltage Control

3.4.1 Distributed Online Algorithm

In this subsection, a distributed online algorithm is developed using dual ascent method. In particular, a closed-form solution is derived for PV systems to locally update P-Q set-points and Lagrangian multipliers.

Dual Ascent Method

In dual ascent method [53], the dual problem is solved using gradient projection algorithm and the primal optimal solution is recovered from the dual optimal solution. Define the dual problem as $\mathcal{D}(\mathbf{y}) = \min_{\mathbf{x}} \mathcal{L}(\mathbf{x},\mathbf{y})$, where $\mathcal{L}(\mathbf{x},\mathbf{y})$ is the Lagrangian function. The iterations of Lagrangian multipliers $\mathbf{y}$ and primal variables $\mathbf{x}$ are given as (3.19) and (3.20), respectively.

$$\mathbf{y}^{k+1} = \left[\mathbf{y}^k + \alpha^k \nabla\mathcal{D}\left(\mathbf{y}^k\right)\right]^Y \tag{3.19}$$

$$\mathbf{x}^{k+1} = \arg\min_{\mathbf{x}} \mathcal{L}(\mathbf{x}, \mathbf{y}^{k+1}) \tag{3.20}$$

where $\nabla \mathcal{D}\left(\mathbf{y}^k\right)$ is the gradient of the dual problem at $\mathbf{y}^k$, α^k is the step size at k-th iteration, Y is the feasible set of $\mathbf{y}$, and $[\cdot]^Y$ denotes the projection operator onto the set Y.

Update Rules for Lagrangian Multipliers

The Lagrangian function of CEN1 is given as,

$$\begin{aligned}\mathcal{L} =& \frac{K+1}{2}\left(\mathbf{p}^c\right)^T \mathbf{R}\mathbf{p}^c - (\mathbf{p}^m - \mathbf{p}^l)^T \mathbf{R}\mathbf{p}^c + \frac{1}{2}\left(\mathbf{q}^s\right)^T \mathbf{R}\mathbf{q}^s + (\mathbf{q}^l)^T \mathbf{R}\mathbf{q}^s \\ &+ \underline{\boldsymbol{\mu}}^T\left(\underline{\mathbf{V}} + \mathbf{R}\mathbf{p}^c - \mathbf{X}\mathbf{q}^s - \mathbf{V}^r\right) + \overline{\boldsymbol{\mu}}^T\left(-\overline{\mathbf{V}} - \mathbf{R}\mathbf{p}^c + \mathbf{X}\mathbf{q}^s + \mathbf{V}^r\right) \\ &+ \underline{\boldsymbol{\nu}}^T(\mathbf{0} - \mathbf{p}^c) + \overline{\boldsymbol{\nu}}^T(\mathbf{p}^c - \mathbf{p}^m) + \underline{\boldsymbol{\omega}}^T(\underline{\mathbf{q}} - \mathbf{q}^s) + \overline{\boldsymbol{\omega}}^T(\mathbf{q}^s - \overline{\mathbf{q}})\end{aligned} \tag{3.21}$$

where $\underline{\boldsymbol{\mu}}$, $\overline{\boldsymbol{\mu}}$, $\underline{\boldsymbol{\nu}}$, $\overline{\boldsymbol{\nu}}$, $\underline{\boldsymbol{\omega}}$ and $\overline{\boldsymbol{\omega}}$ are Lagrangian multipliers associated with (3.18c), (3.18d) and (3.18e), respectively; and $\mathbf{V}^r := \mathbf{R}(\mathbf{p}^m - \mathbf{p}^l) - \mathbf{X}\mathbf{q}^l - \mathbf{V}^c$.

The Lagrangian multipliers are locally updated based on gradient projection method for each PV system [70], given as

$$\underline{\mu}_i^{k+1} = \left[\underline{\mu}_i^k + \underline{\alpha}_i(\underline{V}_i - V_i^k)\right]^+ \tag{3.22a}$$

$$\overline{\mu}_i^{k+1} = \left[\overline{\mu}_i^k + \overline{\alpha}_i(V_i^k - \overline{V}_i)\right]^+ \tag{3.22b}$$

$$\underline{\nu}_i^{k+1} = \left[\underline{\nu}_i^k + \underline{\beta}_i(0 - p_i^{c,k})\right]^+ \tag{3.22c}$$

$$\overline{\nu}_i^{k+1} = \left[\overline{\nu}_i^k + \overline{\beta}_i(p_i^{c,k} - p_i^m)\right]^+ \tag{3.22d}$$

$$\underline{\omega}_i^{k+1} = \left[\underline{\omega}_i^k + \underline{\gamma}_i(\underline{q}_i - q_i^{s,k})\right]^+ \tag{3.22e}$$

$$\overline{\omega}_i^{k+1} = \left[\overline{\omega}_i^k + \overline{\gamma}_i(q_i^{s,k} - \overline{q}_i)\right]^+ \tag{3.22f}$$

where $[\cdot]^+$ denotes the projection operator onto the non-negative range.

Update Rules for Primal Variables

Since $\mathcal{L}$ is a quadratic function of $\mathbf{p}^c$ and $\mathbf{q}^s$, a closed-form solution at k-th iteration can be obtained as

$$\mathbf{p}^{c,k} = \frac{\mathbf{p}^m - \mathbf{p}^l + \overline{\boldsymbol{\mu}}^k - \underline{\boldsymbol{\mu}}^k - \mathbf{R}^{-1}(\underline{\boldsymbol{\nu}}^k - \overline{\boldsymbol{\nu}}^k)}{K+1} \tag{3.23a}$$

$$\mathbf{q}^{s,k} = \mathbf{q}^l + \mathbf{R}^{-1}\mathbf{X}(\underline{\boldsymbol{\mu}}^k - \overline{\boldsymbol{\mu}}^k) + \mathbf{R}^{-1}(\underline{\boldsymbol{\omega}}^k - \overline{\boldsymbol{\omega}}^k) \tag{3.23b}$$

The optimization problem (3.20) boils down to trivial algebraic operations. However, the update of P-Q set-points for each PV system is coupled with all other PV systems through the Lagrangian multipliers. As a result, the global communication is necessary. Fortunately, using the following two propositions, the communication complexity can be reduced substantially such that each PV system only need to exchange multipliers with its neighbors.

Proposition 3 *Denote* $\mathbf{H} := \mathbf{R}^{-1} := \mathbf{A}^T\mathbf{D}_r^{-1}\mathbf{A}$. $\mathbf{H}$ *is a weighted Laplacian matrix induced by the network incidence matrix* $\mathbf{A}$. *For any pair of buses* (i,j) *that are not directly connected, the corresponding entry is zero, i.e.* $(i,j) \notin \mathcal{E} \Leftrightarrow H_{ij} = 0$.

Proof 3 *Let* $\left[\mathbf{A}^T\right]_i$ *denote the i-th row of* $\mathbf{A}^T$ *and* $[\mathbf{D}_r^{-1}\mathbf{A}]^j$ *denote the j-th column of* $\mathbf{D}_r^{-1}\mathbf{A}$. *The entry on l-th row and j-th column of* $\mathbf{D}_r^{-1}\mathbf{A}$ *is* $[\mathbf{D}_r^{-1}\mathbf{A}]_{lj} = A_{lj}/D_{r,ll}$. *Thus, we have*

$$H_{ij} = \left[\mathbf{A}^T\right]_i \left[\mathbf{D}_r^{-1}\mathbf{A}\right]^j = \sum_{l=1}^{N} A_{li}\frac{A_{lj}}{D_{r,ll}}$$

According to the definition of $\mathbf{A}$, *if bus i and bus j are not directly connected,* $A_{li}A_{lj} = 0, \forall\ l$ *and thus* $H_{ij} = 0$. ***Q.E.D.***

Proposition 4 *Since the* x_{ij}/r_{ij} *ratios of the power lines for a distribution network are relatively homogeneous for the practical cases [54],* $\mathbf{R}^{-1}\mathbf{X}$ *can be approximated by c multiple of the N dimensional identity matrix* $\mathbf{I}$, *where c is an approximation of* x_{ij}/r_{ij} *ratios, i.e.* $\mathbf{R}^{-1}\mathbf{X} = c\mathbf{I}$.

Proof 4 $\mathbf{R}^{-1}\mathbf{X} = \mathbf{A}^T\mathbf{D}_r^{-1}\mathbf{A}\mathbf{A}^{-1}\mathbf{D}_x\mathbf{A}^{-T} = \mathbf{A}^T\mathbf{D}_r^{-1}\mathbf{D}_x\mathbf{A}^{-T}$

Since $\mathbf{D}_r$ *and* $\mathbf{D}_x$ *are diagonal matrices constituted by* r_{ij} *and* x_{ij}*,* $\mathbf{D}_r^{-1}\mathbf{D}_x$ *is a diagonal matrix with l-th diagonal entry being* $x_{ij}/r_{ij} = c$*. Therefore,* $\mathbf{R}^{-1}\mathbf{X} = \mathbf{A}^T c\mathbf{I}\mathbf{A}^{-T} = c\mathbf{I}$ ***Q.E.D.***

Applying (3.23) to a particular PV system i, the update of power set-points can be obtained as

$$p_i^{c,k} = \frac{p_i^m - p_i^l + \overline{\mu}_i^k - \underline{\mu}_i^k + H_{ii}(\underline{\nu}_i^k - \overline{\nu}_i^k) + \sum_{j\in\mathcal{N}_i} H_{ij}(\underline{\nu}_j^k - \overline{\nu}_j^k)}{K+1} \tag{3.24a}$$

$$q_i^{s,k} = q_i^l + c(\underline{\mu}_i^k - \overline{\mu}_i^k) + H_{ii}(\underline{\omega}_i^k - \overline{\omega}_i^k) + \sum_{j\in\mathcal{N}_i} H_{ij}(\underline{\omega}_j^k - \overline{\omega}_j^k) \tag{3.24b}$$

where $\mathcal{N}_i$ denotes the set of neighbors of PV system i. Now the update for each PV system is only coupled with its neighbors.

Since constraints (3.18d) and (3.18e) are relaxed, the primal variables obtained from (3.24a) and (3.24b) may be infeasible. In case of infeasibility, they will be projected onto the feasible ranges as

$$p_i^{c,k,a} = \left[p_i^{c,k}\right]_0^{p_i^m} \tag{3.25a}$$

$$q_i^{s,k,a} = \left[q_i^{s,k}\right]_{\underline{q}_i^k}^{\overline{q}_i^k} \tag{3.25b}$$

where $[\cdot]_a^b$ denotes the projection operator onto the range $[a,b]$; $\overline{q}_i^k$ and $\underline{q}_i^k$ are iteratively renewed as $\overline{q}_i^k = \sqrt{S_i^2 - (p_i^m - p_i^{c,k,a})^2}$ and $\underline{q}_i^k = -\overline{q}_i^k$. Compared with the fixed limits in (3.18e), $\overline{q}_i^k$ and $\underline{q}_i^k$ enlarge the reactive power capacity and thereby improving the system performance as will be shown in Section V.

Implementation of the Distributed Algorithm

Fig. 3.3 shows the online implementation of the proposed distributed algorithm. Each bus is equipped with a PV system that could monitor the local bus voltage magnitude and communicate with its neighboring PV systems.

The overall procedure of the algorithm is given as follows.

Step 1: Initialize multipliers and primal variables.

Step 2: Monitor the local bus voltage magnitude V_i.

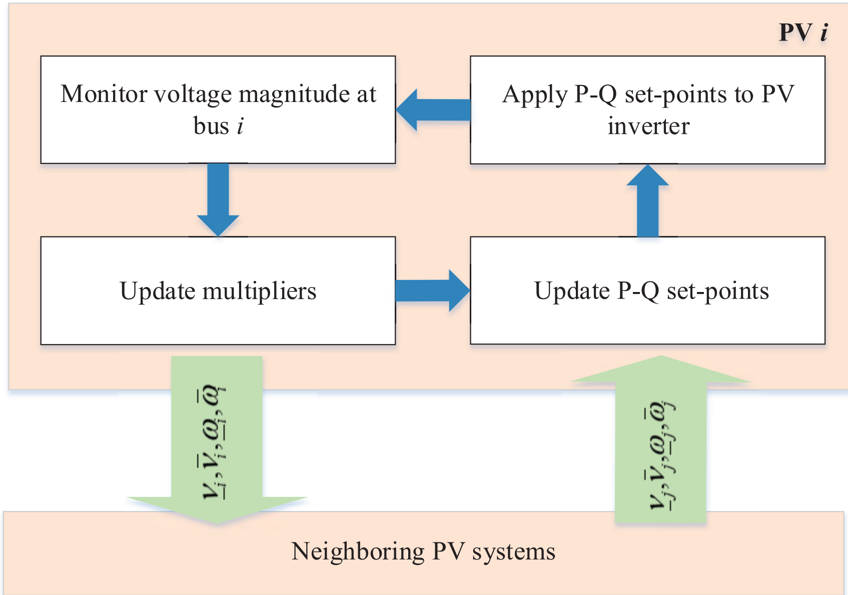

Fig. 3.3 Online implementation of the proposed distributed algorithm, where the green arrows represent the information exchange

Step 3: Update multipliers according to (3.22a)-(3.22f) and exchange multipliers with neighboring PV systems.

Step 4: Update active power curtailment and reactive power set-point according to (3.24a) and (3.24b). Project them onto the feasible ranges as (3.25a) and (3.25b), and apply them to PV inverters.

Step 5: Return to step 2 until the stopping criterion is met.

In this chapter, the voltage stopping criterion is adopted since the optimal solution is directly related to the bus voltages. If the voltage difference of two successive iterations is smaller than the tolerance ϵ, i.e. $|V_i^k - V_i^{k-1}| < \epsilon$, then the update will stop.

The update at each iteration is applied. Fig. 3.4 shows the block diagram of the control scheme for individual PV system at each iteration, which consists of three feedback control loops, i.e. voltage control loop, PV curtailment control loop and PV reactive power control loop. The feedback control is realized through the constant interactions between primal variables and Lagrangian multipliers. For instance, $\overline{\mu}_i > 0$ indicates overvoltage violation at bus i, and it will drive the increase of p_i^c and

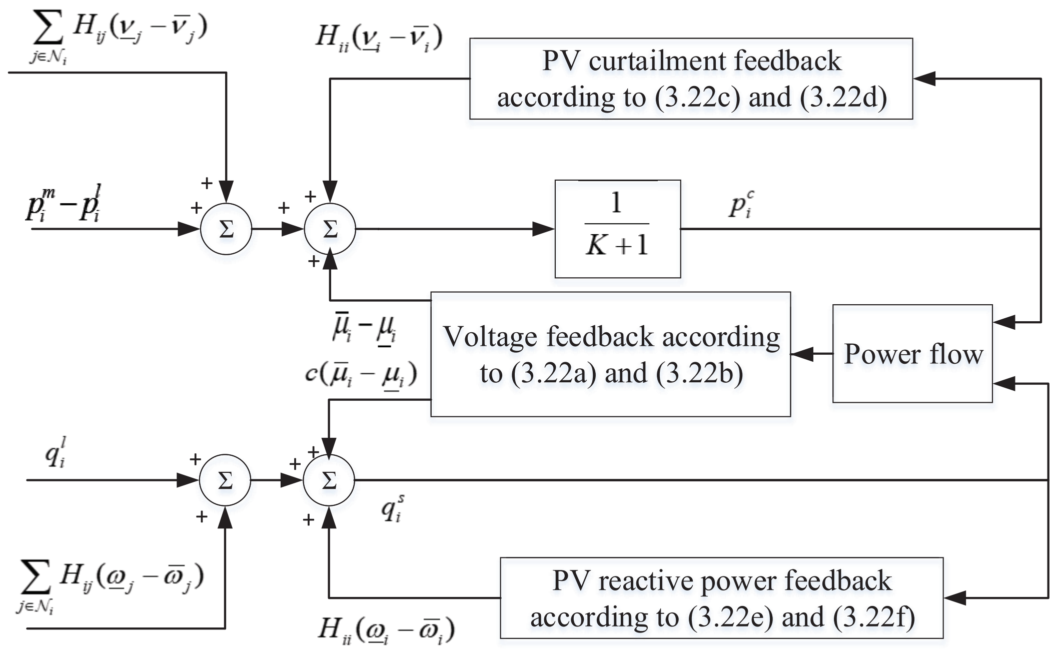

Fig. 3.4 Block diagram of the control scheme for PV system i at each iteration

the decrease of q_i^s, which in turn contributes to the mitigation of overvoltage violation and the decline of $\overline{\mu}_i$. The inputs $\sum_{j\in\mathcal{N}_i} H_{ij}(\underline{\nu}_j - \overline{\nu}_j)$ and $\sum_{j\in\mathcal{N}_i} H_{ij}(\underline{\omega}_j - \overline{\omega}_j)$ represent the influences exerted by the neighbors. Specifically, the multipliers received from the neighbors reveal the inadequacy of active power curtailment and reactive power capacity of the neighbors. By multiplying them with H_{ij}, PV system i will react accordingly to mitigate the inadequacy.

3.4.2 Convergence Analysis

CEN1 is a strongly convex quadratic problem with linear inequality constraints and can be generalized as

$$\min_{\mathbf{x}} \ \frac{1}{2}\mathbf{x}^T\mathbf{Q}\mathbf{x} + \mathbf{c}^T\mathbf{x} \tag{3.26a}$$

$$\text{s.t. } \mathbf{B}\mathbf{x} \leq \mathbf{b} \tag{3.26b}$$

where $\mathbf{x}$ is the vector of decision variables collecting $\mathbf{p}^c$ and $\mathbf{q}^s$. $\mathbf{Q}$ and $\mathbf{B}$ are coefficient matrices, $\mathbf{c}$ and $\mathbf{b}$ are coefficient vectors. The strong convexity of (3.26) implies $\mathbf{Q}$ is PD and invertible. The associated dual problem is given by

$$\max_{\mathbf{y}\geq\mathbf{0}} \; g(\mathbf{y}) = -\frac{1}{2}\mathbf{y}^T\mathbf{B}\mathbf{Q}^{-1}\mathbf{B}^T\mathbf{y} - (\mathbf{B}\mathbf{Q}^{-1}\mathbf{c}+\mathbf{b})^T\mathbf{y} - \frac{1}{2}\mathbf{c}^T\mathbf{Q}^{-1}\mathbf{c} \tag{3.27}$$

where $\mathbf{y}$ is the vector of dual variables collecting $\underline{\boldsymbol{\mu}}$, $\overline{\boldsymbol{\mu}}$, $\underline{\boldsymbol{\nu}}$, $\overline{\boldsymbol{\nu}}$, $\underline{\boldsymbol{\omega}}$ and $\overline{\boldsymbol{\omega}}$. Then the update rules of dual and primal variables are given as

$$\mathbf{y}^{k+1} = \left[\mathbf{y}^k + \mathbf{D}(\mathbf{B}\mathbf{x}^k - \mathbf{b})\right]^+ \tag{3.28}$$

$$\mathbf{x}^{k+1} = -\,\mathbf{Q}^{-1}\mathbf{c} - \mathbf{Q}^{-1}\mathbf{B}^T\mathbf{y}^{k+1} \tag{3.29}$$

where $\mathbf{D}$ is a diagonal matrix whose diagonal entries are constituted by the step sizes.

Theorem 2 *Considering the update rules of (3.28) and (3.29), the trajectories of* $\mathbf{x}^k$ *and* $\mathbf{y}^k$ *asymptotically converge to the optimal solutions* $\mathbf{x}^*$ *and* $\mathbf{y}^*$*, respectively, if the largest eigenvalue of PD matrix* $\mathbf{D}^{\frac{1}{2}}\mathbf{B}\mathbf{Q}\mathbf{B}^T\mathbf{D}^{\frac{1}{2}}$ *is smaller than 2*

Proof 5 *Since problem (3.26) is a strictly convex-quadratic problem with linear constraints, the Slater's condition [71] holds and thus there is no duality gap between (3.26) and (3.27). Therefore, given dual optimal solution* $\mathbf{y}^*$*, the primal optimal solution can be retrieved by minimizing* $\mathcal{L}(\mathbf{x}, \mathbf{y}^*)$*. Plugging (3.29) into (3.28), we obtain*

$$\begin{aligned}\mathbf{y}^{k+1} &= \left[\mathbf{y}^k + \mathbf{D}(-\mathbf{B}\mathbf{Q}^{-1}\mathbf{B}^T\mathbf{y}^k - \mathbf{B}\mathbf{Q}^{-1}\mathbf{c} - \mathbf{b})\right]^+ \\ &= \left[\mathbf{y}^k + \mathbf{D}\nabla g(\mathbf{y}^k)\right]^+\end{aligned}$$

Thus, the iteration of $\mathbf{y}$ *is based on diagonally scaled gradient projection method. To show* $\mathbf{y}^k$ *converges to the optimal solution* $\mathbf{y}^*$*, it is equivalent to show (3.28) is a contraction mapping regarding to the norm of the scaled error. Define* $\bar{\mathbf{y}}^k = \mathbf{D}^{-\frac{1}{2}}\mathbf{y}^k$

and $\bar{\mathbf{y}}^* = \mathbf{D}^{-\frac{1}{2}}\mathbf{y}^*$. *We have*

$$
\begin{aligned}
&\left\|\bar{\mathbf{y}}^{k+1} - \bar{\mathbf{y}}^*\right\| \\
=&\left\|\mathbf{D}^{-\frac{1}{2}}\left[\mathbf{y}^k + \mathbf{D}\nabla g(\mathbf{y}^k)\right]^+ - \mathbf{D}^{-\frac{1}{2}}\left[\mathbf{y}^* + \mathbf{D}\nabla g(\mathbf{y}^*)\right]^+\right\| \\
\leq&\left\|\bar{\mathbf{y}}^k - \bar{\mathbf{y}}^* + \mathbf{D}^{\frac{1}{2}}\left(\nabla g(\mathbf{y}^k) - \nabla g(\mathbf{y}^*)\right)\right\| \\
=&\left\|\bar{\mathbf{y}}^k - \bar{\mathbf{y}}^* - \mathbf{D}^{\frac{1}{2}}\mathbf{B}\mathbf{Q}^{-1}\mathbf{B}^T\mathbf{D}^{\frac{1}{2}}\left(\bar{\mathbf{y}}^k - \bar{\mathbf{y}}^*\right)\right\| \\
=&\left\|\left(\mathbf{I} - \mathbf{D}^{\frac{1}{2}}\mathbf{B}\mathbf{Q}^{-1}\mathbf{B}^T\mathbf{D}^{\frac{1}{2}}\right)\left(\bar{\mathbf{y}}^k - \bar{\mathbf{y}}^*\right)\right\| \\
\leq&\left\|\mathbf{I} - \mathbf{D}^{\frac{1}{2}}\mathbf{B}\mathbf{Q}^{-1}\mathbf{B}^T\mathbf{D}^{\frac{1}{2}}\right\|\left\|\bar{\mathbf{y}}^k - \bar{\mathbf{y}}^*\right\|
\end{aligned}
$$

The first equality holds since $\mathbf{y}^*$ *is a stationary point. The first inequality holds since the projection is non-expansive according to Proposition 1.1.4 in [70]. The second equality holds by plugging in the gradient of dual function* g.

Denote $\mathbf{W} := \mathbf{D}^{\frac{1}{2}}\mathbf{B}\mathbf{Q}\mathbf{B}^T\mathbf{D}^{\frac{1}{2}}$. *By definition, the Euclidean norm of* $\mathbf{I} - \mathbf{W}$ *equals to the largest singular value* ρ *of* $\mathbf{I} - \mathbf{W}$. *Thus,* $\rho = \max_k |1 - \lambda^k|$, *where* λ^k *is k-th eigenvalue of* $\mathbf{W}$. *Since* $\mathbf{W}$ *is positive definite,* $\rho < 1$ *if* $\lambda^{max} < 2$, *where* λ^{max} *is largest eigenvalue of* $\mathbf{W}$. *Therefore, (3.28) is a contraction mapping and* $\mathbf{y}^k$ *converges to dual optimal solution* $\mathbf{y}^*$. *Then* $\mathbf{x}^k$ *converges to the primal optimal solution* $\mathbf{x}^*$ *with* $\mathbf{x}^* = -\mathbf{Q}^{-1}\mathbf{c} - \mathbf{Q}^{-1}\mathbf{B}^T\mathbf{y}^*$. ***Q.E.D.***

3.5 Numerical results

In this section, case studies on the modified IEEE 37-bus and 123-bus distribution systems are carried out to demonstrate the effectiveness of the proposed distributed online algorithm (DIS). Both static and dynamic cases for system loading and PV generation are tested. The performance of DIS is compared with two centralized strategies (CEN1 and CEN2) and a decentralized Q-V droop control scheme (Droop), where CEN2 is to minimize the total loss based on SOCP relaxed branch flow model and is regarded as a benchmark. In addition, the robustness of DIS against communication failure is validated. Note that the actual bus voltage magnitudes obtained from local voltage measurements are used for updating Lagrangian multipliers and hence the approximation error can be avoided. The acceptable range for bus voltage magnitudes is set as [0.95, 1.05] p.u.. All tests are implemented using MATLAB on a personal computer with an Intel Core i5 of 2.4GHz and 12GB memory.

3.5.1 IEEE 37-Bus Distribution System

The system data can be found in [54]. The x_{ij}/r_{ij} ratios are relatively homogeneous, ranging from 0.37 to 0.67. Suppose each bus except the substation bus is equipped with a PV system with 150 kW peak capacity and 1.05×150 kVA rated apparent power. To speed up the convergence, the step sizes are diagonally scaled. Specifically, $\underline{\beta}_i$, $\overline{\beta}_i$, $\underline{\gamma}_i$ and $\overline{\gamma}_i$ are chosen as $0.5/H_{ii}$, where H_{ii} is i-th diagonal entry of matrix $\mathbf{H}$. $\underline{\alpha}_i$ and $\overline{\alpha}_i$ are chosen adaptively in order to quickly eliminate voltage violations. If voltage violation occurs, a big step size will be applied, e.g., 150. Otherwise, a normal step size will be applied, e.g., 30. The stopping criterion is given by $|V_i^k - V_i^{k-1}| < \epsilon$, where the tolerance ϵ is set as 1.0×10^{-4}.

Static Cases

Two representative cases corresponding to high negative net load and positive net load will be considered, as the former leads to overvoltage issues and the latter leads to undervoltage issues.

Case 1: high negative net load during the period of peak PV generation. Without loss of generality, the load at that moment is assumed to be 50% of the peak load.

Case 2: high positive net load during the period of peak load. Since the peak load often occurs at night, PV generation is not available at that moment.

Fig. 3.5 and 3.6 show the convergence of the total loss for cases 1 and 2, where the stopping criterion $|V_i^k - V_i^{k-1}| < \epsilon$ is not invoked. It is observed that the total loss of case 1 is much higher than that of case 2. Besides, the convergence of case 2 is much faster than that of case 1. This is because during the peak PV period the reactive power capacities of PV systems are inadequate to alleviate overvoltage violations alone. Therefore, PV active power curtailment is required, which results in a higher total loss and slower convergence rate. Fig. 3.7 and 3.8 depict the convergence of

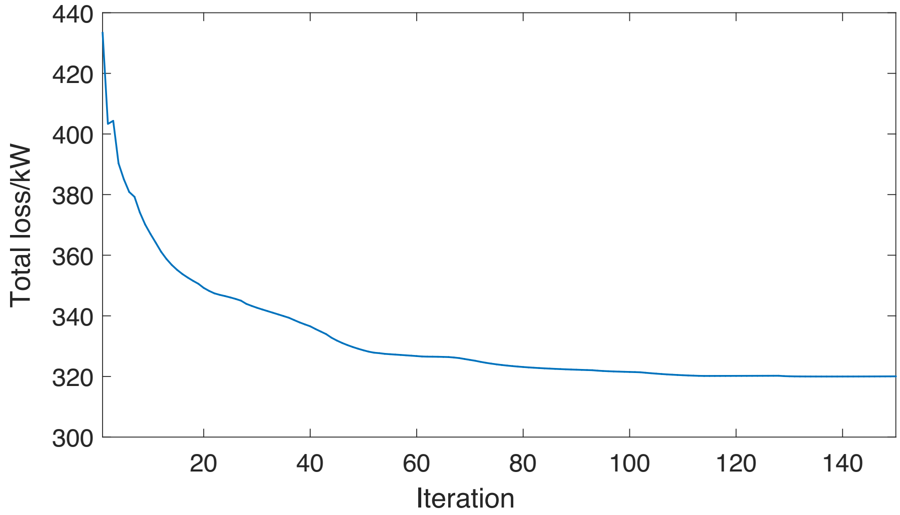

Fig. 3.5 Convergence of the total loss for case 1

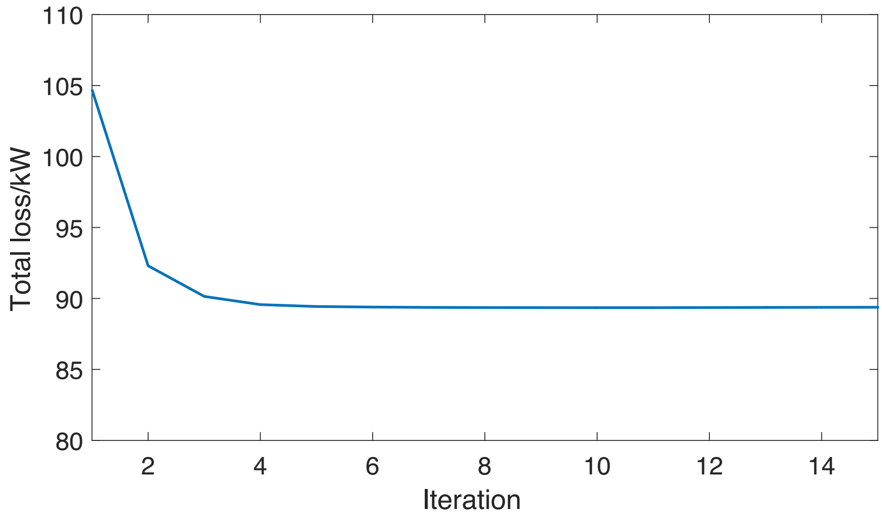

Fig. 3.6 Convergence of the total loss for case 2

the bus voltage magnitudes for cases 1 and 2 when the voltage stopping criterion is invoked. Each curve denotes the variation of voltage magnitude on one bus. Prior to the iterations, severe overvoltage and undervoltage violations are observed for cases 1 and 2, respectively. However, all violations are eliminated with only one iteration for both cases and since then voltages on all buses are maintained within the limits, which validates the high efficiency of the proposed voltage control algorithm.

Tables 3.1 and 3.2 summarize the performance comparisons of four different approaches for cases 1 and 2, respectively, where P^{cur} and P^{loss} denote the PV

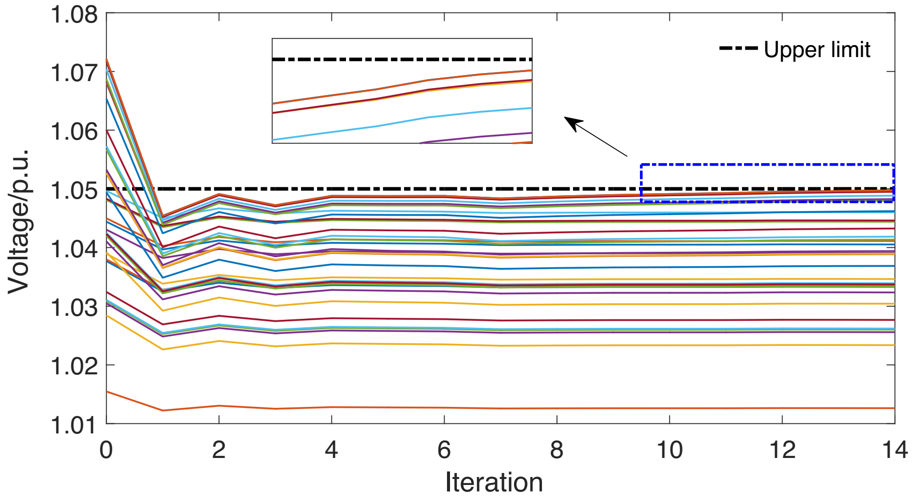

Fig. 3.7 Convergence of the bus voltage magnitudes for case 1

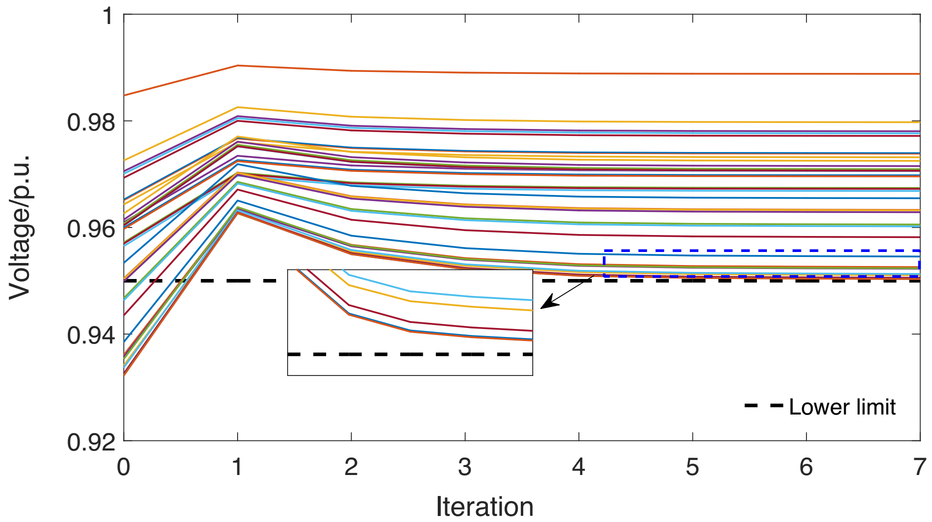

Fig. 3.8 Convergence of the bus voltage magnitudes for case 2

Table 3.1 Performance Comparisons of Different Methods for Case 1

Methods	P^{cur}/kW	P^{loss}/kW	Total loss/kW	Ratio
DIS	20.8	296.8	317.6	1.006
CEN1	154.8	273.5	428.3	1.348
CEN2	25.1	290.5	315.6	1
Droop	–	–	–	–

curtailment and the network loss, respectively. Since droop strategy and CEN2 result in voltage violations in cases 1 and 2, respectively, the corresponding results are

Table 3.2 Performance Comparisons of Different Methods for Case 2

Methods	P^{cur}/kW	P^{loss}/kW	Total loss/kW	Ratio
DIS	0	89.4	89.4	1.001
CEN1	–	–	–	–
CEN2	0	89.3	89.3	1
Droop	0	246.1	246.1	2.753

Note: oscillation is observed in Droop

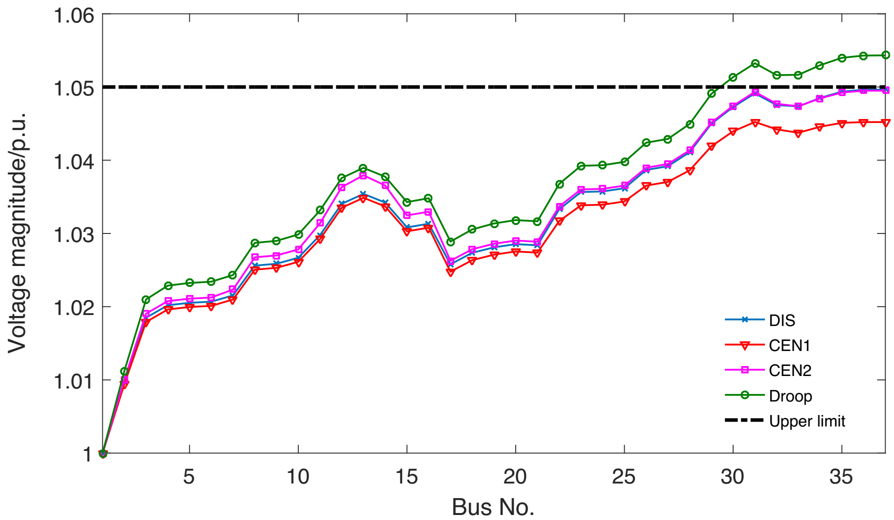

Fig. 3.9 Voltage profiles under different methods for case 1

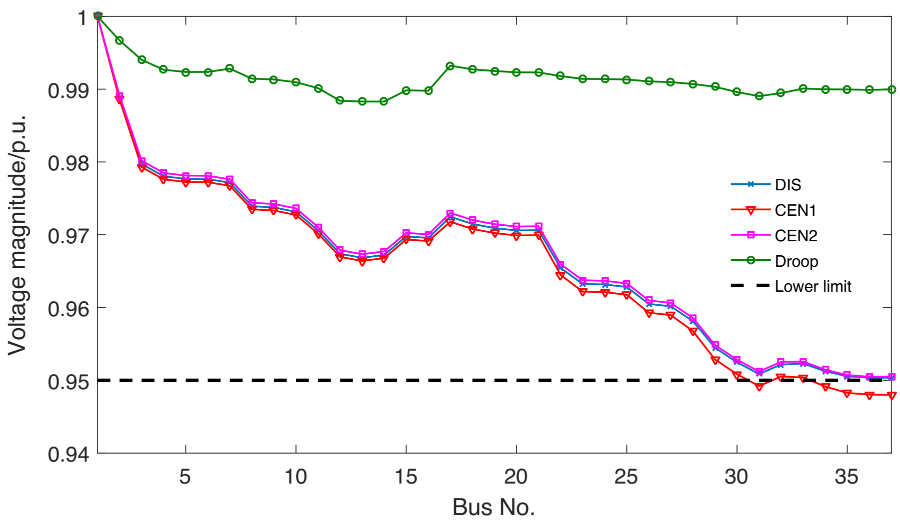

Fig. 3.10 Voltage profiles under different methods for case 2

not indicated in the tables. For each method, the total loss is compared with the benchmark result, i.e. the total loss under CEN2, and the ratios to the benchmark result are exhibited in the tables. The corresponding voltage profiles are plotted in Fig. 3.9 and Fig. 3.10, where the voltage profiles under DIS are almost overlapped with the voltage profiles under CEN2. This phenomenon results from the equally matched performance of DIS and CEN2, which can be observed from Tables 3.1 and 3.2 as well. It is interesting to notice that DIS achieves a better performance in loss minimization and voltage control than CEN1, even though DIS is derived from CEN1. One reason is that in CEN1 the reactive power capacity is fixed at a restricted value, while it is iteratively renewed in DIS. Thus, DIS yields a lower total loss than CEN1. Another reason is that in CEN1 the voltages are approximated using LinDistFlow model. Therein, approximation error could result in voltage violations as observed in Fig. 3.10. By contrast, in DIS the actual voltage values obtained from local voltage measurements are used to update the multipliers and thereby avoiding approximation error. Furthermore, since PV curtailment is necessary in case 1, droop strategy fails to eliminate overvoltage violations as shown in Fig. 3.9. In case 2, it leads to instability and a much higher total loss. Therefore, DIS achieves a near-optimality of CEN2. In addition, it outperforms CEN1 and Droop in terms of voltage control and loss minimization.

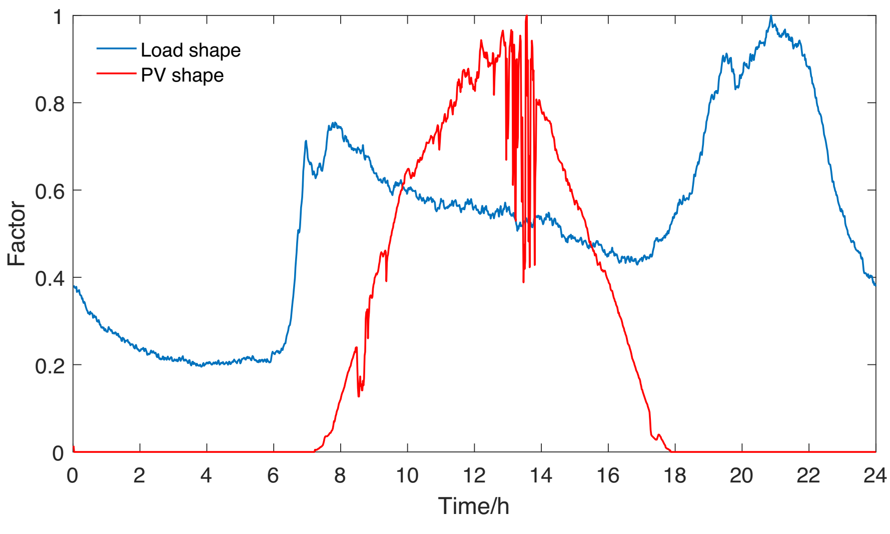

Fig. 3.11 Daily load shape factors and PV shape factors

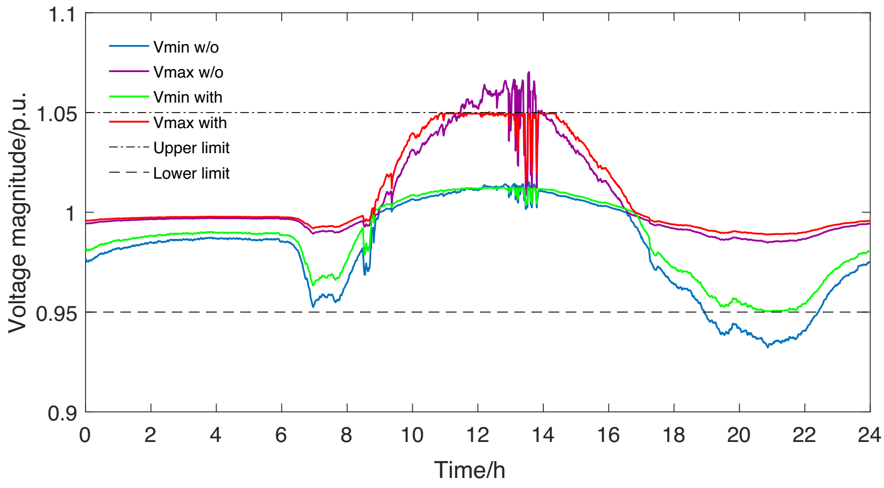

Fig. 3.12 Daily maximum and minimum bus voltage magnitudes with and without DIS control for IEEE 37-bus system

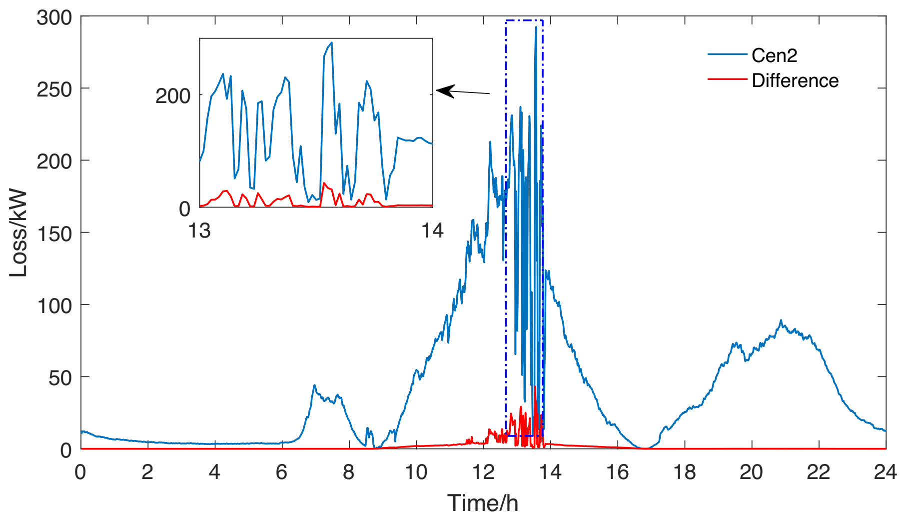

Fig. 3.13 Daily total loss profile of CEN2 and the difference of total loss between DIS and CEN2 for IEEE 37-bus system

Dynamic cases

The dynamic cases for system loading and solar energy are included to verify the effectiveness of our proposed algorithm for online application. The instantaneous maximum available PV active power and load are calculated by multiplying PV and load shape factors with the peak PV capacity and the peak load, respectively. Fig. 3.11 plots the daily load and PV shape factors with one-minute resolution, where the load data and solar irradiance date are obtained from [72] and [56], respectively. Since DIS only involves simple algebraic operations and the limited communication among the neighboring PV systems, the time required to complete one iteration cycle is very short, which is assumed to be 5 seconds [73]. Thus, the maximum iteration number is set as 12 for each time interval. Fig. 3.12 depicts the daily maximum and minimum bus voltage magnitudes with and without DIS control. Severe overvoltage and undervoltage violations are observed without DIS control during the peak PV period and the peak load period, respectively. As expected, all violations are eliminated by DIS control, which verifies the effectiveness of DIS for online voltage control. Fig. 3.13 shows the difference of total loss between DIS and CEN2 as well as the total loss under CEN2. The difference is relatively small and is negligible for most periods. Therefore, DIS achieves a near-optimality of CEN2 even for the dynamic cases.

3.5.2 IEEE 123-bus Distribution System

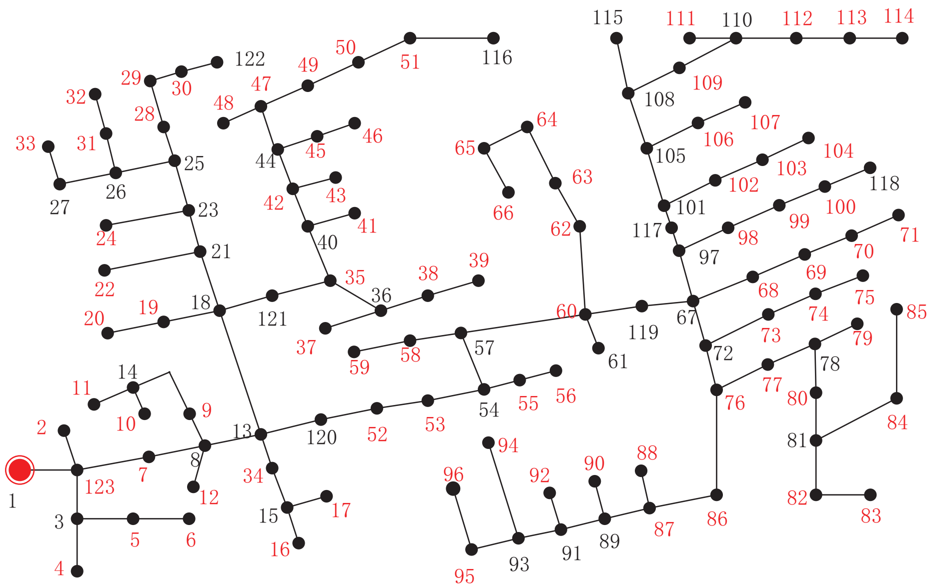

Fig. 3.14 IEEE 123-bus distribution system with PV system location (indicated by red numbers)

To verify the voltage control capability of DIS for large systems, the dynamic cases on the modified IEEE 123-bus distribution system are carried out. Fig. 3.14 depicts

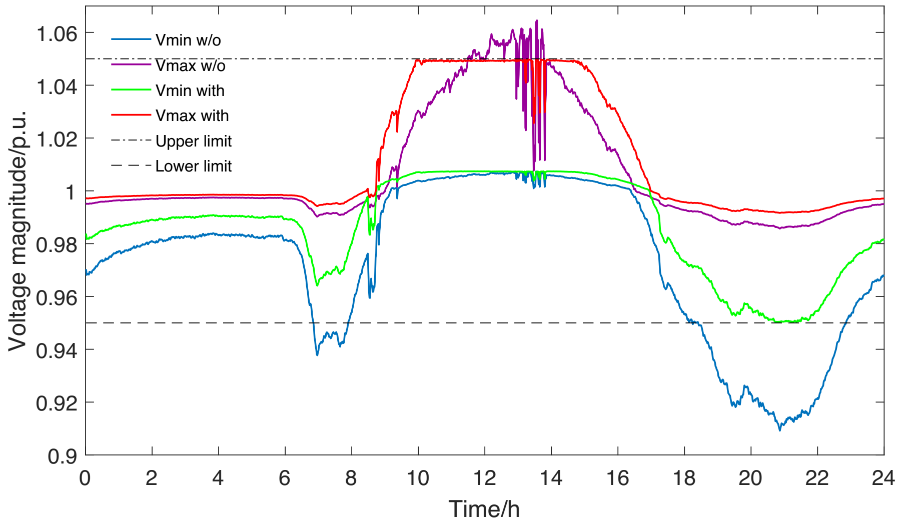

Fig. 3.15 Daily maximum and minimum bus voltage magnitudes with and without DIS control for IEEE 123-bus system

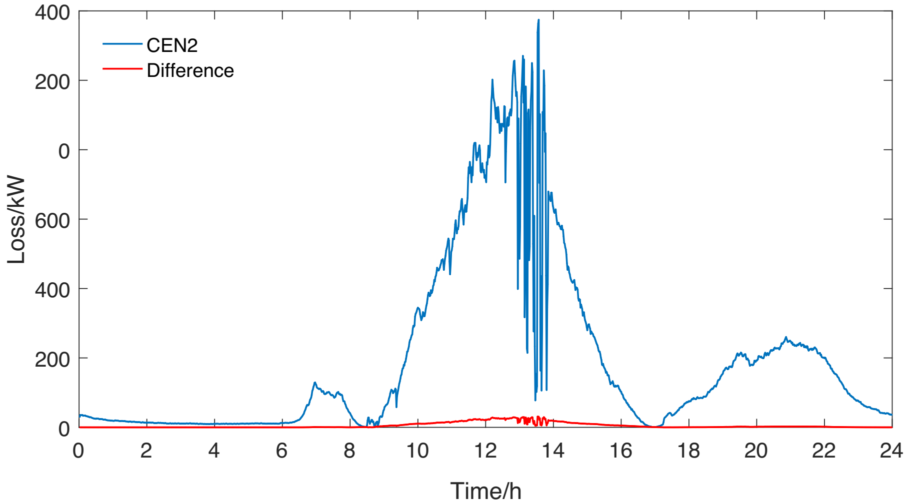

Fig. 3.16 Daily total loss profile of CEN2 and the difference of total loss between DIS and CEN2 for IEEE 123-bus system

the network topology of IEEE 123-bus distribution system, where the locations of PV installations are indicated. The peak capacity of PV system is adjusted as 120 kW and the same load and PV shape factors are applied. Fig. 3.15 shows the daily minimum and maximum bus voltage magnitudes with and without DIS control. As observed, DIS is effective in alleviating overvoltage and undervoltage violations. The comparison on total loss is exhibited in Fig. 3.16 which plots the difference of total

Table 3.3 Comparisons of Robust Performance for 37-bus System

Probability ρ	Case1		Case2	
	Loss/kW	Iteration	Loss/kW	Iteration
0	378.4	6	89.4	7
0.1	381.9	9.8	89.4	8.6
0.2	383.8	10.1	89.4	9.5
0.3	386.0	10.5	89.4	10.2

Table 3.4 Comparisons of Robust Performance for 123-bus System

Probability ρ	Case1		Case2	
	Loss/kW	Iteration	Loss/kW	Iteration
0	568.1	13	131.3	6
0.1	568.3	14	131.3	13.6
0.2	568.5	15	131.3	15.6
0.3	568.7	15.8	131.3	16.2

loss and the total loss under CEN2. For all periods, the difference is negligible, which means the total losses under DIS and CEN2 are almost the same. Thus, DIS could track the near-optimality of CEN2 under the dynamic variations of system conditions.

3.5.3 Robust Performance

Assume that the communication interruptions, e.g. packet drop, occur randomly between PV systems with a probability of ρ. In case of failure in receiving the information from the neighbors for some PV systems, these PV systems would use the information obtained from last iteration. Tables 3.3 and 3.4 list the average total loss and iteration number for 500 simulations under different probabilities for 37-bus and 123-bus system when voltage stopping criterion is invoked. $\rho = 0$ represents intact communication and is the benchmark. Compare with the benchmark, the communication interruptions have little influence on the total loss and slightly increase the iteration number. Therefore, the proposed DIS algorithm is robust against communication failures.

3.6 Summary

In this chapter, a distributed online voltage control algorithm is proposed for multiple PV systems in DNs using dual ascent method. In the proposed algorithm, the voltage control can be implemented immediately. In addition, a close-form solution is derived for PV systems to locally update their active and reactive power set-points based on local voltage measurements and information exchange between neighboring PV systems. The convergence is established analytically and the optimality is guaranteed. The numerical results show the voltage violations can be eliminated with only one iteration and the total loss converges to the near-optimality of a benchmark centralized optimization problem. The robustness against communication interruptions is also validated.

Chapter 4

MPC based Ramp Minimization in Active Distribution Network Using ESSs

4.1 Introduction

The distribution networks (DNs) are undergoing a transition from traditional passive networks to active networks due to the growing integration of distributed energy resources (DERs), the infusion of smart metering and automation infrastructures as well as the emergence of advanced information and communication technologies (ICT) [74]. The active distribution network (ADN) is featured with the capability to actively control and manage the multiple distributed generations (DGs) and other network facilities based on real-time measurements [75]. To this end, a non-profit distribution system operator (DSO) is required to fulfil the reliable and secure operation of the DN like an ISO in transmission network [76]. While the transition of DNs may benefit the society, economy and environment, it also causes troubles to the system operation and control especially when the penetration of renewable DGs, e.g. distributed wind turbines and rooftop PV installations, is high. One of biggest challenges arises from the scarcity of flexible ramping products to tackle the significant variation of net load and thus resulting in the reduction of operational reliability [77]. Since the ramping effect in the DNs will be translated into the transmission network and aggravate the shortage of ramping capability, it is necessary for DSOs to address the ramping problem locally with local flexible resources, e.g. energy storage systems.

Net load, defined as the difference between the actual load and the renewable generation, has been widely used to investigate the impact of renewable energy sources (RESs) integration. Over the years, the California Independent System Operator (CAISO) has observed a sharp decline during the sunrise and a steep rise during the sunset of the daily net load curve, which is known the "duck curve" [34]. As a result, the duck curve of net load imposes a hard ramp-down and ramp-up requirement on power systems. In order to address this issue, several approaches have been proposed. For instance, ref. [78] proposes a ramp limitation oriented control strategy for large scale PV power plants considering the PV curtailment. Though it is effective in controlling the PV ramp, it also leads to the reduction of economic and environmental benefit of RES. Another method is to design new products called flexible ramping products (FRPs) and procure them from the market, which has been extensively studied before recent implementation by CAISO and Midcontinent ISO (MISO) [79]. Ref. [77] evaluates the influence of FRPs on the optimal economic dispatch and shows that FRPs can reduce dispatch cost. Ref. [35] presents a comprehensive review on the modelling and utilization of FRPs. Ref. [80] focuses on the FRP requirement design and demonstrates that FRPs can effectively handle the great variation of net load. To sum up, much effort has been made to alleviate the ramping effect in transmission networks. Nevertheless, few works have studied the ramping problem in DNs even though it can aggravate the shortage of ramping capacity in transmission networks.

Energy storage system (ESS) is believed to be an effective option to accommodate the high penetration of RES. It has gained overwhelming popularity around the world because of its considerable benefits, e.g. deferring the upgrade of generation and network, reducing operating cost and RES curtailment, enhancing system operational flexibility, achieving low-carbon objective, etc. In 2015, the installed capacity of ESSs in U.S. is increased by 243% and is expected to reach 1.5 GW by 2020 [81]. ESS can be classified into utility-scale ESS installed in transmission system and distributed ESS located in DNs and microgrids (MGs). Both types of ESS can provide various services to the power system. In [82], the large-scale ESSs are employed to relieve transmission congestion. In [83], a mobile ESS is used to shift the renewable energy power to peak load periods. In [84], the authors investigate the battery ESSs on providing voltage and frequency regulation in a microgrid. In [85], ESSs play an important role in providing flexible ramping products to transmission network. In [86], ESSs are utilized to enhance the system security by taking corrective action after a contingency. In this chapter, the author endeavours to minimize ramping effect in DNs using distributed ESSs.

To deal with the uncertainties of load demand and renewable energy output, several methods have been proposed, e.g. deterministic optimization [87], stochastic programming [88], robust optimization [89] and model predictive control (MPC) [90]. However, MPC is recognized to be more suitable for short-term operation problem due to its underlying rolling process and effectiveness in dealing with both current and future information. Thus, MPC will be used to carry out the proposed ramp-minimization oriented dispatch model in this chapter. The key idea of MPC is to solve a finite horizon optimization problem in a receding horizon manner and each time only apply the optimal solution of the current time slot to the system. Up to now, MPC has been widely applied in power systems, such as appliance scheduling of a residential building [90], energy management of isolated microgrids [91], real-time power system protection [92].

In ADNs, the power flow no longer unidirectionally moves from the substation to the end-use customers. In order to effectively model bidirectional power flow in ADNs, Baran and Wu proposed a branch flow model in [93], [94]. However, the original branch flow model is nonconvex, which poses challenge in finding a global optimal solution. In this regard, a convexified branch flow model was derived by Farivar and Low in [51] based on the second-order cone (SOC) relaxation and has been widely used since then. For example, ref. [14] applied the SOC relaxed branch flow model to the renewable DG planning problem in ADNs. To guarantee the global optimality, the SOC relaxed branch flow model is also used in the proposed ramp minimization problem.

This chapter proposes a novel MPC based dispatch model for ramp minimization in ADNs using distributed ESSs. The fast responding ESSs are employed to offset the ramp-up and ramp-down effect caused by the diurnal generation pattern of PV systems. MPC is used to carry out the proposed dispatch model, which incorporates both current information and newly updated forecast information. Consequently, ESSs can be appropriately scheduled to avoid latent over-charging or over-discharging during some periods. Numerical results demonstrate that the proposed model and approach can bring about significant reduction of ramping effect and line losses, i.e. more than 80% reduction of maximum ramp and roughly 50% reduction of line losses.

The nomenclature of symbols used in this chapter is given as follows,

Indices and Set

$i/\mathcal{E}$	Index and set of distribution lines
$i/\mathcal{N}$	Index and set of distribution buses
$k/\mathcal{N}^g$	Index and set of PV systems
$m/\mathcal{N}^s$	Index and set of ESSs
$t/\mathcal{T}$	Index and set of time slots
ω	Index of uncertainty scenarios

Parameters

b^g_{ik}	Binary indicator, $b^g_{ik}=1$ if k-th PV system is located at bus i, $b^g_{ik}=0$ otherwise
b^s_{im}	Binary indicator, $b^s_{im}=1$ if m-th ESS is located at bus i, $b^s_{im}=0$ otherwise
$I^{\max}_i$	Line current capacity of the line i
$p^{c,\max}_m$	Maximum charging power of ESS m
$p^{d,\max}_m$	Maximum discharging power of ESS m
$p^g_{k,t}$	Active power output of PV system k in time slot t
$p^{g,\omega}_{k,\tau}$	Active power output of PV system k in time slot τ for scenario ω

$p_{i,t}^{l}$	Active power demand at bus i in time slot t
$p_{i,\tau}^{l,\omega}$	Active power demand at bus i in time slot τ for scenario ω
$q_{i,t}^{l}$	Reactive power demand at bus i in time slot t
$q_{i,\tau}^{l,\omega}$	Reactive power demand at bus i in time slot τ for scenario ω
r_i	Resistance of the line i
$S_m^{\min}$	Minimum allowed energy level of ESS m
$S_m^{\max}$	Maximum allowed energy level of ESS m
$V_i^{\min}$	Lower bound of voltage magnitude at bus i
$V_i^{\max}$	Upper bound of voltage magnitude at bus i
x_i	Reactance of the line i
η_m^c	Charging efficiency of ESS m
η_m^d	Discharging efficiency of ESS m
π_ω	Probability of scenario ω
$\theta_1,\ \theta_2,\ \theta_3$	Weighting factors
Δt	Length of one time slot

Variables

$l_{i,t}$	Squared line current magnitude of line i in time slot t
$l_{i,\tau}^{\omega}$	Squared line current magnitude of line i in time slot τ for scenario ω
$p_{0,t}$	Active power injection into the transmission grid in time slot t
$p_{0,\tau}^{\omega}$	Active power injection into the transmission grid in time slot τ for scenario ω
$p_{i,t}$	Active power injection at bus i in time slot t
$p_{m,t}^{c}$	Charging power of ESS m in time slot t
$p_{m,\tau}^{c,\omega}$	Charging power of ESS m in time slot τ for scenario ω
$p_{m,t}^{d}$	Discharging power of ESS m in time slot t
$p_{m,\tau}^{d,\omega}$	Discharging power of ESS m in time slot τ for scenario ω
$P_{j,t}$	Active flow on the line j in time slot t
$P_{j,\tau}^{\omega}$	Active flow on the line j in time slot τ for scenario ω
$q_{0,t}$	Reactive power injection into the transmission grid in time slot t

$q_{0,\tau}^{\omega}$ Reactive power injection into the transmission grid in time slot τ for scenario ω

$q_{i,t}$ Reactive power injection at bus i in time slot t

$Q_{j,t}$ Reactive flow on the line j in time slot t

$Q_{j,\tau}^{\omega}$ Reactive flow on the line j in time slot τ for scenario ω

$S_{m,t}$ Energy level of ESS m at the end of time slot t

$S_{m,\tau}^{\omega}$ Energy level of ESS m at the end of time slot τ for scenario ω

$v_{i,t}$ Squared voltage magnitude at bus i in time slot t

$v_{i,\tau}^{\omega}$ Squared voltage magnitude at bus i in time slot τ for scenario ω

4.2 System Model and Problem Formulation

4.2.1 Branch Flow Model in Distribution Networks

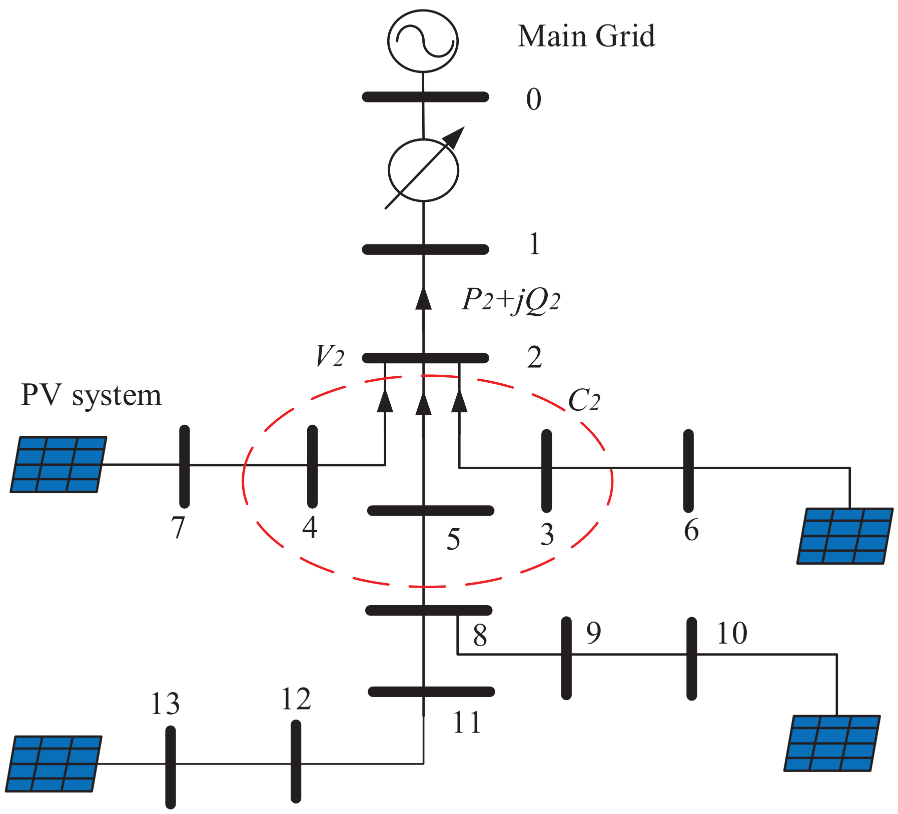

Fig. 4.1 A typical distribution network topology

Consider a distribution network, which is typically radial as shown in Fig. 4.1. Let $\mathcal{G} := (\mathcal{N}, \mathcal{E})$ denote the topology of the DN, where $\mathcal{N} := \{0, 1, ..., N\}$ represents the set of buses and $\mathcal{E}$ represents the set of directed lines. Note that each bus i except the substation bus (indexed by 0) has a unique ancestor bus, denoted by A_i, and a set of child buses, denoted by C_i. For instance, bus 2 has a unique ancestor which is bus 1 and several child buses including bus 3, 4 and 5, i.e. $A_2 = 1$ and $C_2 = \{3, 4, 5\}$. Moreover, the direction of each line is assume to be from a bus i to its ancestor bus A_i as illustrated in Fig. 4.1. Thus, the line from bus i to its ancestor bus A_i can be uniquely labeled as i so that the line index is consistent with the bus index. Then, the line set can be expressed as $\mathcal{E} := \{1, ..., N\}$. In a radial distribution network, branch flow model (BFM) has been widely used to model the power flow equations [51], as shown below.

$$\sum_{j \in C_0} (P_{j,t} - r_j l_{j,t}) + p_{0,t} = 0 \tag{4.1a}$$

$$\sum_{j \in C_i} (P_{j,t} - r_j l_{j,t}) + p_{i,t} = P_{i,t} \qquad \forall i \in \mathcal{N} \backslash 0 \tag{4.1b}$$

$$\sum_{j \in C_0} (Q_{j,t} - x_j l_{j,t}) + q_{0,t} = 0 \tag{4.1c}$$

$$\sum_{j \in C_i} (Q_{j,t} - x_j l_{j,t}) + q_{i,t} = Q_{i,t} \qquad \forall i \in \mathcal{N} \backslash 0 \tag{4.1d}$$

$$v_{i,t} - v_{A_i,t} = 2(r_i P_{i,t} + x_i Q_{i,t}) - (r_i^2 + x_i^2) l_{i,t} \qquad \forall i \in \mathcal{E} \tag{4.1e}$$

$$l_{i,t} = \frac{P_{i,t}^2 + Q_{i,t}^2}{v_{i,t}} \qquad \forall i \in \mathcal{E} \tag{4.1f}$$

where (4.1a) and (4.1b) represent the active power balance equations at substation bus and other buses, respectively; (4.1c) and (4.1d) represent the reactive power balance equations at substation bus and other buses, respectively. (4.1e) describes the voltage drop at each line and (4.1f) denotes the relationship between $l_{i,t}$ and $v_{i,t}$.

Note that (4.1f) is nonconvex, which makes it difficult to find the global optimal solution to the BFM based OPF problem. In order to convexify (4.1f), it is relaxed into an inequality as (4.2) and then reformulated into a second-order cone (SOC) constraint as (4.3).

$$l_{i,t} \geq \frac{P_{i,t}^2 + Q_{i,t}^2}{v_{i,t}} \qquad \forall i \in \mathcal{E} \tag{4.2}$$

$$\|(2P_{i,t},\ 2Q_{i,t},\ l_{i,t} - v_{i,t})\|_2 \leq l_{i,t} + v_{i,t} \qquad \forall i \in \mathcal{E} \tag{4.3}$$

It has been proved in [51] that the relaxation is exact as long as the network is radial and the objective function of the OPF problem is strictly increasing in l_i. In the proposed model, the equality in (4.2) also holds since the network loss is a strict increasing function of l_i.

In an OPF problem, the voltage magnitude of each bus and current magnitude of each line should be ensured not to exceed the bounds.

$$(V_i^{\min})^2 \leq v_{i,t} \leq (V_i^{\max})^2 \qquad \forall i \in \mathcal{N} \tag{4.4}$$

$$l_{i,t} \leq (I_i^{\max})^2 \qquad \forall i \in \mathcal{E} \tag{4.5}$$

4.2.2 Ramp-events and Ramp Index

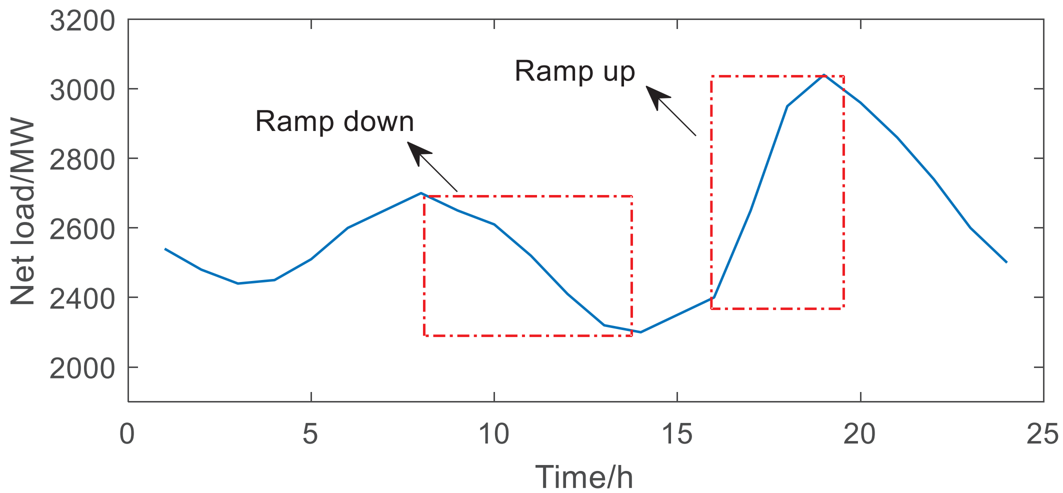

Fig. 4.2 A typical daily net load curve with illustration of ramp-events

The growing integration of PV generation introduces significant variability to the system net load. Specifically, the daily net load curve has been observed a sharp decline during the sunrise and a steep rise during the sunset as shown in Fig. 4.2. As a result, more flexible resources, e.g. fast start generators, are required to provide ramping support. In transmission level, the market mechanism has been established to procure the flexible ramping products in several electricity markets, e.g. California market and midcontinent market in U.S. However, few works have investigated the ramp problem in distribution networks even though it will aggravate the inadequacy of overall ramping capacity. Therefore, a novel dispatch model is proposed for the ramp minimization in DNs so as to enhance the reliability and efficiency of the entire power system. To this end, the author first defines the ramp index in DNs for each time slot t to quantify the ramping effect, as shown below.

$$IR_t = |p_{0,t} - p_{0,t-1}| \tag{4.6}$$

where $p_{0,t}$ represents net load of the entire distribution network in time slot t.

4.2.3 Energy Storage System Model

Over the past few years, great advances have been made in the battery storage technologies, especially in the lithium-ion battery. As a result, the installation of battery energy storages is experiencing a remarkable growth over the world. In this chapter, the battery ESSs are utilized to mitigate the ramping effect through charging during the ramp-down periods and discharging during the ramp-up periods. Since the detailed battery ESS technologies are beyond the scope of this chapter, only the general mathematical model of ESSs is presented. The charging and discharging power at each time slot t should be maintained within the allowable ranges, as shown below.

$$0 \le p^c_{m,t} \le p^{c,\max}_m \qquad \forall m \in \mathcal{N}^s,\ \forall t \in \mathcal{T} \tag{4.7}$$

$$0 \le p^d_{m,t} \le p^{d,\max}_m \qquad \forall m \in \mathcal{N}^s,\ \forall t \in \mathcal{T} \tag{4.8}$$

The dynamics of ESSs between two consecutive time slots can be described as

$$S_{m,t} = S_{m,t-1} + (\eta_m^c \cdot p_{m,t}^c - 1/\eta_m^d \cdot p_{m,t}^d) \cdot \Delta t \tag{4.9}$$

The amount of stored energy should not exceed the maximum allowed energy level $S_m^{\max}$ or fall below the minimum allowed level $S_m^{\min}$.

$$S_m^{\min} \leq S_{m,t} \leq S_m^{\max} \qquad \forall m \in \mathcal{N}^s,\ \forall t \in \mathcal{T} \tag{4.10}$$

Frequent employment of ESS will shorten its life span. Therefore, the degradation cost should be taken into account to avoid overuse of ESS. In the proposed model, the degradation cost is modeled as a linear function of charging and discharging power like [95].

$$C_{m,t}^d = c_m^d \cdot (\eta_m^c p_{m,t}^c + p_{m,t}^d/\eta_m^d) \cdot \Delta t \tag{4.11}$$

where $C_{m,t}^d$ is degradation cost of ESS m in time slot t and c_m^d is the unit degradation cost.

4.2.4 Look-ahead Dispatch Model for Ramp Minimization

In this subsection, a look-ahead dispatch model is presented for distribution system operators to minimize the ramping effect and meanwhile to ensure the system is under a normal operating condition by leveraging the full potential of ESSs in providing voltage support and ramping support. Besides the ramp index, network loss and ESS degradation cost are also taken into account. Thus, the objective function is the weighted sum of the three items. The problem formulation is written as below.

$$\min \quad \theta_1 \cdot IR_t + \theta_2 \cdot \sum_{i \in \mathcal{E}} r_i l_{i,t} + \theta_3 \sum_{m \in \mathcal{N}^s} C_{m,t}^d \tag{4.12a}$$

variables: $p_{0,t}, q_{0,t}, p_{m,t}^d, p_{m,t}^c, P_{j,t}, Q_{j,t}, l_{j,t}, v_{i,t}, S_{m,t}$

$$\text{s.t. } p_{0,t} = -\sum_{j \in C_0} (P_{j,t} - r_j l_{j,t}) \tag{4.12b}$$

$$\sum_{k\in\mathcal{N}^g} b^g_{ik} p^g_{k,t} + \sum_{m\in\mathcal{N}^s} (b^s_{im} p^d_{m,t} - b^s_{im} p^c_{m,t}) - p^l_{i,t} = P_{i,t} - \sum_{j\in C_i} (P_{j,t} - r_j l_{j,t}) \quad \forall j \in \mathcal{N}\backslash 0 \tag{4.12c}$$

$$q_{0,t} = -\sum_{j\in C_0} (Q_{j,t} - x_j l_{j,t}) \tag{4.12d}$$

$$-q^l_{i,t} = Q_{i,t} - \sum_{j\in C_i} (Q_{j,t} - x_j l_{j,t}) \qquad \forall i \in \mathcal{N}\backslash 0 \tag{4.12e}$$

$$v_{i,t} - v_{A_i,t} = 2(r_i P_{i,t} + x_i Q_{i,t}) - (r_i^2 + x_i^2) l_{i,t} \qquad \forall i \in \mathcal{E} \tag{4.12f}$$

$$\left\|(2P_{i,t},\ 2Q_{i,t},\ l_{i,t} - v_{i,t})\right\|_2 \le l_{i,t} + v_{i,t} \qquad \forall i \in \mathcal{E} \tag{4.12g}$$

$$v_{0,t} = 1 \tag{4.12h}$$

$$(V_i^{\min})^2 \le v_{i,t} \le (V_i^{\max})^2 \qquad \forall i \in \mathcal{N}\backslash 0 \tag{4.12i}$$

$$l_{j,t} \le (I_j^{\max})^2 \qquad \forall j \in \mathcal{E} \tag{4.12j}$$

$$0 \le p^c_{m,t} \le p^{c,\max}_m \qquad \forall m \in \mathcal{N}^s \tag{4.12k}$$

$$0 \le p^d_{m,t} \le p^{d,\max}_m \qquad \forall m \in \mathcal{N}^s \tag{4.12l}$$

$$S_{m,t} = S_{m,t-1} + (\eta^c_m \cdot p^c_{m,t} - 1/\eta^d_m \cdot p^d_{m,t}) \cdot \Delta t \qquad \forall m \in \mathcal{N}^s \tag{4.12m}$$

$$S_m^{\min} \le S_{m,t} \le S_m^{\max} \qquad \forall m \in \mathcal{N}^s \tag{4.12n}$$

where $\theta_1,\ \theta_2$ and θ_3 are weighting factors, the second term in the objective represents the network loss; (4.12b) and (4.12c) are active power balance equations at substation bus and other buses, respectively. (4.12d) and (4.12e) are reactive power balance equations at substation bus and other buses, respectively. (4.12f) describes the voltage drop on line i. (4.12g) is a second-order cone constraint relaxed from (4.1f). (4.12h) denotes the voltage magnitude at the substation bus and (4.12i) are voltage constraints at other buses. (4.12j) represents the distribution line capacity constraint. (4.12k)-(4.12n) are constraints related to ESSs.

4.3 Model Predictive Control based Dispatch Model for Ramp Minimization

4.3.1 Model Predictive Control (MPC)

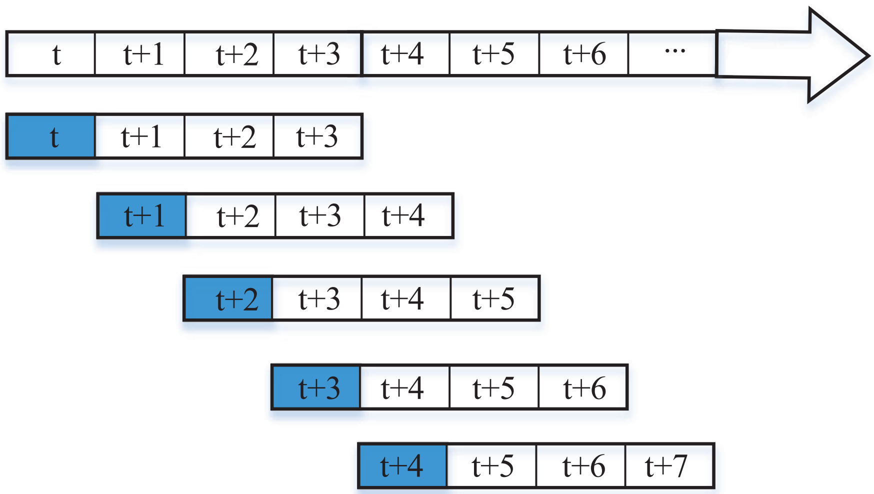

Fig. 4.3 Illustration of model predictive control with a horizon of 4 time slots

The MPC method is employed to carry out the proposed ramp-minimization oriented dispatch model. The key idea of MPC is to solve a finite horizon optimization problem in a receding horizon manner based on the latest updated information. Each time only the optimization result of the current time slot will be applied. Fig. 4.3 illustrates the process of a model predictive control with a horizon of 4 time slots. In order to implement the MPC method, the single-period look-ahead dispatch problem (4.12) needs to be extended into a multi-period dispatch problem that covers the operation of current time slot and the following $N-1$ time slots. Moreover, it is assumed that at any time slot t, the actual load and PV information is known to the DSO as assumed in problem (4.12). The detailed process to implement the MPC based dispatch model is illustrated as below.

i) At time slot t, the DSO collects the load and PV information of the current time slot and updates their forecast information for the following $N-1$ time slots.

ii) Based on the information obtained in step i), the DSO solves the multi-period dispatch problem for ramp minimization and only applies the optimal solution of the current time slot t to the ESSs.

iii) When the time moves forward to $t+1$, the DSO executes exactly the same procedure described in step i) and ii).

The major difference between the MPC based model and the single-period model is that the former considers not only the current information but also some future information. Consequently, the short-sightedness can be avoided. For instance, it is likely that solving problem (4.12) leads to a situation where the energy stored in ESSs is inadequate to mitigate the ramp-up effect of the next few time slots due to the depletion of stored energy at current time slot. However, such situation can be successfully ruled out using the MPC based dispatch model. Note that increasing the horizon length may produce a more robust result against the uncertainties, but it also leads to the decline of forecast accuracy and increase of optimization complexity. Thus, there is trade-off in selecting the length of the horizon. In this application, the author considers a horizon of 4 time slots with the duration of each time slot being 1h.

4.3.2 Stochastic PV and Load Model

It is assumed that except the current time slot t, the future information of PV generation and load demand are random variables and unknown to the DSO. Therefore, the DSO needs to predict the PV output and load value for the next $N-1$ time slots. In this chapter, to obtain the forecasting scenarios of PV and load over the next three time slots, the Gaussian copula approach [96] is employed. Firstly, the marginal predictive distributions of PV and load are derived, respectively, based on the historical information up to the forecast time. Subsequently, a set of multivariate Gaussian random numbers is generated, in which the interdependence is modeled by exponential covariance structure [96, 97]. Eventually, these Gaussian random numbers are transformed into a set of temporal realizations (e.g. 1000) through all

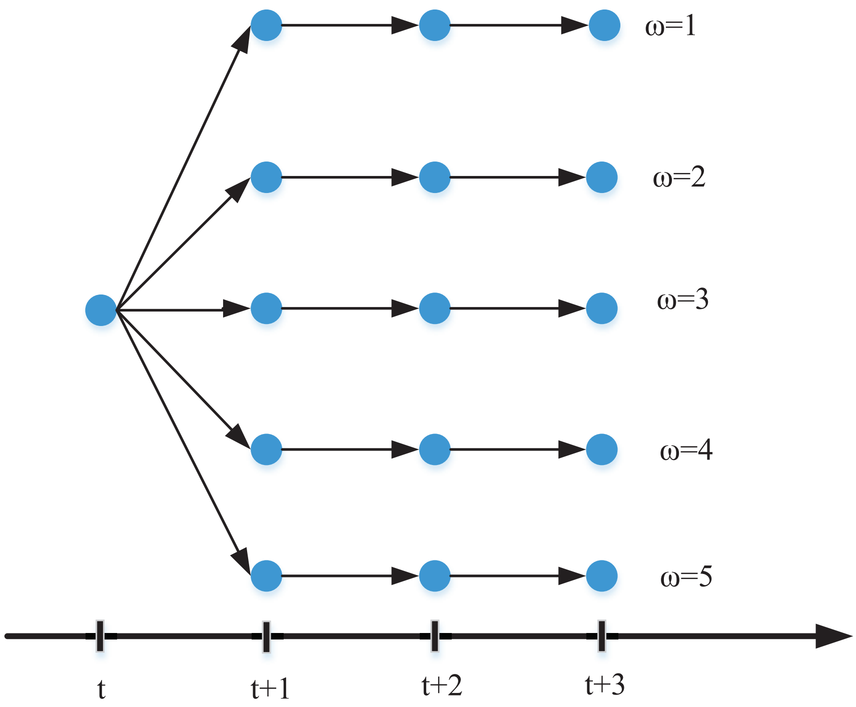

Fig. 4.4 A scenario tree with 5 scenarios over 4 time slots

predictive distributions of PV and load. Given a small number of trajectories are more favored by the decision-makers, a Kantorovich distance (KD) based backward reduction technique [98] is used to curtail the generated scenarios. Fig. 4.4 depict a scenario tree with 5 scenarios over four time slots, where each trajectory represents a scenario. Since the methodology of scenario generation and reduction is beyond the scope of this chapter, the author will not go into detail of it.

4.3.3 MPC-based Stochastic Dispatch Model

The cost function for a given scenario ω and time slot τ is defined as below, which is the same as objective function of problem (4.12).

$$F_{\tau}^{\omega} = \theta_1 \cdot \left| p_{0,\tau}^{\omega} - p_{0,\tau-1}^{\omega} \right| + \theta_2 \cdot \sum_{i \in \mathcal{E}} r_i l_{i,\tau}^{\omega} + \theta_3 \sum_{m \in \mathcal{N}^s} C_{m,\tau}^{d,\omega} \tag{4.13}$$

$$\tau = t, t+1, t+2, t+3 \quad \omega = 1, 2, 3, 4, 5$$

For mathematical conciseness, the decision variables of the current time slot t are also labelled with a superscript ω. Actually, they are independent of the scenario index ω as the only scenario of that time slot is the realized information of load and PV generation. In other words, there is one dispatch result for the current time slot and only it will be applied. Likewise, $p^{\omega}_{0,t-1}$ and $S^{\omega}_{m,t-1}$ are also independent of ω as they are parameters representing the information of the last time slot.

The objective of the MPC based dispatch model is to minimize the weighted sum of F^{ω}_{τ} with the weights being the scenario probabilities π_{ω}. The constraints for each time slot and each scenario is exactly the same as the constraints in problem (4.12).

$$\min \quad \sum_{\omega=1}^{5}\sum_{\tau=t}^{t+3} \pi_{\omega} F^{\omega}_{\tau} \tag{4.14a}$$

$$\text{variables: } p^{\omega}_{0,\tau}, q^{\omega}_{0,\tau}, p^{d,\omega}_{m,\tau}, p^{c,\omega}_{m,\tau}, P^{\omega}_{j,\tau}, Q^{\omega}_{j,\tau}, l^{\omega}_{j,\tau}, v^{\omega}_{i,\tau}, S^{\omega}_{m,\tau}$$

$$\tau = t, t+1, t+2, t+3 \quad \omega = 1,2,3,4,5$$

$$\text{s.t. } p^{\omega}_{0,\tau} = -\sum_{j\in C_0} (P^{\omega}_{j,\tau} - r_j l^{\omega}_{j,\tau}) \tag{4.14b}$$

$$\sum_{k\in\mathcal{N}^g} b^g_{ik} p^{g,\omega}_{k,\tau} + \sum_{m\in\mathcal{N}^s} (b^s_{im} p^{d,\omega}_{m,\tau} - b^s_{im} p^{c,\omega}_{m,\tau}) - p^{l,\omega}_{i,\tau} = P^{\omega}_{i,\tau} - \sum_{j\in C_i} (P^{\omega}_{j,\tau} - r_j l^{\omega}_{j,\tau}) \quad \forall j \in \mathcal{N}\backslash 0 \tag{4.14c}$$

$$q^{\omega}_{0,\tau} = -\sum_{j\in C_0} (Q^{\omega}_{j,\tau} - x_j l^{\omega}_{j,\tau}) \tag{4.14d}$$

$$-q^{l,\omega}_{i,\tau} = Q^{\omega}_{i,\tau} - \sum_{j\in C_i} (Q^{\omega}_{j,\tau} - x_j l^{\omega}_{j,\tau}) \qquad \forall i \in \mathcal{N}\backslash 0 \tag{4.14e}$$

$$v^{\omega}_{i,\tau} - v^{\omega}_{A_i,\tau} = 2(r_i P^{\omega}_{i,\tau} + x_i Q^{\omega}_{i,\tau}) - (r_i^2 + x_i^2) l^{\omega}_{i,\tau} \qquad \forall i \in \mathcal{E} \tag{4.14f}$$

$$\left\| \left(2P^{\omega}_{i,\tau},\ 2Q^{\omega}_{i,\tau},\ l^{\omega}_{i,\tau} - v^{\omega}_{i,\tau}\right) \right\|_2 \le l^{\omega}_{i,\tau} + v^{\omega}_{i,\tau} \qquad \forall i \in \mathcal{E} \tag{4.14g}$$

$$v^{\omega}_{0,\tau} = 1 \tag{4.14h}$$

$$(V_i^{\min})^2 \le v^{\omega}_{i,\tau} \le (V_i^{\max})^2 \qquad \forall i \in \mathcal{N}\backslash 0 \tag{4.14i}$$

$$l^{\omega}_{j,\tau} \le (I_j^{\max})^2 \qquad \forall j \in \mathcal{E} \tag{4.14j}$$

$$0 \le p^{c,\omega}_{m,\tau} \le p^{c,\max}_{m} \qquad \forall m \in \mathcal{N}^s \tag{4.14k}$$

$$0 \le p^{d,\omega}_{m,\tau} \le p^{d,\max}_{m} \qquad \forall m \in \mathcal{N}^s \tag{4.14l}$$

$$S^{\omega}_{m,\tau} = S^{\omega}_{m,\tau-1} + (\eta^c_m \cdot p^{c,\omega}_{m,\tau} - 1/\eta^d_m \cdot p^{d,\omega}_{m,\tau}) \cdot \Delta t \qquad \forall m \in \mathcal{N}^s \tag{4.14m}$$

$$S_m^{\min} \leq S_{m,\tau}^{\omega} \leq S_m^{\max} \qquad \forall m \in \mathcal{N}^s \tag{4.14n}$$

where $p_{k,t}^{g,\omega}$, $p_{i,t}^{l,\omega}$ and $q_{i,t}^{l,\omega}$ are PV output, active load and reactive load of present time slot t, respectively; $p_{k,\tau}^{g,\omega}$, $p_{i,\tau}^{l,\omega}$ and $q_{i,\tau}^{l,\omega}$ are forecasted PV output, active load and reactive load for time slot $\tau(\tau = t+1, t+2, t+3)$ and scenario $\omega(\omega = 1,2,3,4,5)$. Note the objective function is non-smooth. But it can be equivalently converted into a smooth function by replacing the absolute value with a new variable and including two additional inequality constraints.

4.4 Case Studies

In this section, both the single-period dispatch model (denoted as **single t**) and MPC-based dispatch model (denoted as **MPC**) are tested on the modified IEEE 37-bus distribution network for the ramp minimization of a day. Detailed information of the network can be found in [54]. The nominal voltage value of the distribution system is $4.8kV$ and per-unit value is used in the case studies. Fig. 4.5 shows the network topology of IEEE 37-bus distribution feeder with 20 distributed PV installations and 10 distributed ESSs. Fig. 4.6 depicts the realized total active load and PV generation of a day. The parameters related to the PV system and ESS are listed in Table 4.1 along with other parameters.

4.4.1 Performance Comparisons

Fig. 4.7 and 4.8 show the total net load and ramp index of a day under three cases, respectively. Without ESS, the net load experiences a significant ramp-down event from 9:00 to 13:00 and a substantial ramp-up event from 13:00 to 19:00 due to the rapid variation of PV output. But the ramping effect is significantly mitigated when ESSs are integrated as shown in Fig. 4.7 and 4.8. Moreover, ESSs also facilitate the valley-filling and peak-shaving of net load to a great extent. Fig. 4.7 and 4.8 also demonstrate that the MPC based model has a much better performance than the single-period model in terms of ramp mitigation and load-shift. The maximum

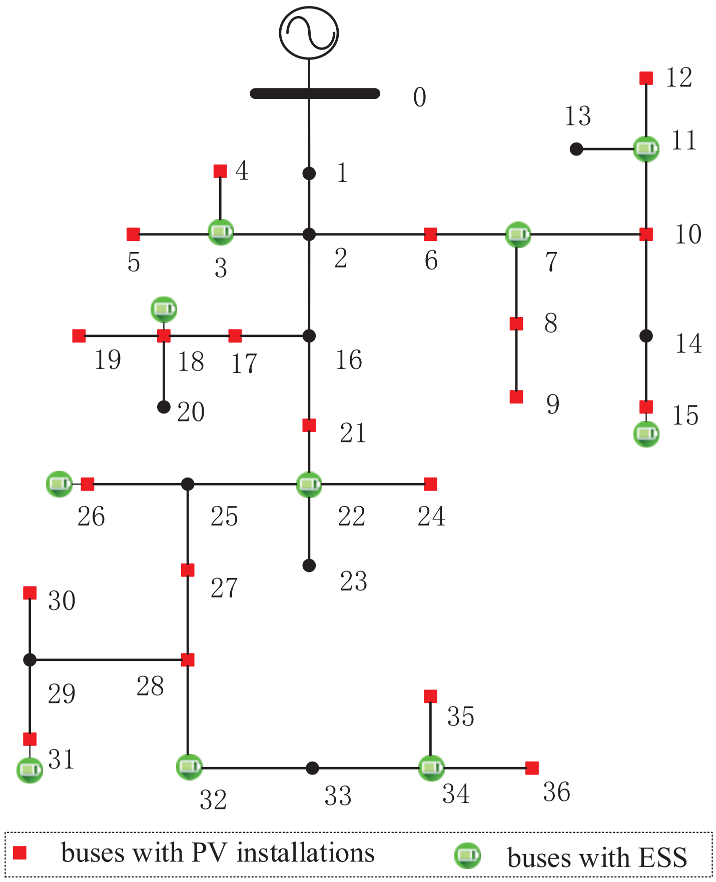

Fig. 4.5 IEEE 37-bus distribution network with PV installations and ESSs

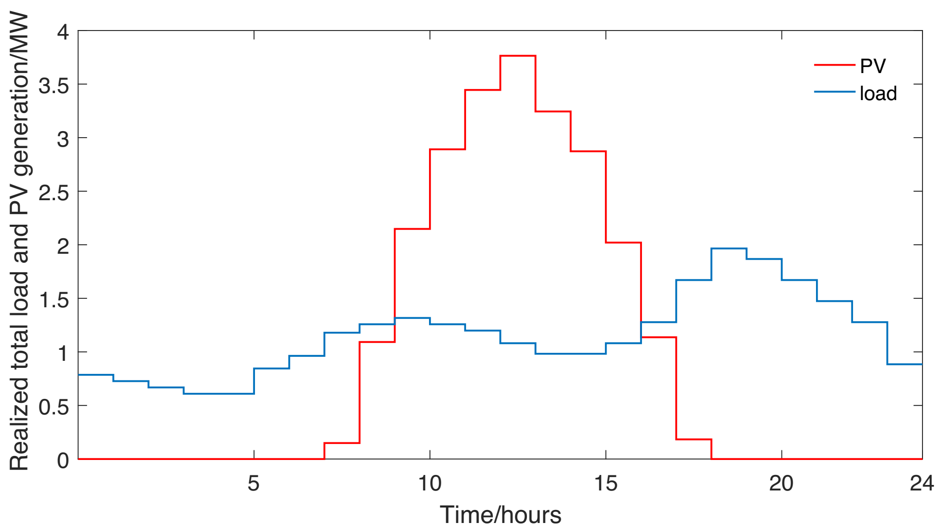

Fig. 4.6 Realized total active load and PV generation of the distribution network

Table 4.1 Parameters for single-period dispatch model and MPC based dispatch model

PV system capacity $p_k^{g,\max}$	200 kVA
Maximum charging power $p_m^{c,\max}$	200 kW
Maximum discharging power $p_m^{d,\max}$	200 kW
Minimum allowed energy level $S_m^{\min}$	100 kWh
Maximum allowed energy level $S_m^{\max}$	1000 kWh
Charging efficiency η_m^c	90%
Discharging efficiency η_m^d	90%
Unite degradation cost c_m^d	\$10/MWh
Lower voltage limit $V_i^{\min}$	0.95 p.u.
Upper voltage limit $V_i^{\max}$	1.05 p.u.
Weight θ_1	0.8
Weight θ_2	0.1
Weight θ_3	0.1

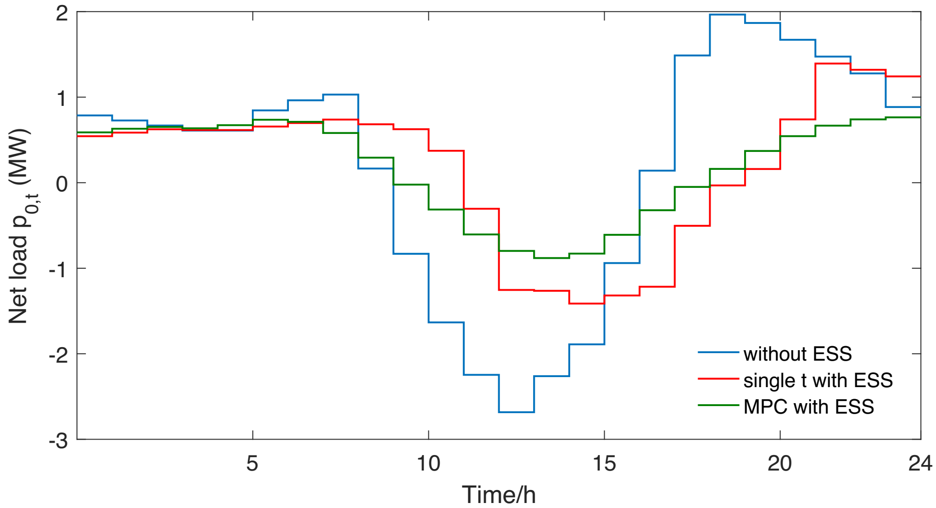

Fig. 4.7 Daily net load of the distribution system under three cases, without ESS, single t with ESS and MPC with ESS

ramp is only reduced by roughly 25% and is shifted to another period using the single-period model. In contrast, the MPC based model mitigates the maximum ramp by more than 80% and maintain the ramp indices at relatively low values over the whole day. The reason is that MPC based model takes future forecast information into account and thus avoiding over-charging or over-discharging of ESSs. Fig. 4.9 shows the voltage mismatch error of the three cases. The voltage mismatch error is defined as the 2-norm of the voltage difference between the actual bus voltages and

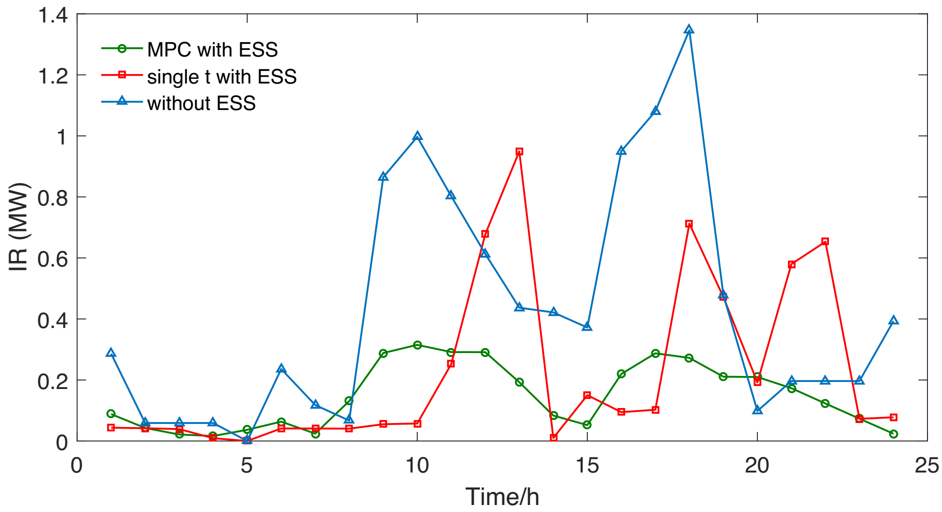

Fig. 4.8 Ramp index under three cases, without ESS, single t with ESS and MPC with ESS

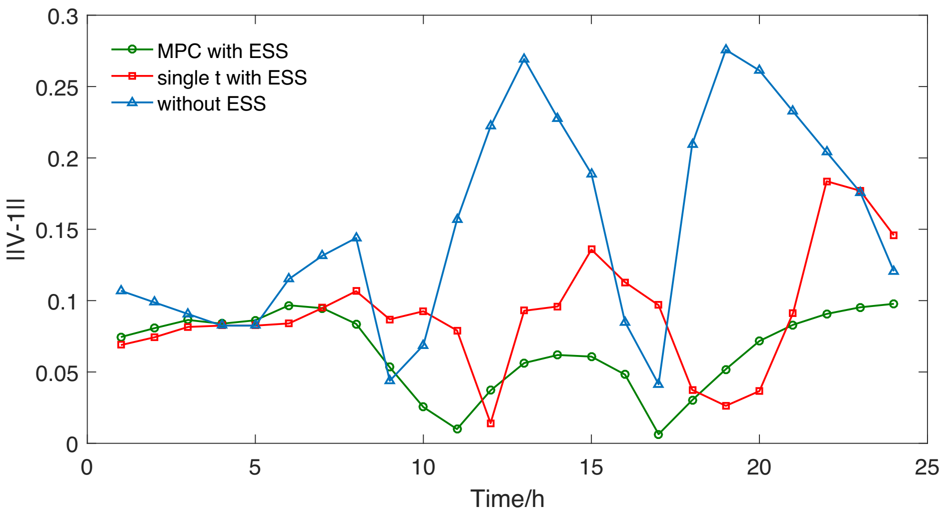

Fig. 4.9 Voltage mismatch error under three cases, without ESS, single t with ESS and MPC with ESS

the reference values. Thus, the smaller voltage mismatch error indicates a better voltage profile. Since ESS has the voltage regulation capability in DNs, integration of ESSs will reduce the voltage mismatch error as shown in Fig. 4.9. In addition, MPC based model leads to a better voltage regulation due to its appropriate ESS scheduling.

To further illustrate the superiority of MPC based model over the single-period model, the author depicts the daily variation of the stored energy level in ESSs for

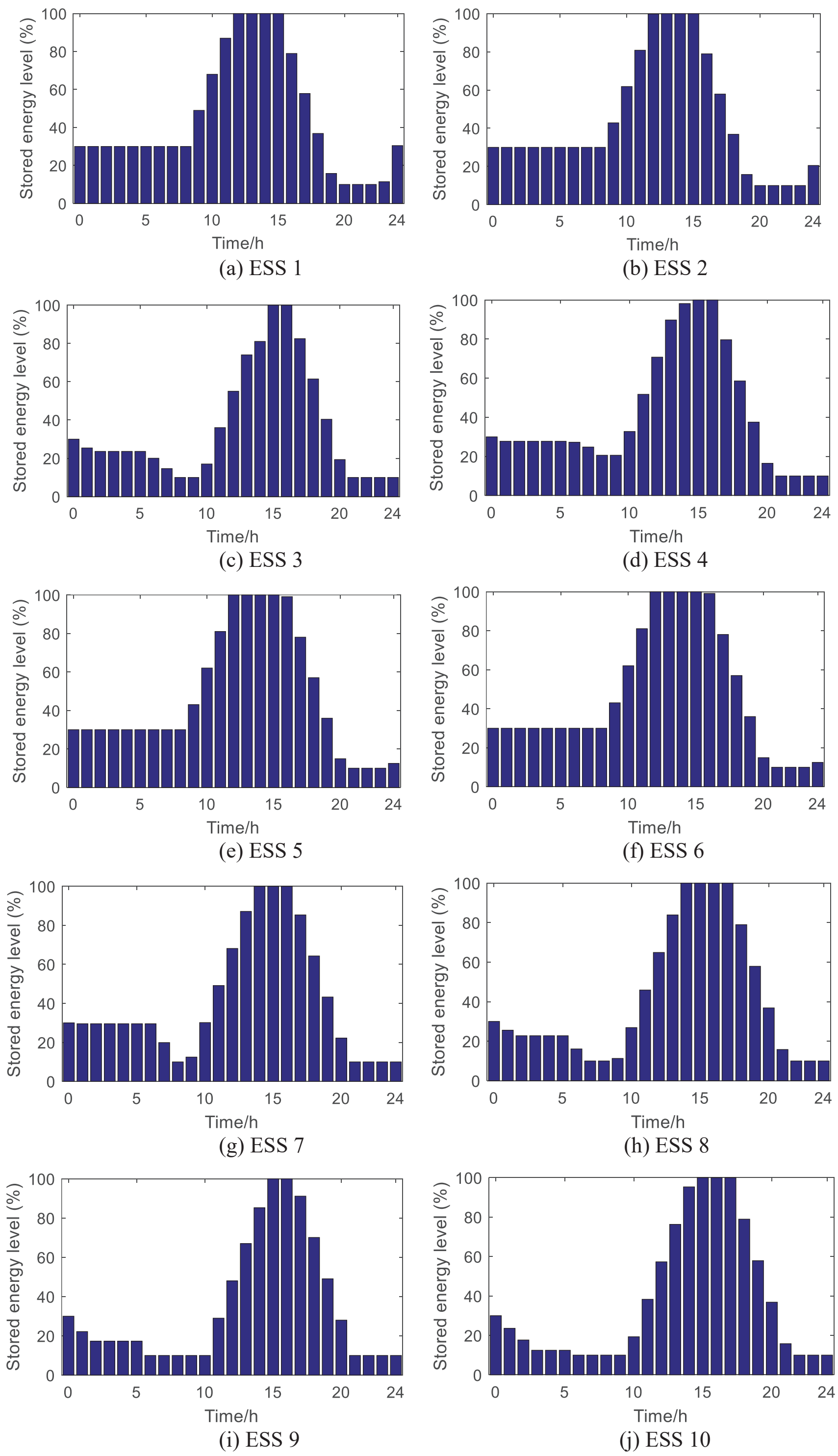

Fig. 4.10 The variation of stored energy level in ESSs for the single-period model

the single-period model and MPC based model in Fig. 4.10 and 4.11, respectively. Moreover, the author also compares the charging/discharging plans of ESSs under two

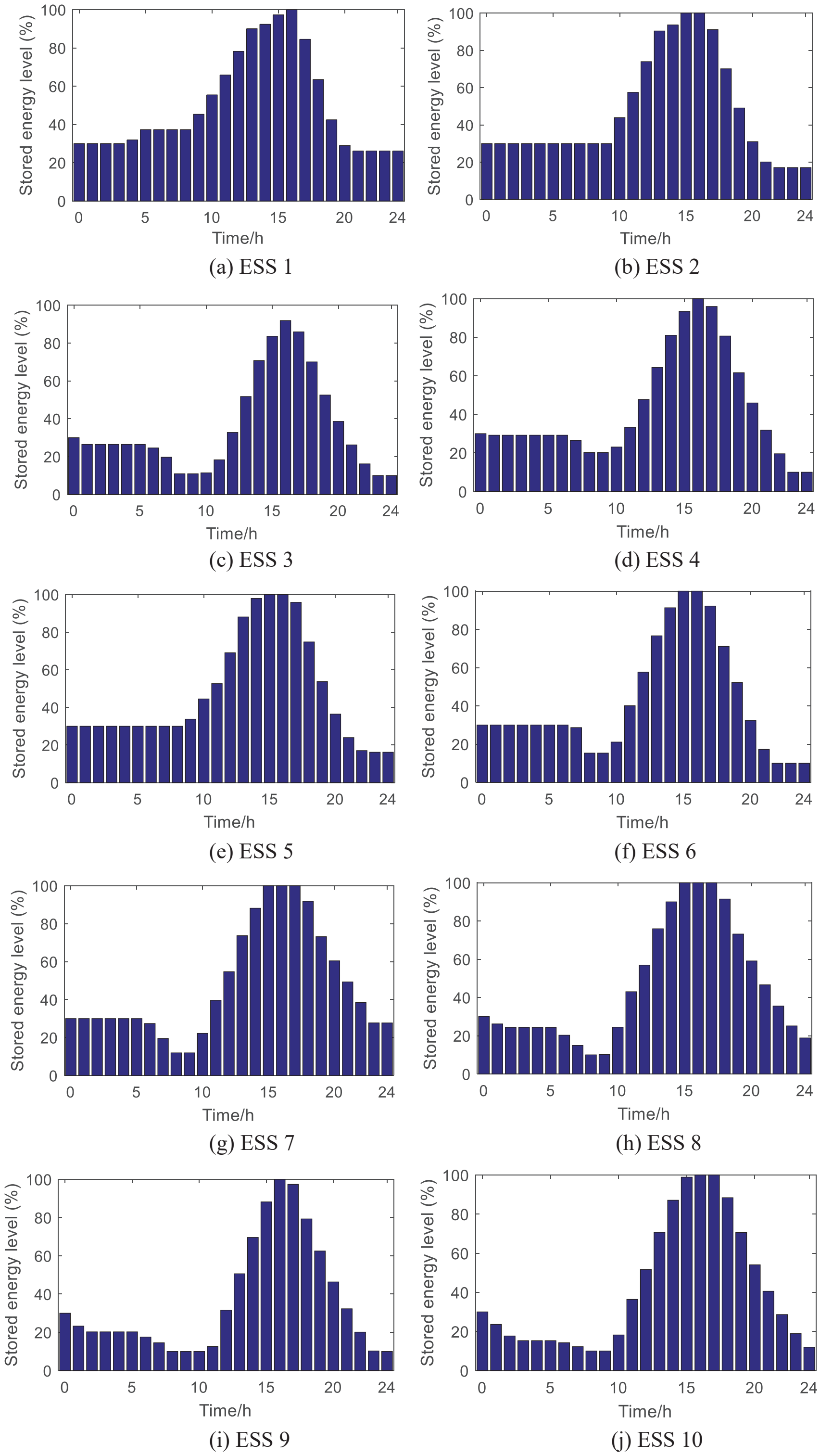

Fig. 4.11 The variation of stored energy level in ESSs for the MPC based model

models in Fig. 4.12. It can be observed from Fig. 4.10 that under the single-period model most ESSs are fully charged from 13:00 to 15:00 and fully discharged from

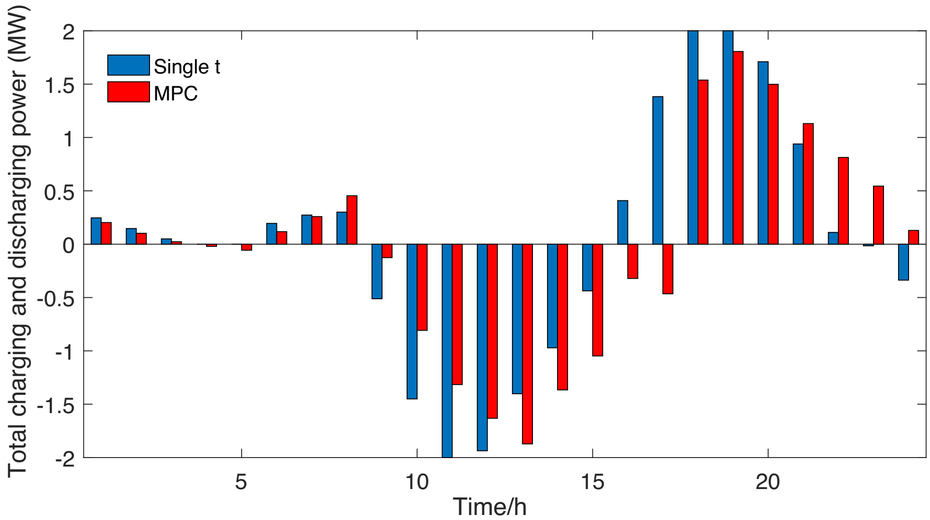

Fig. 4.12 Total charging (-) and discharging (+) power of ESSs of single-period model and MPC based model

20:00-24:00, which implies the inadequacy of energy capacities of ESSs to sustain such a charging/discharging plan. However, the energy levels of ESSs under the MPC based model vary less significantly and ESSs are never fully charged or discharged simultaneously as shown in Fig. 4.11. Hence, the ESS capacities have less influence on the MPC-based model than the single-period model. The inadequacy of ESS capacity in the single-period model arises from the inappropriate charging/discharging arrangement. It can observed from Fig. 4.12 that the ESSs under the single-period model always react faster to the PV and load variation than the ESSs under the MPC based model. Moreover, the charging/discharging power of the former is too large and thus cannot last for a long period. Consequently, the ramp mitigation ability of ESSs is greatly weakened. Therefore, the MPC based dispatch model outperforms single-period dispatch model as the former encourages the ESSs to be used more appropriately.

Table 4.2 Comparison of network loss, ESS degradation cost and ramp index

	Single t			MPC		
	Loss (kWh)	Degradation cost ($)	Ramp index (MW)	Loss (kWh)	Degradation cost ($)	Ramp index (MW)
Total	318	189	5.365	145	177	3.531

Table 4.2 lists the total network loss, ESS degradation cost and ramp index of the single-period model and the MPC-based model. A substantial reduction of network loss and ramp index can be observed using the MPC-based model. Furthermore, the degradation cost of the MPC-based model is also smaller than that of the single period model.

4.4.2 Impact of the ESS capacity

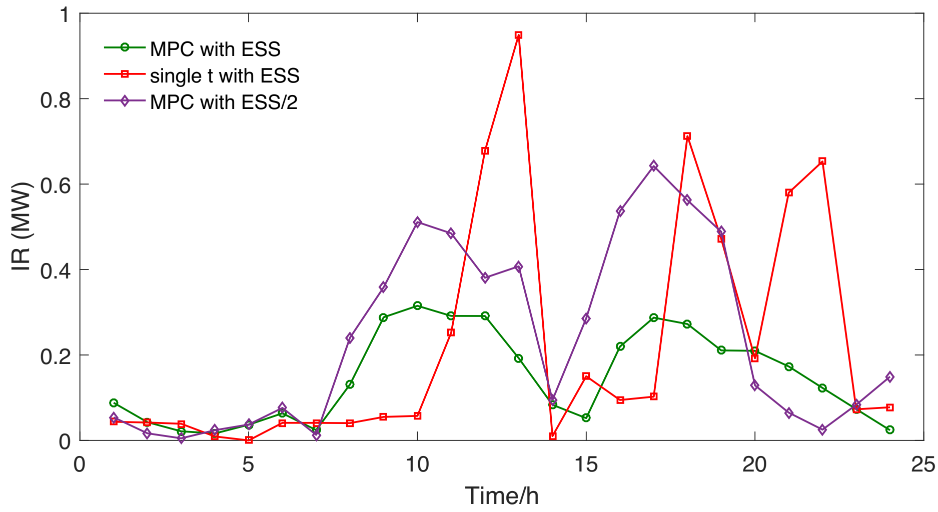

Fig. 4.13 Ramp index under three cases, MPC with ESS, single period with ESS and MPC with ESS/2

Table 4.3 Comparison of network loss, ESS degradation cost and ramp index

	MPC with ESS			MPC with ESS/2		
	Loss (kWh)	Degradation cost ($)	Ramp index (MW)	Loss (kWh)	Degradation cost ($)	Ramp index (MW)
Total	145	177	3.531	352	100	5.670

In this subsection, the author investigates the impact of the ESS capacity on the system performance. Specifically, the author reduces both the maximum charging/discharging power and the energy capacity by half and resolve the MPC-based dispatch problem. Denote this case as **MPC with ESS/2**. Fig. 4.13 depicts the ramp index under three cases, i.e. MPC with ESS, single-period with ESS and MPC with ESS/2. Table 4.3 shows the impact of the ESS capacity on the network loss, degradation cost and total ramp index. It can be seen from Fig. 4.13 when the ESS capacity is halved, the maximum ramp index is almost doubled. The total ramp index also increases substantially when the ESS capacity is halved, as shown by the table. Hence, the ESS capacity has a significant impact on the ramp minimization, which is consistent with our intuition. Also note that the ramping mitigation effect using MPC method with half ESS capacity is still slightly better than that using single-period method with full ESS capacity. Therefore, MPC method can compensate the capacity inadequacy of ESS.

4.5 Summary

The distribution networks are under a transition from passive ones to active ones with the increasing integration of distributed generations. However, the significant variation of renewable energy generations, especially the rooftop PV systems, will aggravate the ramping effect in transmission networks. Aiming at addressing this issue, a novel MPC based dispatch model is proposed to minimize the ramping effect in ADNs using distributed ESSs. In particular, the dispatch model with ESS scheduling is formulated as a multi-period optimization problem which is carried out using the MPC method. Since the MPC method considers both current and future information, it will produce an appropriate ESS scheduling result and keep the ramp at low level over the whole day. Moreover, second-order cone relaxed branch flow model is used to model the power flow in DNs so as to guarantee the global optimality. Numerical results on IEEE 37-bus distribution network demonstrate that the proposed model brings about significant reduction of maximum ramp and line losses.

Chapter 5

A Robust Dispatch Model for Distribution Networks Considering PV Ramp

5.1 Introduction

With the increasing penetration of PV generations in distribution networks, the impact of high variability of PV generations on the distribution system operation will become more remarkable. For instance, the sudden change of solar irradiance known as PV Ramp Event (PRE) may cause severe power imbalance and voltage variations. According to [99], a large ramp-down event was observed in the ERCOT operation area on February 26, 2008, which forced the system to activate the emergent measures. On the other hand, the minute-to-minute ramp event is hard to be predicted since it mainly arises from the cloud movement and climate change. Therefore, it is necessary to take effective measures to address this issue so as to improve the PV hosting capacity.

Several efforts have been made to deal with the PV ramp event. Ref. [100] proposed a preventative dispatch model to address the imbalence issue in a stand-alone microgrid considering the possible PV ramp-event. Ref. [101] presented a probabilistic approach to evaluate the operational adequacy of a stand-alone microgrid taking into account the PV ramp event and uncertainty of energy storage systems. In [102, 103], the energy storage is used to mitigate the ramp rate of the PV output, while in [104] the electric double-layer capacitor is employed to control the ramp rate. Nevertheless, the impact of the fast ramp event on the voltage profile of the distribution networks is not well studied.

In this chapter, a novel dispatch model is proposed for the distribution networks to address the PRE-induced voltage violations. The on-load tap changer (OLTC) is coordinated with PV inverters to ensure the voltage magnitudes within the allowable ranges. OLTC cannot be adjusted too frequently; otherwise, its life span will be shortened significantly. Thus, without loss of generality, the author assumes it can only be adjusted one time per hour and will be fixed in the following one hour. But PV inverters can be adjusted flexibly and continuously within that hour to complement the voltage regulation of OLTC. Normally, to prevent over-voltage violations caused by over-generation of PV systems, the step of OLTC is selected at a position with lower secondary voltage magnitude. But in such case, the under-voltage violation can be so severe that PV inverters cannot eliminate it when a PV ramp event takes place. Hence, the OLTC step is deliberately reselected to ensure the PV ramp-induced under-voltage violations can be effectively removed by the PV inverters alone. Meanwhile, the concept of maximum admissible PV output (MAPO) is proposed to quantify the PV hosting capacity for that hour. The MAPO is predetermined and is fed into the PV inverter controller to guide the operation of PV system. At any time of the covered periods, the active power of PV system should not exceed this value even when the MPPT value is higher than this. Moreover, the author assumes the substation bus is a slack bus, which means it can draw/inject any amount of power from/to the transmission network to balance the generation and load in distribution network.

The proposed model is formulated as a two-stage robust optimization problem, where the first stage determines the OLTC position and maximum admissible PV output (MAPO), and the second stage evaluates the feasibility of the first stage result under all possible realizations of PV ramp events. The column-and-constraint generation (CCG) algorithm is utilized to solve the proposed model.

The nomenclature of symbols used in this chapter is given as follows,

Indices and Sets

$\mathcal{E}$	Set of distribution lines
$i/\mathcal{N}$	Index and set of distribution buses
$k/\mathcal{N}^s$	Index and set of PV systems
$t/\mathcal{T}$	Index and set of time slots

Parameters

b^s_{ik}	Binary indicator, $b^s_{ik}=1$ if k-th PV system is located at bus i, $b^s_{ik}=0$ otherwise
n_r	Number of OLTC steps
$p^l_{i,t}$	Active power demand at bus i in time slot t
$P^{\max}_k$	Power capacity of PV panel k
$P^L_{k,t}$	Lower bound of predicted output interval for PV panel k in time slot t
$P^U_{k,t}$	Upper bound of predicted output interval for PV panel k in time slot t
$q^l_{i,t}$	Reactive power demand at bus i in time slot t
$Q^{\max}_k$	Upper bound of reactive power output of PV inverter k
r_{ij}	Resistance of the line connecting bus i and bus j
S_k	Rated apparent power of PV inverter k
V^0_m	Voltage magnitude on the secondary side of OLTC when the k-th step is selected
$V^{\min}_i$	Lower bound of voltage magnitude at bus i
$V^{\max}_i$	Upper bound of voltage magnitude at bus i
V_r	Nominal value of voltage magnitude
x_{ij}	Reactance of the line connecting bus i and bus j
θ	Angle corresponding to the minimum allowed power factor
Γ_k	Temporal uncertainty budget for PV inverter k
Γ_t	Spatial uncertainty budget in time slot t

Variables

$p_{0,t}$	Active power extraction from the transmission grid in time slot t
$p^a_{k,t}$	Realized maximum available power of PV system k in time slot t
$p^s_{k,t}$	Active power set-point of PV system k in time slot t
$P^{apo}_{k,t}$	Maximum admissible output of PV system k in time slot t
$P_{ij,t}$	Active flow on the line (i,j) from bus i to bus j in time slot t
$q_{0,t}$	Reactive power injection into the transmission grid in time slot t
$q^s_{k,t}$	Reactive power set-point of PV system k in time slot t
$Q_{ij,t}$	Reactive flow on the line (i,j) from bus i to bus j in time slot t
V_0	Voltage magnitude on the secondary side of OLTC
$V_{i,t}$	Voltage magnitude at bus i in time slot t
$s^l_{i,t}/s^u_{i,t}$	Positive slack variables for relaxing voltage constraints
$z_{k,t}$	Binary indicator, $z_{k,t}=1$ if there is a ramp down event on PV system k in time slot t, $z_{k,t}=0$ otherwise
χ_m	Binary indicator, $\chi_m=1$ if the m-th step of OLTC is selected, $\chi_m=0$ otherwise

5.2 Robust Intra-hour Dispatch Model

5.2.1 PV Inverter Dispatch

The PV inverters can be used for voltage regulation by adjusting the active and reactive power set-points [105]. The maximum admissible PV outputs is predetermined to quantify the operational PV hosting capacity of a distribution network. It is fed into the PV inverter controller prior to the dispatch time to guide the operation of PV system. If the maximum available PV power in real time exceeds MAPO, the excess power will be curtailed to prevent the PRE-induced voltage violations. Thus, the set of PV inverter operating points is given by

$$\Phi_k = \Big\{(p^s_{k,t}, q^s_{k,t}): \; p^s_{k,t} = \min\left(P^{apo}_{k,t}, p^a_{k,t}\right) \tag{5.1a}$$

$$\left|q^s_{k,t}\right| \leq Q^{\max}_k \tag{5.1b}$$

$$-\tan\theta \cdot p^s_{k,t} \leq q^s_{k,t} \leq \tan\theta \cdot p^s_{k,t}\Big\} \tag{5.1c}$$

where $Q_k^{\max} = \sqrt{S_k^2 - (P_k^{\max})^2}$. (5.1a) is to determine the active power set-point $p_{k,t}^s$ by selecting the smaller one between $P_{k,t}^{apo}$ and $p_{k,t}^a$, where $P_{k,t}^{apo}$ is maximum admissible PV output and $p_{k,t}^a$ is the maximum available active power obtained from maximum power point tracking technique. (5.1b) is to maintain the reactive power output within its capacity $Q_k^{\max}$. (5.1c) imposes the minimum power factor requirement on the PV inverter.

5.2.2 Modelling PV Ramp Events

In this subsection, the uncertainty set is constructed to model PV ramp events, which is the key step in applying robust optimization. Generally, the uncertainty set is modelled as a interval set with uncertainty budget [106]. The core idea of robust optimization is to find an optimal solution that is immune against worst case of uncertainty realization. Given the upper and lower bounds of the intervals as well as the uncertainty budgets, the worst realizations of PV ramp events can be modelled as

$$U = \Bigg\{ p_{k,t}^a | z_{k,t} \in \{0,1\} \quad \forall k \in \mathcal{N}^s,\ \forall t \in \mathcal{T} \tag{5.2a}$$

$$p_{k,t}^a = (1 - z_{k,t}) P_{k,t}^U + z_{k,t} P_{k,t}^L \quad \forall k \in \mathcal{N}^s,\ \forall t \in \mathcal{T} \tag{5.2b}$$

$$\sum_{k \in \mathcal{N}^s} z_{k,t} \leq \Gamma_t \quad \forall t \in \mathcal{T} \tag{5.2c}$$

$$\sum_{t \in \mathcal{T}} z_{k,t} \leq \Gamma_k \quad \forall k \in \mathcal{N}^s \Bigg\} \tag{5.2d}$$

where $P_{k,t}^U$ and $P_{k,t}^L$ are the upper bound and lower bound of the interval. $z_{k,t}$ is a binary indicator for PV ramp down event. (5.2b) shows that the worst case occurs when either the upper bound or the lower bound is attained. (5.2c) and (5.2d) represent uncertainty budget limit constraint.

5.2.3 Two-stage Coordinated Intra-hour Dispatch Model

A two-stage coordinated intra-hour dispatch model (CID) is formulated to maximize PV hosting capacity. The horizon and resolution are 1 hour and 5 minutes, respectively. The formulation of CID is given as follows,

$$\max_{P_{k,t}^{apo},\chi_m} \sum_{t\in\mathcal{T}}\sum_{k\in\mathcal{N}^s} P_{k,t}^{apo} \tag{5.3a}$$

$$\text{s.t. } P_{k,t}^{apo} \le P_{k,t}^{U} \quad \forall k\in\mathcal{N}^s,\ \forall t\in\mathcal{T} \tag{5.3b}$$

$$\chi_m \in \{0,1\}, \quad \sum_{m=1}^{n_r} \chi_m = 1 \tag{5.3c}$$

$$V_0 = \sum_{m=1}^{n_r} V_m^0 \cdot \chi_m \tag{5.3d}$$

$$\forall \{p_{k,t}^a\} \in U,\ \exists \left(p_{k,t}^s, q_{k,t}^s\right) \in \Phi_k \quad \forall k\in\mathcal{N}^s,\ \forall t\in\mathcal{T} \text{ such that} \tag{5.3e}$$

$$p_{0,t} = \sum_{j:0\to j} P_{0j,t} \quad \forall t\in\mathcal{T} \tag{5.3f}$$

$$\sum_{k\in\mathcal{N}^s} b_{ik}^s p_{k,t}^s - p_{i,t}^l = \sum_{j:i\to j} P_{ij,t} - P_{fi,t} \quad \forall i\in\mathcal{N}/0\ \forall t\in\mathcal{T} \tag{5.3g}$$

$$q_{0,t} = \sum_{j:0\to j} Q_{0j,t} \quad \forall t\in\mathcal{T} \tag{5.3h}$$

$$\sum_{k\in\mathcal{N}^s} b_{ik}^s q_{k,t}^s - q_{i,t}^l = \sum_{j:i\to j} Q_{ij,t} - Q_{fi,t} \quad \forall i\in\mathcal{N}/0\ \forall t\in\mathcal{T} \tag{5.3i}$$

$$V_{j,t} = V_{i,t} - \frac{r_{ij}P_{ij,t} + x_{ij}Q_{ij,t}}{V_r} \quad \forall (i,j)\in\mathcal{E} \tag{5.3j}$$

$$V_{0,t} = V_0 \quad \forall t\in\mathcal{T} \tag{5.3k}$$

$$V^{\min} \le V_{i,t} \le V^{\max} \quad \forall i\in\mathcal{N}\backslash 0,\quad \forall t\in\mathcal{T} \tag{5.3l}$$

where the objective (5.3a) is to maximize the total MAPO that represents the PV hosting capacity of the entire distribution system. (5.3b) keeps MAPO below the predicted upper bound of PV output. (5.3c) and (5.3d) are constraints related to the voltage regulation of OLTC, where χ_m is a binary variable with 1 indicating the selection of m-th step of OLTC and V_m^0 is the voltage magnitude corresponding to χ_m. Note that (5.3b)-(5.3d) are first stage constraints and $P_{k,t}^{apo}, \chi_m$ are first stage decision variables determined before the realization of PV uncertainty. (5.3e)-(5.3l) are second stage constraints and $p_{k,t}^s, q_{k,t}^s$ are second stage decision variables determined after the realization of PV uncertainty. (5.3e)-(5.3l) means that for any realization of PV uncertainty there exits at least one PV dispatch strategy that satisfies all operation constraints, which implies the robustness. Specifically, (5.3e) is the constraint related to the PV inverter dispatch. (5.3f) and (5.3g) show the active power balance at the substation bus and other buses, respectively. (5.3h) and (5.3i) describe the reactive power balance at the substation bus and other buses, respectively. (5.3j) denotes the voltage relationship between two neighbouring buses. (5.3k) and (5.3l) represent the voltage constraints for the substation bus and other buses, respectively.

Problem (5.3) is generally computationally intractable due to the intractable second stage constraints (5.3e)-(5.3l). In order to effectively solve the above problem, the second stage problem is reformulated as the following optimization problem.

$$\max_{p^a_{k,t}\in U} \min_{p^s_{k,t},q^s_{k,t},s^l_{i,t},s^u_{i,t}} \sum_{t\in\mathcal{T}} \sum_{i\in\mathcal{N}\backslash 0} \left(s^l_{i,t} + s^u_{i,t}\right) \tag{5.4a}$$

$$\text{s.t. } (5.3\text{e}) - (5.3\text{k}) \tag{5.4b}$$

$$V_{i,t} \geq V^{\min} - s^l_{i,t} \quad \forall i \in \mathcal{N}\backslash 0 \quad \forall t \in \mathcal{T} \tag{5.4c}$$

$$V_{i,t} \leq V^{\max} + \mathrm{s}^u_{i,t} \quad \forall i \in \mathcal{N}\backslash 0 \quad \forall t \in \mathcal{T} \tag{5.4d}$$

$$s^l_{i,t} \geq 0, \quad s^u_{i,t} \geq 0 \quad \forall i \in \mathcal{N}\backslash 0 \quad \forall t \in \mathcal{T} \tag{5.4e}$$

where $s^l_{i,t}$ and $s^u_{i,t}$ are non-negative slack variables. The voltage constraints (5.3l) are relaxed to (5.4c) and (5.4d). Thus, the objective function (5.4a) quantifies the voltage violations. Note that problem (5.4) is a bi-layer problem, where the inner layer is to minimize the voltage violations by adjusting the power set-points of PV inverters and the outer lay is to maximize the voltage violations by selecting the worst case of PV ramp events. The robustness requires the optimal value of (5.4) to always be 0.

5.3 Solution Method and Algorithm

The column-and-constraint generation(CCG) method is used to solve the above two-stage robust optimization problem [107]. By clarity, it will first be reformulated into a compact form as

$$\max_{\mathbf{x}=[\mathbf{x}_1^T \ \mathbf{x}_2^T]^T} \mathbf{c}^T\mathbf{x}_1 \tag{5.5a}$$

$$\text{s.t. } \mathbf{A}\mathbf{x}_1 \le \mathbf{b} \tag{5.5b}$$

$$\mathbf{B}\mathbf{x}_2 = \mathbf{d} \tag{5.5c}$$

$$\mathbf{x}_2 \in \{0,1\} \tag{5.5d}$$

$$\left(\max_{\mathbf{u}\in U} \min_{\mathbf{y},\mathbf{s}\le 0} \mathbf{1}^T\mathbf{s}\right) = 0 \tag{5.5e}$$

$$\Omega_1(\mathbf{x}) = \{\mathbf{y},\mathbf{u} : \mathbf{D}\mathbf{y} + \mathbf{E}\mathbf{u} + \mathbf{F}\mathbf{x} \le \mathbf{g}\} \tag{5.5f}$$

$$\Omega_2 = \{\mathbf{y},\mathbf{s} : \mathbf{C}\mathbf{y} \le \mathbf{f} + \mathbf{s}\} \tag{5.5g}$$

where $\mathbf{x}_1$ and $\mathbf{x}_2$ collect the continuous and binary variables of the first stage, respectively. (5.5b) and (5.5c) represent the first stage constraints, where the former summarizes (5.3b), and the latter summarizes (5.3c) and (5.3d). $\mathbf{y}$ and $\mathbf{s}$ collect the second stage variables and slack variables, respectively. (5.5e)-(5.5g) corresponds to the second stage problem (5.4). Particularly, (5.5f) summarizes (5.4b), and (5.5g) summarizes (5.4c) and (5.4d).

The core idea of CCG is to decompose the original two-stage problem into a master problem and a sub-problem. By solving the sub-problem, CCG constraints are iteratively generated and added to the master problem. The master problem is given by

$$\max_{\mathbf{x}=[\mathbf{x}_1^T\ \mathbf{x}_2^T]^T,\ \mathbf{y}^l} \mathbf{c}^T\mathbf{x}_1 \tag{5.6a}$$

$$\text{s.t. } \mathbf{A}\mathbf{x}_1 \le \mathbf{b} \tag{5.6b}$$

$$\mathbf{B}\mathbf{x}_2 = \mathbf{d} \tag{5.6c}$$

$$\mathbf{x}_2 \in \{0,1\} \tag{5.6d}$$

$$\mathbf{D}\mathbf{y}^l + \mathbf{E}\mathbf{u}^l + \mathbf{F}\mathbf{x} \le \mathbf{g} \quad l = 1, 2..., K \tag{5.6e}$$

$$\mathbf{C}\mathbf{y}^l \le \mathbf{f} \quad l = 1, 2..., k \tag{5.6f}$$

where K is the iteration index. (5.6e) and (5.6f) are CCG constraints. $\mathbf{x}$ and $\mathbf{y}^l$ are decision variables of (5.6). $\mathbf{u}^l$ is the worst case of PV uncertainty obtained by solving the sub-problem at l-th iteration.

The suproblem is formulated by replacing the inner lay of (5.4) with its dual, as shown below.

$$\max_{\mathbf{u}\in U,\ \boldsymbol{\lambda},\ \boldsymbol{\omega}} \quad -\mathbf{f}^T\boldsymbol{\lambda}+\mathbf{u}^T\mathbf{E}^T\boldsymbol{\omega}+\mathbf{x}^T\mathbf{F}^T\boldsymbol{\omega}-\mathbf{g}^T\boldsymbol{\omega} \tag{5.7a}$$

$$\text{s.t. } \mathbf{C}^T\boldsymbol{\lambda}+\mathbf{D}^T\boldsymbol{\omega}=\mathbf{0} \tag{5.7b}$$

$$\mathbf{0}\le\boldsymbol{\lambda}\le\mathbf{1} \tag{5.7c}$$

$$\boldsymbol{\omega}\ge\mathbf{0} \tag{5.7d}$$

where $\boldsymbol{\lambda}$ and $\boldsymbol{\omega}$ are dual variables associated with (5.5f) and (5.5g), respectively. Since constraints (5.5f) and (5.5g) are linear, the strong duality holds [71]. Hence, (5.7) is equivalent to the second stage problem (5.5e)-(5.5g). Note there is bilinear term in (5.7a). Big M method can be applied to linearize the bilinear term or outer approximation method can be used to solve (5.7). Interested readers can refer to [108–110].

Algorithm 2 summarizes the overall algorithm for solving the proposed two-stage robust optimization problem.

Algorithm 2: CCG Algorithm for the Two-stage Robust Optimization Problem

Initialize the iteration index $K=1$;
repeat
  Solve the master problem (5.6) and obtain the optimal solution $\mathbf{x}^K$;
  Fix $\mathbf{x}$ at $\mathbf{x}^K$ and solve the sub-problem (5.7). Obtain the optimal solution $\mathbf{u}^K$ and the optimal value p^*;
  K=K+1;
  Create additional variable $\mathbf{y}^{K+1}$ and add new CCG cuts (5.6e) and (5.6f) to the master problem (5.6);
until $p^*=0$;
Return the optimal first stage decision $\mathbf{x}^{K-1}$

5.4 Case Study

The proposed coordinated dispatch (CID) model is tested on IEEE 33-bus distribution network [111], where 8 PV systems are installed at bus 14, 15, 16, 17, 21, 24, 31 and

32, respectively. The capacity of each PV system is 800 kW. The solar PV power is calculated using the actual solar irradiance data provided by [56]. The lower bound of PV output is set as 20% of predicted value. The algorithm is implemented on MATLAB with CPLEX 12.6 solver [112].

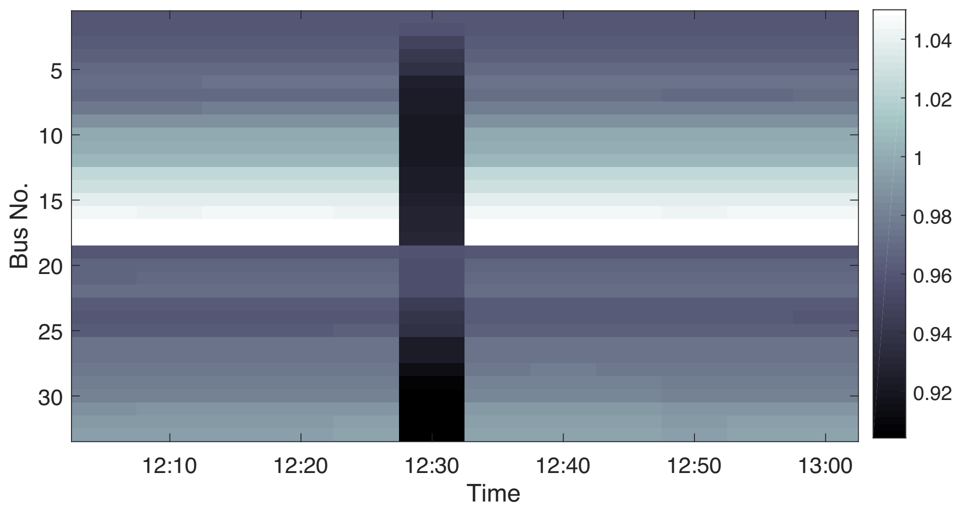

Fig. 5.1 Bus voltage magnitudes under DM

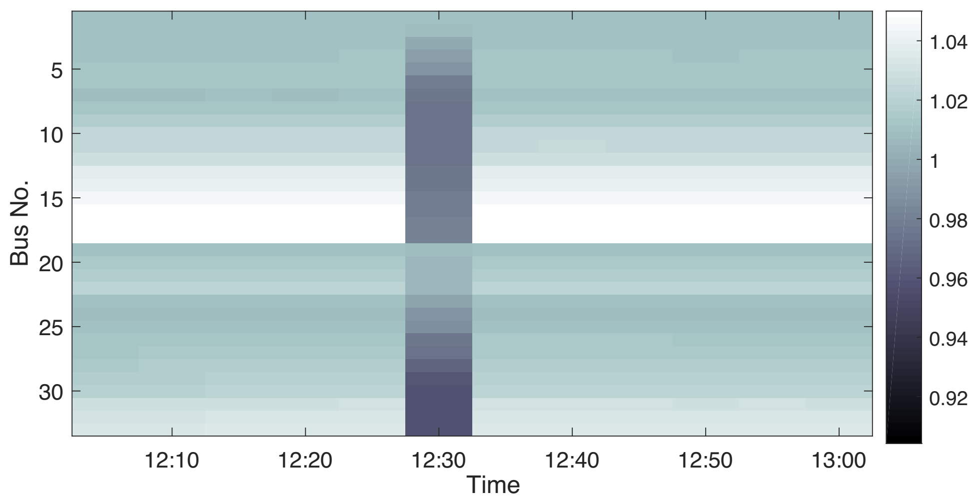

Fig. 5.2 Bus voltage magnitudes under CID

Deterministic model (DM) is used as a benchmark, whose objective is to minimize PV curtailment without considering PV ramp events. Fig. 5.1 and 5.2 depict the bus voltage magnitudes over the period from 12:00 to 13:00 under the DM and CID,

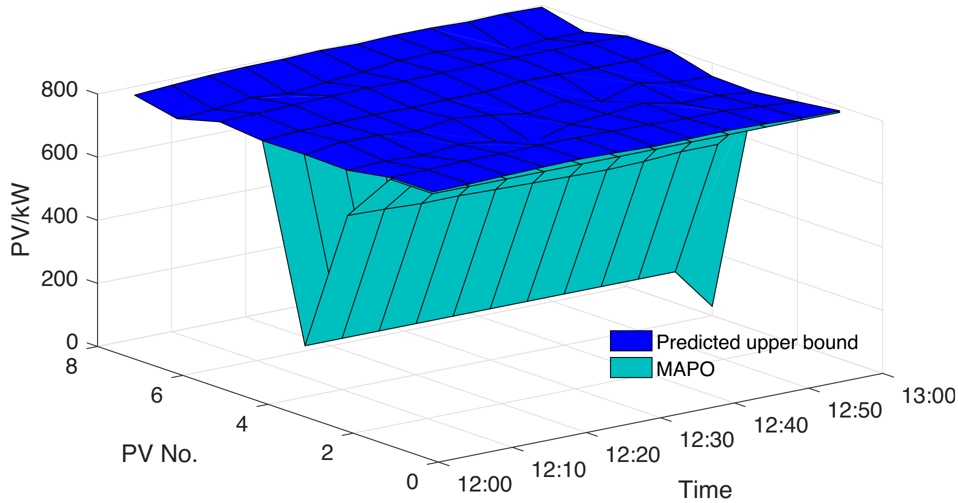

Fig. 5.3 Maximum PV output and predicted upper bound

respectively. In DM case, severe undervoltage violations are observed when a PRE takes place at 12:30. By contrast, the bus voltage magnitudes under CID are always maintained within the allowable range which is $[0.95, 1.05]$. The reason is that CID considers all possible scenarios of PV ramp events and takes preventative measures by properly selecting the OLTC step and predetermining the maximum admissible PV output. Therefore, CID outperforms DM in terms of dealing with PRE-induced voltage violations. In addition, MAPO as well as the predicted upper bound are demonstrated in Fig.5.3. It can be observed that MAPO remains the same with the upper bound for the most PV inverters. Thus, the PV curtailment is relatively small (roughly 6.3% of total PV generation), which validates the effectiveness of the proposed model in coping with the PREs and maximizing the solar energy utilization.

5.5 Summary

In this chapter, the author presents a novel coordinated intra-hour dispatch model for distribution networks considering minute-to-minute PV ramp events. The model is formulated as a two-stage robust optimization problem, where the first stage is to determine the OLTC step as well as the operational PV hosting capacity and the second stage is to ensure the voltage security by properly scheduling PV inverters.

Numerical results on IEEE 33-bus validate the effectiveness of the proposed model in addressing the PRE-induced voltage problem.

Chapter 6

Conclusions and Future Works

6.1 Conclusions

The widespread adoption of DERs introduces considerable challenges to the distribution system operation because of their uncertain and intermittent nature and the complexity in coordinating them. The focus of this thesis is on overcoming these challenges by developing advanced management approaches. Both centralized and decentralized strategies are proposed to cope with the economic and technical issues within the distribution system operation domain with the ultimate goal of improving DER accommodation capability. In particular, the author investigates the distribution system operation problem in the following four aspects.

1) To overcome the complexity in coordinating various devices and promote the competitive energy trading, a novel transactive energy trading framework is proposed for the end-use customers by leveraging the recent emerging transactive energy concept. Specifically, an innovative bilateral energy trading mechanism is developed by utilizing Nash bargaining theory and is seamlessly integrated with an efficient distributed optimal power flow technique. By doing so, the market issues and distribution system operation issues can be dealt with in a holistic manner. With some rigorous analysis, the author converts the proposed transactive energy trading problem into an equivalent two-stage problem, where the first stage determines the optimal energy trading and dispatch, and the

second stage settles the optimal payment. Furthermore, an efficient distributed algorithm is developed that enables the proposed framework to be implemented in a decentralized manner to preserve the autonomy and privacy of customers. The optimality and convergence of the proposed algorithm is guaranteed. Numerical results on IEEE 37-bus and 123-bus distribution systems demonstrate the economic and technical effectiveness of the proposed framework and the efficiency of the proposed algorithm.

2) To address the severe voltage variations caused by the intermittent PV output, a distributed online voltage control algorithm is proposed for the distribution networks. Conventional distributed algorithms implement voltage control only when the algorithms converge. However, the proposed algorithm is able to carry out voltage control immediately. Specifically, the author formulates the voltage control problem as an optimization problem where the objective is to minimize the total loss while maintaining the bus voltages within the acceptable rang. Then a distributed algorithm is developed by applying dual ascend method to this optimization problem. With this distributed algorithm, each PV system is able to locally update and apply its active and reactive power set-points based on the local voltage measurement and information exchange with neighboring PV systems. The convergence to the optimality is established analytically. Moreover, the close-form solution for each update is derived so as to significantly improve the control efficiency. Numerical tests on IEEE 37-bus and 123-bus system validate the effectiveness of the proposed distributed online algorithm.

3) To mitigate significant load ramps arisen from the diurnal pattern of solar PV power, a novel look-ahead dispatch model is proposed for the active distribution networks using distributed ESSs. The dispatch problem is modelled as a finite horizon optimization problem and is carried out utilizing the model predictive control method that takes both current and future information into account. Consequently, ESSs can be appropriately scheduled to avoid latent over-charging or over-discharging during some periods. Numerical results on IEEE 37-bus

distribution system show that the proposed model brings about more than 80% reduction of maximum ramp and roughly 50% reduction of distribution line losses.

4) To alleviate the minute-to-minute PV ramp induced voltage violations, a novel intra-hour dispatch model is proposed that enables coordination between OLTC and PV inverters. Specifically, this model is formulated as a two-stage robust optimization problem, where the first stage determines the OLTC step and maximum admissible PV output (MAPO), and the second stage evaluates the feasibility of the first stage result under all possible realizations of PV ramp events (PREs). MAPO is proposed to quantify the operational PV hosting capacity and is fed into PV inverter controllers prior to the dispatch time to guide the operation of PV systems. Besides, the proposed model is not a standard two-stage robust optimization problem. Thus, it is reformulated before applying CCG algorithm to solve it. Case study on IEEE 33-bus distribution network verifies the effectiveness of the proposed model in addressing PRE induced voltage problem.

6.2 Future Works

This thesis has proposed several advanced methods for the management of the active distribution networks with high penetration of DERs. Some assumptions have been made to simplify the complicated realistic problems, such as the distribution networks are three-phase balanced and customers are rational. To make the proposed methods more implementable, the author will investigate the following problems in the future.

1) In fact, distribution networks are inherently three-phase unbalanced due to the untransposed lines, unbalanced load and multi-phase feeders [12]. It presents considerable complexity to the modelling of distribution networks, not to mention the analysis of practical operation problems, such as voltage regulation and energy management. Therefore, the author will first endeavor to develop

more accurate models, e.g. multi-phase optimal power flow model, to assist the investigation of the operation problems.

2) Beside the voltage variations, the voltage unbalance across different phases is a severe problem in practice. The unbalance should be maintained below certain level; otherwise, it will cause detrimental effects to various devices, such as transformers and electric motors. Moreover, since a large portion of DERs are single-phase generators, the widespread of them may further aggravate the voltage unbalance. Therefore, the author will investigate the voltage variation and voltage unbalance problems and develop effective control strategies by employing the potential of DERs to address the voltage problems.

3) In chapter 2, the author only develops a transactive energy framework for energy trading. With the evolution of power systems, more ancillary services, e.g. reactive power support, ramping product and frequency regulation, are required to ensure the system reliability, security and resilience. One ideal way to procure these services is to encourage end-users to provide them. Therefore, the author will design a transactive energy model considering both energy and ancillary services. In addition, the author will study the customers' behaviors in a more comprehensive way.

4) In chapter 2 and 3, the author develops distributed algorithms to implement the transactive energy design and voltage control in a distributed manner. However, the uncertainties of load demand and renewable energies are not taken into account since up to now it is still mathematically challenging in incorporating uncertainties into distributed operation and control schemes. In the future, the author will study the possibility to integrate robust optimization or stochastic programming with distributed algorithms.

Appendix A

A.1 Proof of Proposition 1

To obtain the explicit form of $\mathbf{x}_i$-update problem, first we need to specify the related Lagrangian multipliers, as shown in Table A.1. Through expanding the quadratic and collecting terms, the $\mathbf{x}_i$-update problem (2.28) can be further decomposed into three subproblems. The tedious process is not elaborated here for clarity. Interested readers may refer to the subsection III-B of [48].

The first subproblem solves the optimal $(P_i^x, Q_i^x, l_i^x, v_i^x)$, i.e.

$$\begin{aligned} \min \ & \left(P_i^x - \widehat{P}_i\right)^2 + \left(Q_i^x - \widehat{Q}_i\right)^2 + \left(l_i^x - \widehat{l}_i\right)^2 \\ & + \frac{|C_i|+1}{2}\left(v_i^x - \widehat{v}_i\right)^2 \end{aligned} \tag{A.1a}$$

$$\begin{aligned} \text{over } & P_i^x, Q_i^x, l_i^x, v_i^x \\ \text{s.t. } & (2.25\text{f}) \text{ and } (2.25\text{g}) \end{aligned} \tag{A.1b}$$

where

$$\widehat{P}_i = \frac{P^z_{i(i)} + P^z_{i(A_i)}}{2} - \frac{\mu^{(1)}_{i(i)} + \mu^{(1)}_{i(A_i)}}{2\rho}$$

Table A.1 Multipliers associated with consensus constraints

$\mu^{(1)}_{i(j)}$: $P_i^x = P^z_{i(j)}$ $j \in i \cup A_i$	$\mu^{(2)}_{i(j)}$: $Q_i^x = Q^z_{i(j)}$ $j \in i \cup A_i$
$\mu^{(3)}_{i(j)}$: $l_i^x = l^z_{i(j)}$ $j \in i \cup A_i$	$\mu^{(4)}_{i(j)}$: $v_i^x = v^z_{i(j)}$ $j \in i \cup C_i$
$\mu^{(5)}_{i(i)}$: $p_i^x = p^z_{i(i)}$	$\mu^{(6)}_{i(i)}$: $q_i^x = q^z_{i(i)}$
$\mu^{(7)}_{ij(i)}$: $e^x_{ij} = e^z_{ij(i)}$ $j \in \mathcal{N}\backslash i$	$\mu^{(7)}_{ji(i)}$: $e^x_{ji} = e^z_{ji(i)}$ $j \in \mathcal{N}\backslash i$

$$\widehat{Q}_i = \frac{Q^z_{i(i)} + Q^z_{i(A_i)}}{2} - \frac{\mu^{(2)}_{i(i)} + \mu^{(2)}_{i(A_i)}}{2\rho}$$
$$\widehat{l}_i = \frac{l^z_{i(i)} + l^z_{i(A_i)}}{2} - \frac{\mu^{(3)}_{i(i)} + \mu^{(3)}_{i(A_i)}}{2\rho}$$
$$\widehat{v}_i = \frac{v^z_{i(i)} + \sum_{j\in C_i} v^z_{i(j)}}{|C_i| + 1} - \frac{\mu^{(4)}_{i(i)} + \sum_{j\in C_i} \mu^{(4)}_{i(j)}}{\rho(|C_i| + 1)}$$

According to [48], (A.1) has a closed form solution.

The second subproblem solves the optimal q^x_i, i.e.

$$\min_{q^x_i} \ \left(q^x_i - \widehat{q}_i\right)^2 \tag{A.2a}$$
$$\text{s.t. } \underline{q}_i \le q^x_i \le \overline{q}_i \tag{A.2b}$$

where $\widehat{q}_i = q^z_{i(i)} - \frac{\mu^{(6)}_{i(i)}}{\rho}$. The optimal solution can be easily obtained as $\left[\widehat{q}_i\right]^{\overline{q}_i}_{\underline{q}_i}$, where $[\cdot]^b_a$ represents the projection operator onto the range $[a, b]$.

The third subproblem solves the optimal (p^x_i, e^x_{ij}), i.e.

$$\min_{p^x_i, e^x_{ij}} \ (\alpha_i + \frac{\rho}{2})\left(p^x_i - \widehat{p}_i\right)^2 + \sum_{j\in\mathcal{N}\setminus i} \rho\left(e^x_{ij} - \widehat{e}_{ij}\right)^2 \tag{A.3a}$$
$$\text{s.t. } \underline{p}_i \le p^x_i \le \overline{p}_i \tag{A.3b}$$
$$\underline{e}_i \le \sum_{j\in\mathcal{N}\setminus i} e^x_{ij} \le \overline{e}_i \tag{A.3c}$$

where

$$\widehat{p}_i = \frac{1}{2\alpha_i + \rho}\left(2\alpha_i(p^g_i - D_i) + \rho p^z_{i(i)} + \lambda - \pi_i - \mu^{(5)}_{i(i)}\right)$$
$$\widehat{e}_{ij} = \frac{e^z_{ij(i)} + e^z_{ij(j)}}{2} + \frac{\lambda - \mu^{(7)}_{ij(i)} - \mu^{(7)}_{ij(j)}}{2\rho}$$

The values of λ, $\underline{e}_i$ and $\overline{e}_i$ depend on the sign of p^x_i. If $p^x_i \le 0$, then $\lambda = \lambda^b$, $\underline{e}_i = 0$, $\overline{e}_i = -p^x_i$; otherwise $\lambda = \lambda^s$, $\underline{e}_i = -p^x_i$, $\overline{e}_i = 0$.

As long as the problem (A.3) can be solved in closed form, we would complete the proof. Indeed, we derive the closed form solution to (A.3). Since (A.3) is a convex quadratic optimization problem with linear inequalities, it has a unique global minimizer. Without loss of generality, suppose $p_i^x \leq 0$ and update $\overline{p}_i$ as $\min(\overline{p}_i, 0)$. Then (A.3) is transformed to

$$\min_{p_i^x, e_{ij}^x} \ (\alpha_i + \frac{\rho}{2})\Big(p_i^x - \widehat{p}_i\Big)^2 + \sum_{j \in \mathcal{N}\setminus i} \rho\Big(e_{ij}^x - \widehat{e}_{ij}\Big)^2 \tag{A.4a}$$

$$\text{s.t. } \underline{p}_i \leq p_i^x \leq \overline{p}_i \tag{A.4b}$$

$$0 \leq \sum_{j \in \mathcal{N}\setminus i} e_{ij}^x \leq -p_i^x \tag{A.4c}$$

In the following, we will derive its closed form solution by enumerating the activeness of the inequality constraints.

Case 1: (A.4c) is inactive.

Then $p_i^{x*} = \Big[\widehat{p}_i\Big]_{\underline{p}_i}^{\overline{p}_i}$ and $e_{ij}^{x*} = \widehat{e}_{ij}, \ j \in \mathcal{N}\setminus i$.

Case 2: (A.4c) is active and $\sum_{j \in \mathcal{N}\setminus i} e_{ij}^x = 0$.

Then (A.4) can be decomposed into two subproblems. One subproblem only involves variable p_i^x, i.e.

$$\min_{p_i^x} \ (\alpha_i + \frac{\rho}{2})\Big(p_i^x - \widehat{p}_i\Big)^2$$
$$\text{s.t. } \underline{p}_i \leq p_i^x \leq \overline{p}_i$$

whose optimal solution is $p_i^{x*} = \Big[\widehat{p}_i\Big]_{\underline{p}_i}^{\overline{p}_i}$. The other subproblem only involves variables e_{ij}^x, i.e.

$$\min_{e_{ij}^x} \ \sum_{j \in \mathcal{N}\setminus i} \rho\Big(e_{ij}^x - \widehat{e}_{ij}\Big)^2$$
$$\text{s.t. } \sum_{j \in \mathcal{N}\setminus i} e_{ij}^x = 0$$

it can be generalized as the problem (2.33). Thus, it can be solved in closed form.

Case 3: (A.4c) is active and $\sum_{j \in \mathcal{N}\setminus i} e_{ij}^x = -p_i^x$.

Then (A.4) can be reformulated as the problem below by eliminating p_i^x.

$$\min_{e_{ij}^x} \ F_i(\{e_{ij}^x | j \in \mathcal{N}\setminus i\}) \tag{A.7a}$$

$$\text{s.t.} \ -\overline{p}_i \leq \sum_{j \in \mathcal{N} \setminus i} e^x_{ij} \leq -\underline{p}_i \tag{A.7b}$$

where $F_i(\{e^x_{ij} | j \in \mathcal{N} \setminus i\}) = (\alpha_i + \frac{\rho}{2})\Big(\sum_{j \in \mathcal{N} \setminus i} e^x_{ij} + \widehat{p}_i\Big)^2 + \sum_{j \in \mathcal{N} \setminus i} \rho\Big(e^x_{ij} - \widehat{e}_{ij}\Big)^2$. Similarly, we solve (A.7) in closed form by enumerating the activeness of the constraint (A.7b).

- **Subcase 3.1:** (A.7b) is inactive .

  Then the optimal solution can be obtained by solving the following linear system:

$$\frac{\partial F_i(\{e^x_{ij} | j \in \mathcal{N} \setminus i\})}{\partial e^x_{ij}} = 0 \quad j \in \mathcal{N} \setminus i$$

  Denote $X := \sum_{j \in \mathcal{N} \setminus i} e^x_{ij}$. Then, we have

$$X^* = \frac{-(N-1)(\rho + 2\alpha_i)\widehat{p}_i + 2\rho \sum_{j \in \mathcal{N} \setminus i} \widehat{e}_{ij}}{(N-1)(\rho + 2\alpha_i) + 2\rho}$$
$$e^{x*}_{ij} = \widehat{e}_{ij} - \frac{\rho + 2\alpha_i}{2\rho}(X^* + \widehat{p}_i)$$

- **Subcase 3.2:** (A.7b) is active and $\sum_{j \in \mathcal{N} \setminus i} e^x_{ij} = -\overline{p}_i$.

  Then, the problem (A.7) can be converted to the following problem.

$$\min_{e^x_{ij}} \ \sum_{j \in \mathcal{N} \setminus i} \rho\Big(e^x_{ij} - \widehat{e}_{ij}\Big)^2 \tag{A.9a}$$
$$\text{s.t.} \ \sum_{j \in \mathcal{N} \setminus i} e^x_{ij} = -\overline{p}_i \tag{A.9b}$$

  With a slight abuse of notation, (A.9) can be generalized as

$$\min_{\mathbf{z}} \ \frac{1}{2}\mathbf{z}^T\mathbf{Q}\mathbf{z} + \mathbf{c}^T\mathbf{z} \tag{A.10a}$$
$$\text{s.t.} \ \mathbf{A}\mathbf{z} = \mathbf{b} \tag{A.10b}$$

  where $\mathbf{z}$ is the vector of decision variables constituted by e^x_{ij}; $\mathbf{Q} := 2\rho\mathbf{I}_{N-1}$; $\mathbf{c}$ is a vector constituted by $-2\rho\widehat{e}_{ij}$; $\mathbf{A} = \mathbf{1}^T$ and $\mathbf{b} = -\overline{p}_i$; $\mathbf{I}_{N-1}$ is a $N-1$

dimensional identity matrix. (A.10) has a closed form solution given by

$$\begin{aligned}\mathbf{z}^* =&\Big(\mathbf{Q}^{-1}\mathbf{A}^T(\mathbf{A}\mathbf{Q}^{-1}\mathbf{A}^T)^{-1}\mathbf{A}\mathbf{Q}^{-1} - \mathbf{Q}^{-1}\Big)\mathbf{c}\\ &+ \mathbf{Q}^{-1}\mathbf{A}^T(\mathbf{A}\mathbf{Q}^{-1}\mathbf{A}^T)^{-1}\mathbf{b}\end{aligned}$$

- **Subcase 3.3:** (A.7b) is active and $\sum_{j\in\mathcal{N}\backslash i} e^x_{ij} = -\underline{p}_i$.

  Then the optimal $\{e^x_{ij}|j \in \mathcal{N}\backslash i\}$ can be obtained similarly as the subcase 3.2.

A.2 Proof of Proposition 2

Let $\mu'_{ij(i)}$ and $\mu'_{ji(i)}$ denote the multiplier for (2.37c) and (2.37d), respectively. Then for a given penalty parameter $\rho > 0$, the augmented Lagrangian is defined as

$$\mathcal{L}_\rho(\mathbf{x}', \mathbf{y}', \boldsymbol{\mu}') := \sum_{i\in\mathcal{N}} \mathcal{L}_{\rho,i}(\phi^x_{ij}, \phi^z_{ij(i)}, \phi^z_{ij(j)}, \mu'_{ij(i)}, \mu'_{ij(j)}) \tag{A.11}$$

where

$$\begin{aligned}\mathcal{L}_{\rho,i}(\phi^x_{ij}, \phi^z_{ij(i)}, \phi^z_{ij(j)}, \mu'_{ij(i)}, \mu'_{ij(j)}) :=& -\ln\Big(\theta_i - \sum_{j\in\mathcal{N}\backslash i} \phi^x_{ij}\Big)\\ &+ \sum_{j\in\mathcal{N}\backslash i}\Big(\mu'_{ij(i)}(\phi^x_{ij} - \phi^z_{ij(i)}) + \frac{\rho}{2}(\phi^x_{ij} - \phi^z_{ij(i)})^2\Big)\\ &+ \sum_{j\in\mathcal{N}\backslash i}\Big(\mu'_{ij(j)}(\phi^x_{ij} - \phi^z_{ij(j)}) + \frac{\rho}{2}(\phi^x_{ij} - \phi^z_{ij(j)})^2\Big)\end{aligned}$$

At each iteration k, each agent i solves the problem below to update ϕ^x_{ij} based on the current value of $\phi^{z,k}_{ij(i)}$, $\phi^{z,k}_{ij(j)}$, $\mu'^{,k}_{ij(i)}$ and $\mu'^{,k}_{ij(j)}$.

$$\begin{aligned}&\min\ \mathcal{L}_{\rho,i}(\phi^x_{ij}, \phi^{z,k}_{ij(i)}, \phi^{z,k}_{ij(j)}, \mu'^{,k}_{ij(i)}, \mu'^{,k}_{ij(j)}))\\ &\text{over } \{\phi^x_{ij}|j \in \mathcal{N}\backslash i\}\end{aligned} \tag{A.12}$$

Its optimal solution can be obtained by solving the equations below.

$$\frac{\partial\mathcal{L}_{\rho,i}(\phi^x_{ij}, \phi^{z,k}_{ij(i)}, \phi^{z,k}_{ij(j)}, \mu'^{,k}_{ij(i)}, \mu'^{,k}_{ij(j)})}{\partial\phi^x_{ij}} = 0 \quad j \in \mathcal{N}\backslash i$$

Denote $Y_i = \sum_{j \in \mathcal{N} \setminus i} \phi_{ij}^x$. Then the optimal Y_i^* can be obtained by solving the following equation.

$$Y_i^2 + (\frac{a_i}{2\rho} - \theta_i)Y_i - \frac{a_i\theta_i}{2\rho} - \frac{N-1}{2\rho} = 0$$

where

$$a_i = \sum_{j \in \mathcal{N} \setminus i} \left(\mu_{ij(i)}^{\prime,k} + \mu_{ij(j)}^{\prime,k} - \rho\phi_{ij(i)}^{z,k} - \rho\phi_{ij(j)}^{z,k}\right)$$

Finally, the optimal solution to (A.12) is obtained as

$$\phi_{ij}^{x*} = \frac{\phi_{ij(i)}^{z,k} + \phi_{ij(j)}^{z,k}}{2} - \frac{\mu_{ij(i)}^{\prime,k} + \mu_{ij(j)}^{\prime,k}}{2\rho} - \frac{1}{2\rho}\frac{1}{\theta_i - Y_i^*}$$

References

[1] R. Labastida and B. Feldman, "Global DER deployment forecast database," *Navigant Research*, 2017.

[2] M. H. Bollen and F. Hassan, *Integration of distributed generation in the power system.* John wiley & sons, 2011, vol. 80.

[3] C. S. Initiative *et al.*, "California solar statistics," 2015.

[4] G. I. Strahs and C. Tombari, *Laying the Foundation for a Solar America: The Million Solar Roofs Initiative. Final Report, October 2006.* National Renewable Energy Laboratory, 2006.

[5] IEA, *Prospects for distributed energy systems in China.* IEA publications, 2017.

[6] J. L. Sawin, F. Sverrisson, K. Seyboth, R. Adib, H. E. Murdock, C. Lins, I. Edwards, M. Hullin, L. H. Nguyen, S. S. Prillianto *et al.*, "Renewables 2017 global status report," 2017.

[7] J. Zhao, "Optimal operation and planning of smart grid with electric vehicle penetration," Ph.D. dissertation, The Hong Kong Polytechnic University, 2017.

[8] J. Zhao, Z. Xu, J. Wang, C. Wang, and J. Li, "Robust distributed generation investment accommodating electric vehicle charging in a distribution network," *IEEE Transactions on Power Systems*, 2018.

[9] P. Cazzola, M. Gorner, R. Schuitmaker, and E. Maroney, "Global EV outlook 2017," *International Energy Agency, France*, 2017.

[10] V. M. Balijepalli, V. Pradhan, S. Khaparde, and R. Shereef, "Review of demand response under smart grid paradigm," in *Innovative Smart Grid Technologies-India (ISGT India), 2011 IEEE PES.* IEEE, 2011, pp. 236–243.

[11] D. Papadaskalopoulos and G. Strbac, "Decentralized participation of flexible demand in electricity markets-part i: Market mechanism," *IEEE Transactions on Power Systems*, vol. 28, no. 4, pp. 3658–3666, 2013.

[12] W. H. Kersting, *Distribution system modeling and analysis.* CRC press, 2001.

[13] C. Wan, J. Lin, W. Guo, and Y. Song, "Maximum uncertainty boundary of volatile distributed generation in active distribution network," *IEEE Transactions on Smart Grid*, 2016.

[14] C. Zhang, J. Li, Y. J. A. Zhang, and Z. Xu, "Optimal location planning of renewable distributed generation units in distribution networks: An analytical approach," *IEEE Transactions on Power Systems*, 2017.

[15] S. Bose, D. F. Gayme, S. Low, and K. M. Chandy, "Optimal power flow over tree networks," in *Communication, Control, and Computing (Allerton), 2011 49th Annual Allerton Conference on.* IEEE, 2011, pp. 1342–1348.

[16] P. N. Vovos, A. E. Kiprakis, A. R. Wallace, and G. P. Harrison, "Centralized and distributed voltage control: Impact on distributed generation penetration," *IEEE Transactions on power systems*, vol. 22, no. 1, pp. 476–483, 2007.

[17] E. Dall'Anese, S. V. Dhople, and G. B. Giannakis, "Optimal dispatch of photovoltaic inverters in residential distribution systems," *IEEE Transactions on Sustainable Energy*, vol. 5, no. 2, pp. 487–497, 2014.

[18] V. Calderaro, G. Conio, V. Galdi, G. Massa, and A. Piccolo, "Optimal decentralized voltage control for distribution systems with inverter-based distributed generators," *IEEE Transactions on Power Systems*, vol. 29, no. 1, pp. 230–241, 2014.

[19] R. B. Melton, "Gridwise transactive energy framework," Pacific Northwest National Laboratory (PNNL), Richland, WA (US), Tech. Rep., 2013.

[20] M. Akter, M. Mahmud, and A. M. Oo, "A hierarchical transactive energy management system for microgrids," in *Power and Energy Society General Meeting (PESGM), 2016.* IEEE, 2016, pp. 1–5.

[21] S. M. Sajjadi, P. Mandal, T.-L. B. Tseng, and M. Velez-Reyes, "Transactive energy market in distribution systems: A case study of energy trading between transactive nodes," in *North American Power Symposium (NAPS), 2016.* IEEE, 2016, pp. 1–6.

[22] Y. K. Renani, M. Ehsan, and M. Shahidehpour, "Optimal transactive market operations with distribution system operators," *IEEE Transactions on Smart Grid*, 2017.

[23] S. Bahramirad, A. Khodaei, and R. Masiello, "Distribution markets," *IEEE Power and Energy Magazine*, vol. 14, no. 2, pp. 102–106, 2016.

[24] M. Akter, M. Mahmud, and A. M. Oo, "An optimal distributed transactive energy sharing approach for residential microgrids," in *Power & Energy Society General Meeting, 2017 IEEE.* IEEE, 2017, pp. 1–5.

[25] J. Lee, J. Guo, J. K. Choi, and M. Zukerman, "Distributed energy trading in microgrids: A game-theoretic model and its equilibrium analysis," *IEEE Transactions on Industrial Electronics*, vol. 62, no. 6, pp. 3524–3533, 2015.

[26] H.-G. Yeh, D. F. Gayme, and S. H. Low, "Adaptive var control for distribution circuits with photovoltaic generators," *IEEE Transactions on Power Systems*, vol. 27, no. 3, pp. 1656–1663, 2012.

[27] S. Bolognani, R. Carli, G. Cavraro, and S. Zampieri, "Distributed reactive power feedback control for voltage regulation and loss minimization," *IEEE Transactions on Automatic Control*, vol. 60, no. 4, pp. 966–981, 2015.

[28] V. Calderaro, G. Conio, V. Galdi, G. Massa, and A. Piccolo, "Optimal decentralized voltage control for distribution systems with inverter-based distributed generators," *IEEE Transactions on Power Systems*, vol. 29, no. 1, pp. 230–241, 2014.

[29] M. Farivar, L. Chen, and S. Low, "Equilibrium and dynamics of local voltage control in distribution systems," in *Decision and Control (CDC), 2013 IEEE 52nd Annual Conference on*. IEEE, 2013, pp. 4329–4334.

[30] P. Jahangiri and D. C. Aliprantis, "Distributed volt/var control by pv inverters," *IEEE Transactions on power systems*, vol. 28, no. 3, pp. 3429–3439, 2013.

[31] E. Dall?Anese, S. V. Dhople, B. B. Johnson, and G. B. Giannakis, "Decentralized optimal dispatch of photovoltaic inverters in residential distribution systems," *IEEE Transactions on Energy Conversion*, vol. 29, no. 4, pp. 957–967, 2014.

[32] W. Zheng, W. Wu, B. Zhang, H. Sun, and Y. Liu, "A fully distributed reactive power optimization and control method for active distribution networks," *IEEE Transactions on Smart Grid*, vol. 7, no. 2, pp. 1021–1033, 2016.

[33] C. Feng, Z. Li, M. Shahidehpour, F. Wen, W. Liu, and X. Wang, "Decentralized short-term voltage control in active power distribution systems," *IEEE Transactions on Smart Grid*, 2017.

[34] P. Denholm, M. O'Connell, G. Brinkman, and J. Jorgenson, "Overgeneration from solar energy in california. a field guide to the duck chart," National Renewable Energy Lab.(NREL), Golden, CO (United States), Tech. Rep., 2015.

[35] Q. Wang and B.-M. Hodge, "Enhancing power system operational flexibility with flexible ramping products: A review," *IEEE Transactions on Industrial Informatics*, vol. 13, no. 4, pp. 1652–1664, 2017.

[36] K. Divya and J. Østergaard, "Battery energy storage technology for power systems-an overview," *Electric Power Systems Research*, vol. 79, no. 4, pp. 511–520, 2009.

[37] R. Ambrosio, "Transactive energy systems," *IEEE Electrification Magazine*, vol. 4, no. 4, pp. 4–7, 2016.

[38] H. Hao, C. D. Corbin, K. Kalsi, and R. G. Pratt, "Transactive control of commercial buildings for demand response," *IEEE Transactions on Power Systems*, vol. 32, no. 1, pp. 774–783, 2017.

[39] J. Qiu, J. Zhao, H. Yang, and Z. Y. Dong, "Optimal scheduling for prosumers in coupled transactive power and gas systems," *IEEE Transactions on Power Systems*, 2017.

[40] S. M. Sajjadi, P. Mandal, T.-L. B. Tseng, and M. Velez-Reyes, “Transactive energy market in distribution systems: A case study of energy trading between transactive nodes,” in *North American Power Symposium (NAPS), 2016*. IEEE, 2016, pp. 1–6.

[41] N. Liu, X. Yu, C. Wang, C. Li, L. Ma, and J. Lei, “Energy sharing model with price-based demand response for microgrids of peer-to-peer prosumers,” *IEEE Transactions on Power Systems*, vol. 32, no. 5, pp. 3569–3583, 2017.

[42] H. Wang and J. Huang, “Incentivizing energy trading for interconnected microgrids,” *IEEE Transactions on Smart Grid*, 2017.

[43] D. Gregoratti and J. Matamoros, “Distributed energy trading: The multiple-microgrid case,” *IEEE Transactions on Industrial Electronics*, vol. 62, no. 4, pp. 2551–2559, 2015.

[44] A. Werth, N. Kitamura, and K. Tanaka, “Conceptual study for open energy systems: distributed energy network using interconnected dc nanogrids,” *IEEE Transactions on Smart Grid*, vol. 6, no. 4, pp. 1621–1630, 2015.

[45] Y. Wang, W. Saad, Z. Han, H. V. Poor, and T. Başar, “A game-theoretic approach to energy trading in the smart grid,” *IEEE Transactions on Smart Grid*, vol. 5, no. 3, pp. 1439–1450, 2014.

[46] M. Pilz and L. Al-Fagih, “Recent advances in local energy trading in the smart grid based on game–theoretic approaches,” *IEEE Transactions on Smart Grid*, 2017.

[47] H. Yang, D. Yi, J. Zhao, and Z. Dong, “Distributed optimal dispatch of virtual power plant via limited communication,” *IEEE Transactions on Power Systems*, vol. 28, no. 3, pp. 3511–3512, 2013.

[48] Q. Peng and S. H. Low, “Distributed optimal power flow algorithm for radial networks, i: Balanced single phase case,” *IEEE Transactions on Smart Grid*, 2016.

[49] B. Zhang, A. Y. Lam, A. D. Domínguez-García, and D. Tse, “An optimal and distributed method for voltage regulation in power distribution systems,” *IEEE Transactions on Power Systems*, vol. 30, no. 4, pp. 1714–1726, 2015.

[50] H. J. Liu, W. Shi, and H. Zhu, “Distributed voltage control in distribution networks: Online and robust implementations,” *IEEE Transactions on Smart Grid*, 2017.

[51] M. Farivar and S. H. Low, “Branch flow model: Relaxations and convexification—part i,” *IEEE Transactions on Power Systems*, vol. 28, no. 3, pp. 2554–2564, 2013.

[52] J. F. Nash Jr, “The bargaining problem,” *Econometrica: Journal of the Econometric Society*, pp. 155–162, 1950.

[53] S. Boyd, N. Parikh, E. Chu, B. Peleato, and J. Eckstein, “Distributed optimization and statistical learning via the alternating direction method of multipliers,” *Foundations and Tfds® in Machine Learning*, vol. 3, no. 1, pp. 1–122, 2011.

[54] D. T. F. W. Group *et al.*, "Distribution test feeders," *Available from: ewh. ieee. org/soc/pes/dsacom/testfeeders/index. htmi*, 2010.

[55] C. Zhang, J. Li, Y. J. A. Zhang, and Z. Xu, "Optimal location planning of renewable distributed generation units in distribution networks: An analytical approach," *IEEE Transactions on Power Systems*, 2017.

[56] "Hong Kong Observatory," [online]. Available: http://www.hko.gov.hk/.

[57] K.-C. Toh, M. J. Todd, and R. Tütüncü, "Sdpt3 version 4.0 (beta)–a matlab software for semidefinite-quadratic-linear programming," *[Online] http://www. math. nus. edu. sg/ mattohkc/sdpt3. html*, 2009.

[58] "US solar market insight report 2016," Solar Energy Industries Association [online]. Available: http://www.seia.org/research-resources/solar-market-insight-report-2016-year-review.

[59] H. Zhu and H. J. Liu, "Fast local voltage control under limited reactive power: Optimality and stability analysis," *IEEE Transactions on Power Systems*, vol. 31, no. 5, pp. 3794–3803, 2016.

[60] H.-G. Yeh, D. F. Gayme, and S. H. Low, "Adaptive var control for distribution circuits with photovoltaic generators," *IEEE Transactions on Power Systems*, vol. 27, no. 3, pp. 1656–1663, 2012.

[61] M. J. E. Alam, K. M. Muttaqi, and D. Sutanto, "A multi-mode control strategy for var support by solar pv inverters in distribution networks," *IEEE transactions on power systems*, vol. 30, no. 3, pp. 1316–1326, 2015.

[62] P. Jahangiri and D. C. Aliprantis, "Distributed volt/var control by pv inverters," *IEEE Transactions on power systems*, vol. 28, no. 3, pp. 3429–3439, 2013.

[63] C. Feng, Z. Li, M. Shahidehpour, F. Wen, W. Liu, and X. Wang, "Decentralized short-term voltage control in active power distribution systems," *IEEE Transactions on Smart Grid*, 2017.

[64] K. E. Antoniadou-Plytaria, I. N. Kouveliotis-Lysikatos, P. S. Georgilakis, and N. D. Hatziargyriou, "Distributed and decentralized voltage control of smart distribution networks: models, methods, and future research," *IEEE Transactions on Smart Grid*, 2017.

[65] P. Šulc, S. Backhaus, and M. Chertkov, "Optimal distributed control of reactive power via the alternating direction method of multipliers," *IEEE Transactions on Energy Conversion*, vol. 29, no. 4, pp. 968–977, 2014.

[66] A. Maknouninejad and Z. Qu, "Realizing unified microgrid voltage profile and loss minimization: A cooperative distributed optimization and control approach," *IEEE Transactions on Smart Grid*, vol. 5, no. 4, pp. 1621–1630, 2014.

[67] A. Abessi, V. Vahidinasab, and M. S. Ghazizadeh, "Centralized support distributed voltage control by using end-users as reactive power support," *IEEE Transactions on Smart Grid*, vol. 7, no. 1, pp. 178–188, 2016.

[68] D. B. West *et al.*, *Introduction to graph theory.* Prentice hall Upper Saddle River, 2001, vol. 2.

[69] T. Zhu, Z. Huang, A. Sharma, J. Su, D. Irwin, A. Mishra, D. Menasche, and P. Shenoy, “Sharing renewable energy in smart microgrids,” in *Cyber-Physical Systems (ICCPS), 2013 ACM/IEEE International Conference on.* IEEE, 2013, pp. 219–228.

[70] D. P. Bertsekas, *Nonlinear programming.* Athena scientific Belmont, 1999.

[71] S. Boyd and L. Vandenberghe, *Convex optimization.* Cambridge university press, 2004.

[72] G. Hébrail and A. Bérard, “Individual household electric power consumption data set,” *É. d. France, Ed., ed: UCI Machine Learning Repository*, 2012.

[73] A. Bidram, A. Davoudi, F. L. Lewis, and J. M. Guerrero, “Distributed cooperative secondary control of microgrids using feedback linearization,” *IEEE Transactions on Power Systems*, vol. 28, no. 3, pp. 3462–3470, 2013.

[74] J. Zhao, J. Wang, Z. Xu, C. Wang, C. Wan, and C. Chen, “Distribution network electric vehicle hosting capacity maximization: a chargeable region optimization model,” *IEEE Transactions on Power Systems*, vol. 32, no. 5, pp. 4119–4130, 2017.

[75] J. Zhang, H. Cheng, and C. Wang, “Technical and economic impacts of active management on distribution network,” *International Journal of Electrical Power & Energy Systems*, vol. 31, no. 2-3, pp. 130–138, 2009.

[76] M. Ahlstrom, E. Ela, J. Riesz, J. O’Sullivan, B. F. Hobbs, M. O’Malley, M. Milligan, P. Sotkiewicz, and J. Caldwell, “The evolution of the market: Designing a market for high levels of variable generation,” *IEEE Power and Energy Magazine*, vol. 13, no. 6, pp. 60–66, 2015.

[77] C. Wu, G. Hug, and S. Kar, “Risk-limiting economic dispatch for electricity markets with flexible ramping products,” *IEEE Transactions on Power Systems*, vol. 31, no. 3, pp. 1990–2003, 2016.

[78] B.-I. Crăciun, T. Kerekes, D. Séra, R. Teodorescu, and U. D. Annakkage, “Power ramp limitation capabilities of large pv power plants with active power reserves,” *IEEE Transactions on Sustainable Energy*, vol. 8, no. 2, pp. 573–581, 2017.

[79] L. Xu and D. Tretheway, “Flexible ramping products,” 2012.

[80] C. Wang, P. B.-S. Luh, and N. Navid, “Ramp requirement design for reliable and efficient integration of renewable energy,” *IEEE Transactions on Power Systems*, vol. 32, no. 1, pp. 562–571, 2017.

[81] Y. Zhang, V. Gevorgian, C. Wang, X. Lei, E. Chou, R. Yang, Q. Li, and L. Jiang, “Grid-level application of electrical energy storage: Example use cases in the united states and china,” *IEEE Power and Energy Magazine*, vol. 15, no. 5, pp. 51–58, 2017.

[82] H. Khani, M. R. D. Zadeh, and A. H. Hajimiragha, "Transmission congestion relief using privately owned large-scale energy storage systems in a competitive electricity market," *IEEE Transactions on Power Systems*, vol. 31, no. 2, pp. 1449–1458, 2016.

[83] H. H. Abdeltawab and Y. A.-R. I. Mohamed, "Mobile energy storage scheduling and operation in active distribution systems," *IEEE Transactions on Industrial Electronics*, vol. 64, no. 9, pp. 6828–6840, 2017.

[84] H. Zhao, M. Hong, W. Lin, and K. A. Loparo, "Voltage and frequency regulation of microgrid with battery energy storage systems," *IEEE Transactions on Smart Grid*, 2017.

[85] C. O'Dwyer and D. Flynn, "Using energy storage to manage high net load variability at sub-hourly time-scales," *IEEE Transactions on Power Systems*, vol. 30, no. 4, pp. 2139–2148, 2015.

[86] Y. Wen, C. Guo, H. Pandžić, and D. S. Kirschen, "Enhanced security-constrained unit commitment with emerging utility-scale energy storage," *IEEE Transactions on power Systems*, vol. 31, no. 1, pp. 652–662, 2016.

[87] Y. Wen, C. Guo, D. S. Kirschen, and S. Dong, "Enhanced security-constrained opf with distributed battery energy storage," *IEEE Transactions on Power Systems*, vol. 30, no. 1, pp. 98–108, 2015.

[88] A. Bhattacharya, J. Kharoufeh, and B. Zeng, "Managing energy storage in microgrids: A multistage stochastic programming approach," *IEEE Transactions on Smart Grid*, 2016.

[89] J. Li, Z. Xu, J. Zhao, and C. Wan, "A coordinated dispatch model for distribution network considering pv ramp," *IEEE Transactions on Power Systems*, vol. 33, no. 1, pp. 1107–1109, 2018.

[90] C. Chen, J. Wang, Y. Heo, and S. Kishore, "MPc-based appliance scheduling for residential building energy management controller," *IEEE Transactions on Smart Grid*, vol. 4, no. 3, pp. 1401–1410, 2013.

[91] D. E. Olivares, C. A. Cañizares, and M. Kazerani, "A centralized energy management system for isolated microgrids," *IEEE Transactions on smart grid*, vol. 5, no. 4, pp. 1864–1875, 2014.

[92] L. Jin, R. Kumar, and N. Elia, "Model predictive control-based real-time power system protection schemes," *IEEE Transactions on Power Systems*, vol. 25, no. 2, pp. 988–998, 2010.

[93] M. E. Baran and F. F. Wu, "Optimal capacitor placement on radial distribution systems," *IEEE Transactions on power Delivery*, vol. 4, no. 1, pp. 725–734, 1989.

[94] M. Baran and F. F. Wu, "Optimal sizing of capacitors placed on a radial distribution system," *IEEE Transactions on power Delivery*, vol. 4, no. 1, pp. 735–743, 1989.

[95] D. T. Nguyen and L. B. Le, "Optimal bidding strategy for microgrids considering renewable energy and building thermal dynamics," *IEEE Transactions on Smart Grid*, vol. 5, no. 4, pp. 1608–1620, 2014.

[96] P. Pinson and R. Girard, "Evaluating the quality of scenarios of short-term wind power generation," *Applied Energy*, vol. 96, pp. 12–20, 2012.

[97] X.-Y. Ma, Y.-Z. Sun, and H.-L. Fang, "Scenario generation of wind power based on statistical uncertainty and variability," *IEEE Transactions on Sustainable Energy*, vol. 4, no. 4, pp. 894–904, 2013.

[98] N. M. Razali and A. Hashim, "Backward reduction application for minimizing wind power scenarios in stochastic programming," in *Power Engineering and Optimization Conference (PEOCO), 2010 4th International.* IEEE, 2010, pp. 430–434.

[99] E. Ela and B. Kirby, "Ercot event on february 26, 2008: lessons learned," National Renewable Energy Lab.(NREL), Golden, CO (United States), Tech. Rep., 2008.

[100] J. Zhao and Z. Xu, "Ramp-limited optimal dispatch strategy for pv-embedded microgrid," *IEEE Transactions on Power Systems*, vol. 32, no. 5, pp. 4155–4157, 2017.

[101] L. H. Koh, P. Wang, F. H. Choo, K.-J. Tseng, Z. Gao, and H. B. Püttgen, "Operational adequacy studies of a pv-based and energy storage stand-alone microgrid," *IEEE Transactions on power systems*, vol. 30, no. 2, pp. 892–900, 2015.

[102] M. Alam, K. Muttaqi, and D. Sutanto, "A novel approach for ramp-rate control of solar pv using energy storage to mitigate output fluctuations caused by cloud passing," *IEEE Transactions on Energy Conversion*, vol. 29, no. 2, pp. 507–518, 2014.

[103] V. Salehi and B. Radibratovic, "Ramp rate control of photovoltaic power plant output using energy storage devices," in *PES General Meeting| Conference & Exposition, 2014 IEEE.* IEEE, 2014, pp. 1–5.

[104] N. Kakimoto, H. Satoh, S. Takayama, and K. Nakamura, "Ramp-rate control of photovoltaic generator with electric double-layer capacitor," *IEEE Transactions on Energy Conversion*, vol. 24, no. 2, pp. 465–473, 2009.

[105] T. Ding, C. Li, Y. Yang, J. Jiang, Z. Bie, and F. Blaabjerg, "A two-stage robust optimization for centralized-optimal dispatch of photovoltaic inverters in active distribution networks," *IEEE Transactions on Sustainable Energy*, vol. 8, no. 2, pp. 744–754, 2017.

[106] D. Bertsimas and M. Sim, "The price of robustness," *Operations research*, vol. 52, no. 1, pp. 35–53, 2004.

[107] B. Zeng and L. Zhao, "Solving two-stage robust optimization problems using a column-and-constraint generation method," *Operations Research Letters*, vol. 41, no. 5, pp. 457–461, 2013.

[108] D. Bertsimas, E. Litvinov, X. A. Sun, J. Zhao, and T. Zheng, “Adaptive robust optimization for the security constrained unit commitment problem,” *IEEE Transactions on Power Systems*, vol. 28, no. 1, pp. 52–63, 2013.

[109] W. Wei, F. Liu, S. Mei, and Y. Hou, “Robust energy and reserve dispatch under variable renewable generation,” *IEEE Transactions on Smart Grid*, vol. 6, no. 1, pp. 369–380, 2015.

[110] R. Jiang, J. Wang, and Y. Guan, “Robust unit commitment with wind power and pumped storage hydro,” *IEEE Transactions on Power Systems*, vol. 27, no. 2, pp. 800–810, 2012.

[111] M. E. Baran and F. F. Wu, “Network reconfiguration in distribution systems for loss reduction and load balancing,” *IEEE Transactions on Power delivery*, vol. 4, no. 2, pp. 1401–1407, 1989.

[112] I. I. CPLEX, “V12. 1: User’s manual for cplex,” *International Business Machines Corporation*, vol. 46, no. 53, p. 157, 2009.